Instituto Tecnológico y de Estudios Superiores de Monterrey

Campus Monterrey

School of Engineering and Sciences

Characterization of the Skin Secretions of *Dryophytes arenicolor* and Identification of Arenin, a Novel Kunitz-like Polypeptide

A dissertation presented by

Jesús Hernández-Pérez

Submitted to the
School of Engineering and Sciences
in partial fulfillment of the requirements for the degree of

Doctor

in

Biotechnology

Monterrey Nuevo León, December 14th, 2018

Instituto Tecnológico y de Estudios Superiores de Monterrey

Campus Monterrey

School of Engineering and Sciences

The committee members, hereby, certify that have read the dissertation presented by Jesús Hernández-Pérez and that it is fully adequate in scope and quality as a partial requirement for the degree of Doctor in Biotechnology,

Dr. Jorge A. Benavides Lozano
Tecnológico de Monterrey
School of Engineering and Sciences
Advisor

Dr. Guy A. Cardineau
Tecnológico de Monterrey
Arizona State University
Co-Advisor

Dr. José M. Aguilar Yáñez
Tecnológico de Monterrey
School of Engineering and Sciences
Committee Member

Dr. Katy E. Klymus
U.S. Geological Survey
Columbia Environmental Research Center
Committee Member

Dr. Jorge E. Moreno Cuevas
Universidad de Monterrey
School of Health Sciences
Committee Member

Tecnológico de Monterrey
17 DIC 2018
Dirección Nacional de Posgrado
Dr. Rubén Morales Menéndez

Dr. Rubén Morales Menéndez
Dean of Graduate Studies
School of Engineering and Sciences

Monterrey Nuevo León, December 14th, 2018

Declaration of Authorship

I, Jesús Hernández Pérez declare that this dissertation titled, Characterization of the skin secretions of *Dryophytes arenicolor* and identification of Arenin, a novel Kunitz-like polypeptide and the work presented in it are my own. I confirm that:

- This work was done wholly or mainly while in candidature for a research degree at this University.
- Where any part of this thesis has previously been submitted for a degree or any other qualification at this University or any other institution, this has been clearly stated.
- Where I have consulted the published work of others, this is always clearly attributed.
- Where I have quoted from the work of others, the source is always given. With the exception of such quotations, this thesis is entirely my own work.
- I have acknowledged all main sources of help.
- Where the thesis is based on work done by myself jointly with others, I have made clear exactly what was done by others and what I have contributed myself.

Jesús Hernández Pérez
Monterrey Nuevo León, December 14th, 2018

“Against that positivism which stops before phenomena,
saying "there are only facts," I should say:
no, it is precisely facts that do not exist,
only interpretations…”

Friedrich Nietzsche
Notebooks (Summer 1886 – Fall 1887)

A Saucerful of Secrets
Roger Waters, Richard Wright, Nick Mason and David Gilmour
Pink Floyd (1968)

Dedication

To all the frogs that participated on this research, their lives will not be forgotten.

To my Mother, my Grandmother and my family for being the first ones who have put their trust on me.

To Brenda for all her love, support, patience and companionship along this road.

To Jorge Benavides for his guidance, trust and friendship, thank you for being a life and career role-model.

To Guy Cardineau for taking me under his mentorship 8 years ago, for all his teachings inside and outside the lab, for his friendship and honesty.

To Edgar and Karla for their friendship and support in the long nights and the short days.

To Daniel, David, Elias, Felipe, Manuel, Rebeca, Roberto and Sergio for their friendship and for all the journeys we have shared and all the teachings we have learned together.

To Alex G, Calef, Constantino, David, Fanny, Isabela, Tere and Wendy for their confidence, support, friendship and all the drinks we have had together.

To Eduardo, Emilio and Ricardo for continue teaching me with their own lives.

To Done, David, Panxho, Tsuru, Rola and all the community which have provide friendship and joy.

To Pepe, Alex A, Beatriz, Sole, Mario, Hector, Alex R, Cesar for all their help, support, advice and friendship.

To Jean, Glendon, Daniel, Lina, Florence, Kate, Keylin, Moon, Kehan, Prem, Zhong Yang, Edgar for their friendship and having welcomed me while at Singapore.

To Bernardo, Humberto, Manuel, Roberto, Rocío, Salomón, Samara for their long-lasting friendship even though we have lived in different cities for 11 years.

To Zaida, Fer and Sabrina for their friendship and the time they invested assisting this research.

Acknowledgements

I would like to express my deepest gratitude to all those who have supported this research through knowledge, time, resources, advice and friendship.

To Tecnológico de Monterrey for tuition support and Consejo Nacional de Ciencia y Tecnología (CONACyT) for living support through the Ph.D. scholarship No. 391089.

To the financial support from the Research Group with strategic focus on Bioengineering, Biosystems and Synthetic Biology of Tecnológico de Monterrey (Account number 0020209I13).

Special thanks to Marilena Antunes-Ricardo for her teaching and advice on analytical techniques. To Javier Villela-Castrejón and Alejandro Robles for their technical advice on cell viability assays.

To Jorge Benavides, Guy Cardineau, Katy Klymus, José Manuel Aguilar and Jorge Moreno for their time, advice, support and knowledge invested in this dissertation.

To Aida Serra, Siu Kwan Sze, Patricia Conway and Jørgen Schlundt for their support while at NTU.

Characterization of the skin secretions of *Dryophytes arenicolor* and Identification of Arenin, a novel Kunitz-like polypeptide

by

Jesús Hernández-Pérez

Abstract

Zootherapy is the treatment of human ailments with remedies made from animals and their products. Despite its prevalence in the traditional medical practices worldwide, research on this phenomenon has often been neglected in comparison to medicinal plant research. Amphibian skin secretions are enriched with complex cocktails of bioactive molecules such as proteins, peptides, biogenic amines, alkaloids, guanidine derivatives, steroids and other minor components spanning a wide spectrum of pharmacological actions exploited for centuries in folk medicine.

This study presents evidence on the protein profile of the skin secretions of the canyon tree frog, *Dryophytes arenicolor, an* anuran from the Hylidae family, previously described as an ingredient used in Mexican Traditional Medicine practices. At the same time, it presents the reverse-phase liquid chromatography isolation, mass spectrometry characterization, identification at mRNA level and 3D modelling of a *novel* 58 amino acids Kunitz-like polypeptide from the skin secretions of *D. arenicolor*, **arenin**. To evaluate the bioactivity potential of arenin, cell viability assays were performed on HDFa, Caco-2 and MCF7 cells cultured with different concentrations of arenin. At 2 µg/mL of arenin, HDFa and Caco-2 cells showed a viability of 52.1%±2.86 and 108.8%±4.86, respectively. A viability shift was observed at 4 µg/mL of arenin, since HDFa and Caco-2 cells showed a viability of 100.74%±2.60 and 62.77%±1.69. This viability alternance continued being observed at 8 and 16 µg/mL of arenin, suggesting a multi-target interaction in an hormetic-like fashion.

This work demonstrates the lack of typical 12-50 amino acid long peptides in the skin secretions of *D. arenicolor* and proposes that arenin, one of its major constituents, plays a key role in its defense against predators. The hormetic response produced by arenin in cell proliferation assays requires further transcriptomic, metabolomic and proteomic research to unveil the mechanisms underlying the variable effect on cell viability observed at different concentrations of arenin.

Keywords: amphibians - skin secretions - *Dryophytes arenicolor* - Kunitz-like polypeptide - cytotoxicity.

Caracterización de las secreciones epidérmicas de *Dryophytes arenicolor* e Identificación de Arenina, un nuevo polipéptido tipo Kunitz.

por

Jesús Hernández-Pérez

Resumen

La zooterapia es el tratamiento de dolencias humanas con remedios hechos a partir de partes y derivados de animales. A pesar de su prevalencia en prácticas de la medicina tradicional de todo el mundo, la investigación de este fenómeno ha sido desestimada frecuentemente en comparación a la investigación realizada en plantas medicinales. Las secreciones dérmicas de anfibios están enriquecidas con mezclas complejas de moléculas bioactivas tales como proteínas, péptidos, aminas biogénicas, alcaloides, derivados de guanidina, esteroides y otros componentes menores que abarcan un amplio espectro de acciones farmacológicas que han sido aprovechadas por la medicina tradicional por siglos.

Este estudio presenta evidencia del perfil de las secreciones epidérmicas de la ranita de cañón, *Dryophytes arenicolor*; anuro de la familia Hylidae que ha sido descrito previamente como ingrediente utilizado en prácticas de la Medicina Tradicional Mexicana. Al mismo tiempo, se presenta el aislamiento por cromatografía liquida de fase reversa, caracterización por espectrometría de masas, identificación del ARN codificante y modelo 3D de un nuevo polipéptido tipo Kunitz de 58 aminoácidos procedente de las secreciones epidérmicas de *D. arenicolor*, **arenina**. Para evaluar el potencial bioactivo de arenina, se realizaron ensayos de viabilidad celular en las líneas celulas HDFa, Caco2 y MCF7 cultivadas en presencia de distintas concentraciones de arenina. Las células HDFa y Caco-2 tratadas con 2 µg/mL de arenina mostraron una viabilidad de 52.1%±2.86 y 108.8%±4.86, respectivamente. Inversión de la viabilidad fue observada en las células HDFa y Caco-2 tratadas con 4 µg/mL de arenina, mostrando una viabilidad de 100.74%±2.60 y 62.77%±1.69, respectivamente. Esta alternación de la viabilidad continuó siendo observada a 8 y 16 µg/mL de arenina sugiriendo una interacción multi-objetivo de acuerdo a una relación del tipo hormética.

Este trabajo demuestra la ausencia de péptidos defensivos típicos en las secreciones epidérmicas de *D. arenicolor* y propone que arenina, uno de sus constituyentes mayores, ejerce un papel defensivo contra depredadores. La respuesta hormética producida por arenina en los ensayos de viabilidad celular requiere profunda investigación transcriptómica, metabolómica y proteómica para elucidar los mecanismos moleculares responsables del efecto variable en la viabilidad observado a diferentes concentraciones de arenina.

Palabras claves: anfibios - secreciones epidérmicas - *Dryophtes arenicolor* - polipéptido tipo Kunitz - citotoxicidad.

List of Figures

List of Tables

Contents

Chapter 1

1. Introduction

Natural science comprehends the observation and study of the ways in which nature works. Consequently, through centuries scientists have gathered empirical knowledge of the biological and physical world in order to provide a better understanding of the Universe [1]. Throughout human history, people have used various materials from nature to cure their illnesses and improve their health. Traditional human populations have a broad natural pharmacopeia consisting of wild plant and animal species. According to the World Health Organization, 80 percent of the developing world's rural population depends on traditional medicines for its primary healthcare needs [2]. In many parts of the world, traditional medicine is the preferred form of health care, and remains the most available and affordable form of therapy in low income countries. For thousands of years, Nature has been the source of medicinal agents and has provided a scaffold for the development of modern drugs, many of them based on their use in traditional medicine [3].

The use of biological resources for various therapies has been documented in many different parts of the world [4–8]. The phenomenon of zootherapy, the treatment of human ailments with remedies made from animals and their products, is marked both by a broad geographical distribution and very deep historical origins, that even in modern societies constitutes an important alternative among many other known therapies practiced worldwide [3]. Despite its prevalence in traditional medical practices worldwide, medicinal animals' research has received little attention from ethnobiologists and anthropologists in comparison to medicinal plant research. It is only within the past few decades that an awareness of the variety and importance of nonbotanical remedies has emerged [9]. Regardless of the recent surge in publications about zootherapeutics, the subject is still far from being well covered, and even more distant from being exhausted. The lack of zootherapeutic studies has contributed to an underestimation of the importance of zootherapeutic resources [10].

Heparin, a strongly charged polysaccharide anticoagulant isolated from canine liver in 1922 by Howell and McLean [11], is an example of how the zootherapeutic research could shed light on effective drugs. Literature before 1916 abounds with substances from animal tissue that inhibit blood clotting and that sometimes, with hindsight, have been interpreted as being due to heparin [12]. During the first half-century after its discovery, heparin developed into a readily available

useful medicine, recognized as a heavily sulfonated polysaccharide known to require plasmatic antithrombin for its action.

The world is facing a massive loss of wildlife due to anthropogenic factors such as: habitat loss/ fragmentation, overexploitation, and introduction of invasive species and diseases. Transformation of ecosystems through human activities has been putting severe constraints on the availability and accessibility of plant and animal species used for medicinal purposes. Regrettably, the demand created by traditional medicine is one of the causes of the overexploitation of the wild population of numerous animal species [2]. One of the major negative consequences of this trend is that there will be essentially a reduction in the sources of zootherapeutic agents for the future development of medicines.

Amphibians are unique among vertebrates in requiring both aquatic and terrestrial habitats for their life cycle. For this reason they have developed highly evolved immune defenses to survive in a variety of conditions [13]. As many other members in the animal kingdom, adaptive and innate immune systems are defense lines that protects amphibians from external harm. As part of their adaptive immune response, antibodies and T-lymphocyte-mediated reaction acts in response to detection of pathogens by specialized cells with antigens displayed in their surface. On the other hand, macrophages, neutrophils, complement-mediated lysis of pathogens, natural killer cells and skin secretions comprise the innate immune mechanisms used by amphibians [14]. Over millions of years, amphibians have refined a multifunctional skin that is morphologically and biochemically adapted to accomplish general physiological functions such as water regulation and respiration, and, at the same time, it is equipped with highly-specialized dermal granular glands, also known as poison glands, capable of synthesizing and storing a plethora of bioactive compounds focused on host defense against predators and pathogenic microorganisms [15,16].

As amphibians spend a significant part of their life in contact with water, it is not surprising that they have evolved dermal granular glands specialized in the synthesis and storage of chemical defenses capable to halt microorganism's infection. Typical defensive antimicrobial peptides have been demonstrated to inhibit growth of – or even kill – bacteria and fungi through damage of their cell membrane and cell wall [17]. Another mechanism of amphibian defense against microorganisms is through the delivery of molecules to the skin surface to inhibit the activity of pathogen secreted proteases targeted to damage host tissue and promote infection [18]. On the other hand, threats faced by amphibians are not exclusively pathogenic, in some anurans noxious chemicals have been proposed to have a role in host defense against predators. An alkaloid

steroid toxin named batrachotoxin isolated from the skin secretions of the dart-poison frog *Phyllobates aurotaenia* is an example of chemical defense against predators. Batrachotoxin have been described as a potent toxin able to cause ventricular fibrillation and neuromuscular toxicity in the form of flaccid paralysis and seizures through inactivation impairment of voltage gated Na^+ channels, holding open the channels persistently [19]. Chemical predator defenses of proteic nature have been also suggested, such is the case of anntoxin, a kunitz-like polypeptide from *Hyla annectans* that have been demonstrated to, as batrachotoxin, inhibit voltage gated Na^+ channels and whose toxicity have been tested against insect, snake, bird and mouse [20].

Research on characterization of bioactive peptides and proteins from anurans have provided scientific data supporting the usage of animal derived products in traditional therapies [3]. In China, more than 1500 animals are used as sources of drugs. In India 15–20% of the Ayurveda medicine is based on animal-derived substances. In Latin America 584 medicinal animal species have been recorded [21]. México has a great biodiversity of fauna, accounting for about 10% of the reported biological species on the planet and ranks first place in terms of reptiles with 717 species recorded of which 50% are endemic, second in mammals with 491 species, fourth in amphibians with 290 species and tenth in birds with 1054 species [3]. In Mexico, over 100 animals have been described in ethnopharmacological studies as part of Mexican Traditional Medicine (MTM) practices used since pre-Colombian times [8,22]**.** Research on this area could help expand our knowledge about the natural pharmacopeia that our ancestors used to treat diverse illnesses and to provide scientific support behind its usage. However, many factors such as habitat destruction due to human activities, spread of diseases among animal species and the illegal trade have contributed to the decrease of anurans' populations [23]; emphasizing the importance of research focused on describing the activity and potential applications of animal-derived molecules may help to understand its ecological importance and therefore promote conservation policies to reduce species extinction.

The work presented in this dissertation is focused on the isolation and characterization of a Kunitz-like polypeptide from the skin secretions of an amphibian that has been described in the indigenous knowledge recognized as Mexican Traditional Medicine. This research intends to provide scientific evidence to support the usage of the skin of *Dryophytes arenicolor* by inhabitants of indigenous communities in Mexico through elucidation of the molecular participants behind the effects associated with its use. Moreover, the purpose behind the molecular and biochemical characterization of the bioactive compounds in the skin secretions of *D. arenicolor* is to provide knowledge about its potential applications and genetic information that will allow its heterologous

expression to expand its bioactivity research as part of a drug design platform that avoids the unnecessary killing of animals for isolation of bioactive compounds. In a broad sense, this work aims to serve as a research scaffold that allows the investigation of more bioactive compounds derived from animal sources.

1.1 Hypothesis

Due to the high species diversity of amphibians, a potentially enormous array of bioactive molecules that have not been described yet, frogs and toads (anuran) skin secretions are an active area of research interest in the discovery of novel biologically active molecules [17,24]. Although peptides of 10 to 48 residues long comprise the majority of biomolecules described in anurans [17], a considerable number of species from distinct families have been described to lack peptides in their skin secretions [18,25–27].

The vast majority of the bioactive peptides and proteins described belong to the subfamilies Pelodryadinae and Phyllomedusinae, even though the subfamily Hylinae has the widest distribution and the most species [28,29]. From the Hylinae subfamily, the Hyla/Dryophytes genus comprises 35 species from which antimicrobial peptides, neuropeptides, wound-healing peptides, antinociception peptides, protease inhibitor peptides, tryptophyllins and caeruleins have been described [17].

Based on the evidence of the presence of bioactive peptides in amphibian skin secretions and taking advantage of the enormous biodiversity in Mexico, we selected a member of the hylinae subfamily that has been mentioned in ethnopharmacological studies as providing an ingredient used in Mexican Traditional Medicine (MTM) practices [8,22], to study its skin secretions. Here we present the first report about the characterization of the skin secretions of *Dryophytes arenicolor.*

From these points, the hypothesis tested through the experimental work presented in this document is:

- It is possible to isolate, identify and characterize of at least one bioactive polypeptide from the skin secretions of *Dryophytes arenicolor.*

1.2 Dissertation objectives

The main objective of this dissertation is to isolate, identify and characterize a bioactive molecule from the skin secretions of *D. arenicolor*. To systematically test the hypothesis presented and satisfy the main objective, the following specific objectives are stated for the present work:

1. Collect *D. arenicolor* specimens and recover their skin secretions *via* norepinephrine stimulation.

2. Determine the protein profile of the skin secretions of *D. arenicolor* through 2D-PAGE and RP-HPLC.

3. Develop a fractionation method to purify the most abundant compounds from the skin secretions of *D. arenicolor* using semi-preparative RP-HPLC.

4. Assess the potential antiproliferative activity of the HPLC-purified fractions.

5. Characterize the structure of the bioactive fractions through Mass Spectrometry.

6. Identify the encoding cDNA to validate the data obtained with Mass Spectrometry through sequencing of the mRNA isolated from skin secretions.

1.3 Dissertation structure

Here we present the first report about the characterization of the skin secretion of *Dryophytes arenicolor*, formerly known as *Hyla arenicolor* [30], a frog with an atypical skin secretions profile due to the absence of low molecular weight peptides and a preliminary activity characterization of its most abundant fraction.

This dissertation is divided into 5 chapters. **Chapter 1** gives an introduction focused on the importance of studying zootherapeutic agents, since they could serve as scaffolds for the development of modern drugs. Furthermore, the hypothesis, general objective and specific objectives of the present research work are described.

Chapter 2 presents a general background about the research done on amphibian skin secretions. Basic information on *D. arenicolor* is presented as well as elemental background on protease inhibitors since the polypeptide isolated from the skin secretions of *D. arenicolor* exhibits a domain corresponding to this family of proteins. A summary on the state of the art of the main techniques used through this investigation is also reviewed.

Chapter 3 details the methodology employed over the course of this research, comprising: Specimen collection and its genetic identification, recovery of skin secretions and its profiling through analytical techniques, isolation of abundant proteins and assessment of its effect on cell proliferation assays, structural characterization, identification of protein encoding mRNA(s) and 3D structure modelling of the bioactive polypeptide isolated.

Chapter 4 includes the results and discussion developed from the characterization of the skin secretions of *D. arenicolor,* isolation of the bioactive polypeptide and its behavior observed in cell proliferation assays are attended. Results presented in this chapter were published in the International Journal of Molecular Sciences under the title: Identification of Arenin, a Novel Kunitz-Like Polypeptide from the Skin Secretions of *Dryophytes arenicolor*, accepted 19 November 2018.

In **Chapter 5**, conclusions and future work based on the observations made through this research are presented.

In the Appendix section, abbreviations used through this text, a supplemental table and figures about the structural characterization of the polypeptide isolated from the skin secretions of *D. arenicolor* are shown along with the references supporting this dissertation. A Personal *Vitae* and the article describing this research published on November 19th, 2018 in the International Journal of Molecular Sciences (Hernández-Pérez, J.; Serra, A.; Sze, S.K.; Conway, P.L.; Schlundt, J.; Benavides, J. Identification of Arenin, a Novel Kunitz-Like Polypeptide from the Skin Secretions of *Dryophytes arenicolor*. *Int. J. Mol. Sci.* **2018**, *19*, 3644.) are also included in the Appendix.

Chapter ¡Error! No se encuentra el origen de la referencia.

2. Background

The anuran skin presents morpho-functional and behavioral protective adaptations against several adverse factors in the terrestrial environment. The cutaneous glands present in the skin play an essential role in respiration, reproduction, protection against desiccation and defense against predators and infection by microorganisms on the body surface. Secretions produced by these glands have a key role in host protection given by its complex chemical composition with noxious or toxic substances with diverse pharmacological effects, which constitute an important source of biologically active compounds against bacteria, fungi, protozoa, and viruses [31].

Amphibian granular glands (**Fig. 2.1**) are syncytial structures of smooth muscle cells innervated by sympathetic nerves. Following alarm or injury, the sympathetic nervous system is activated, adrenergic receptors are stimulated, and the contents of the gland are released to the surface of the skin [14,32]. Skin secretions have been demonstrated to contain a range of different classes of pharmacologically active molecules such as proteins, peptides, biogenic amines, alkaloids, guanidine derivatives, steroids and other minor components spanning a wide spectrum of pharmacological actions exploited for centuries in folk medicine [16].

By far, peptides of 10 to 48 residues long are the most studied molecules derived from amphibian skin secretions with over 100 families of more than 2000 peptides. These peptide families include antimicrobial peptides, myotropical peptides, opioid peptides, corticotrophin-releasing peptides, angiotensins, protease inhibitor peptides, neuropeptides, antioxidant peptides, lectins, insulin-releasing peptides, mast cells degradation/histamine-releasing peptides, wound-healing peptides, immunomodulatory peptides, neuronal nitric oxide synthase inhibitors, antiviral peptides, antitumor peptides, antiparasitic peptides, pheromone peptides, granains and other peptides [17]. Due to the vast amphibian biodiversity, an enormous array of bioactive molecules with diverse applications that have not yet been described, frogs and toads (anuran) skin secretions continue to draw attention as a sources of novel biological active molecules [17,24]. Although peptides comprise the majority of biomolecules described in literature [17], a considerable number of species from distinct families have been described to lack peptides in their skin secretions [18,25–27].

Figure 2.1. Amphibian skin structure

A) Frog skin cross section with epidermis and dermis layers annotated, poison or granular glands produce and store noxious or toxic skin secretions, mucous glands waterproofs the skin, chromatophores or pigment cells affect skin color changes and blood vessels irrigates the skin tissue [33]. **B)** Scanning electron microscopy (SEM) image of a funnel-type gland outlet in the dorsal skin of *Hyla arborea*. The surface of the cells shows many micro-ridges (x 7000 magnification) [34].

Hylidae is one of the largest families of anurans with over 870 species recognized and is considered a rich source of amphibian bioactive peptides. The vast majority of the bioactive peptides and proteins from skin secretions described belong to the Pelodryadinae and Phyllomedusinae subfamilies even though the Hylinae subfamily has the widest distribution and the most species [28,29]. From the hylinae subfamily, the Hyla genus, recently divided into Old World (Hyla) and New World (Dryophytes) subgenera [30], comprises 35 species from which antimicrobial peptides, neuropeptides, wound-healing peptides, analgesic peptides, protease inhibitor peptides, insulin releasing peptides, smooth muscle stimulation peptides have been described [17]. Based on the vast evidence describing the presence of bioactive peptides in amphibian skin secretions, and taking advantage of the enormous biodiversity in Mexico, we decided to study the skin secretions of the canyon tree frog *Dryophytes arenicolor*, a member of the Hylidae family that has been mentioned in ethnopharmacological studies as an ingredient used in Mexican Traditional Medicine (MTM) practices [8,22], whose skin secretions have not been studied previously and may contain bioactive compounds targeted to host defense that could also have potential therapeutic applications .

2.1 *Dryophytes arenicolor*

The canyon tree frog, *Dryophytes arenicolor* **(Fig. 2.2)** belongs to the Hylidae family, subfamily Hylinae and was transferred in 2016 by Duellman *et al.*[30] from the genus Hyla to the recently resurrected genus Dryophytes.

D. arenicolor adult frogs display a snout vent length (SVL) around 32 to 57 mm. It has rough warty skin which prevents desiccation. Webbing is well developed but does not extend to the hind leg's fifth toe. Toe pads are considerably enlarged. It is distinguished from similar species by having a dark-edged light spot beneath the eye, instead of a dark bar running through the eye. Dorsal coloration is brown to gray and randomly spotted, while ventral coloration is cream to orange-yellow. This coloration aids in its ability to camouflage. When exposed to sun, the dorsal coloration changes from being normally dark to a light green [35]. Adults feed on a variety of insects including beetles, ants, spiders, centipedes and caterpillars, meanwhile larvae eat suspended matter, organic debris, algae, and plant tissue[36]. Breeding period ranges from March to July but can be extended due to insufficient rainfall until August. Vocal calls are hollow, nasal, and explosive, lasting only 1-3 seconds. They are inactive in cold temperatures and hot, dry weather when it retreats to rock cervices. They are most active at night but can be observed among rocks in stream courses diurnally.

Figure 2.2. *Dryophytes arenicolor.* (Jesus Hernández-Pérez, 2016)

D. arenicolor is found at near sea level to about 3,000 m above sea level (asl) in a 200,000 – 2,500,000 km^2 area from (**Fig. 2.3**) northwestern Oaxaca, southwestern Puebla, northern Guerrero, northern Michoacán, through Morelos, Estado de Mexico, Tlaxcala, Querétaro, Guanajuato, western Hidalgo, southwestern San Luis Potosi, southern Aguascalientes, eastern

Jalisco, eastern Nayarit, eastern Sinaloa, western Durango, western Zacatecas, western Chihuahua and eastern Sonora in Mexico to western and southeastern Colorado and southern Utah, through Arizona and Western New Mexico in the USA. Its habitat ranges from arid environments to streambanks and it breeds in pools along canyon-bottom streams. This frog requires temporary or permanent pools in rocky arid scrub and mountains. It can be found in trees and clinging to boulders and along intermittent or permanent streams in semi-arid grassland, tropical scrub forest, pinon-juniper and pine-oak woodlands [36].

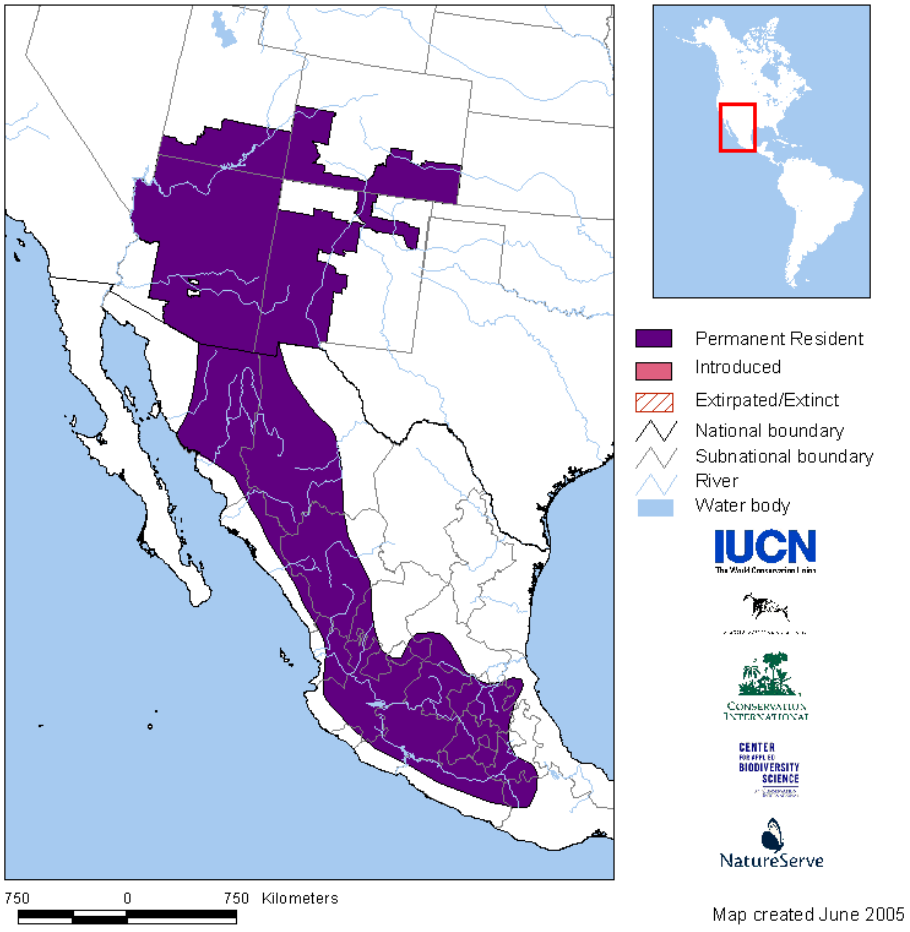

Figure 2.3. *D. arenicolor* distribution

Range Map Compilers: IUCN, Conservation International, NatureServe, and collaborators, 2004 [36].

With an estimated population size of 100,000 – 1,000,000 individuals and according to the Red List of International Union for Conservation of Nature (IUCN), *D. arenicolor* is listed as Least concern (LC) since it is a non-threatened species whose populations is believed to be stable. Also,

since it occurs in a wide variety of habitats and part of its range includes Biosphere Reserves and Natural parks, no extraordinary conservations actions are needed so far [37].

Previous research on *D. arenicolor* have described its complex evolutionary history characterized by several phylogeographically distinct lineages, a probable cryptic species, and multiple episodes of mitochondrial introgression with the sister group, the *Hyla eximia* complex [38,39] and its hormonal-dependent skin reflecting platelets [40]. Also, *D. arenicolor* individuals have been used in experiments to assess the mechanisms of thermoregulation and water uptake by the skin [41]. Before this study, there are no scientific reports about the skin secretions of *D. arenicolor*.

2.2 Protease Inhibitors

Proteases and their inhibitors are ubiquitous molecules within biological systems involved in the regulation of a plethora of fundamental functions. Proteases are generally classified according to the key catalytic amino acid residue within their active sites (serine, cysteine, threonine, aspartic acid) or based on the requirements of cofactors essential for catalytic activity (metalloproteases). Serine proteases are one of the most widely studied grouping of proteins; they are involved in key regulatory processes such as peptide hormone precursor processing and release, blood coagulation, complement fixation and additionally, they are intimately involved in the pathogenesis of numerous diseases, including cancer, pulmonary emphysema and inflammation [42]. Inhibitors of this class of proteases act by binding to their cognate enzyme in a substrate-like manner forming a stable complex. Likewise, protein-based protease inhibitors (PIs) can be classified according to the presence of a defined structural motif (Kunitz, Kasal and Bowman-Birk) or to reflect the actual class of protease that they inhibit (cystitis, serpent, and tissue inhibitors of metalloproteases, TIMPS) [43]. PIs widely found in animals, microorganisms and plants are known to play key roles in the etiology and treatment of human pathologies such as cancer, inflammation and hemorrhage based on their capacity to inhibit the catalytic activity of proteolytic enzymes [44]. In addition to their anti-protease activity that could protect the host against a range of extrinsic proteases, PIs have been demonstrated to exhibit other intrinsic activities that contributes to termination of inflammatory process, including modulation of cytokine expression, signal transduction and tissue remodeling [45].

Many protease inhibitor peptides and polypeptides smaller than 10 kDa have been identified from amphibian skins, primarily Bowman-Birk inhibitors in the skin secretions of ranid frogs and Kunitz inhibitors in the skin secretions of both, toads and frogs [46]. HV-BBI from *Huia versabilis*, pYR

from *Rana sevosa* and pLR from *Lithobates pipiens*, members of the ORB family, identified as Bowman-Birk-like trypsin inhibitors, share a highly conserved precursor structure of 65-70 aa, including a highly conserved N-terminal signal peptide before an acidic aa-rich domain and a mature peptide domain located at the C-terminus. Comparisons of mature peptide sequences show that they have a conserved GCWTKSXXPKPC motif [43].

Most amino acid sequences presenting the Kunitz/bovine pancreatic trypsin inhibitor (BPTI) family domain (also known as the MEROPS inhibitor family 12, clan 1B)[47] inhibits proteases of the S1 family and are restricted to the metazoa. They are short (57 to 60 residues) alpha/beta proteins with few secondary structures, no overall conservation of amino acids, one reactive loop and typically the fold is constrained by 3 disulfide bonds in a conserved pattern: -----C-------CBZXXXXXCXXXXXXYXXXCXXC----------C (where X is any aa and - is a gap). The type example for this family is aprotinin (BPTI), but the family includes numerous other members such as dendrotoxins from mamba (Dendroaspis) snake venoms [48], the mammalian inter-alpha-trypsin inhibitors [49]; a domain found in an alternatively-spliced form of Alzheimer's amyloid beta-protein [50]; domains at the C-termini of the alpha (1) and alpha (3) chains of type VII and type VI collagens [26]; and tissue factor pathway inhibitor precursor [51]. Kunitz-type PIs isolated from amphibian skin secretions include BSTI, BMTI, BOTI and BVTI from *Bombina bombina, Bombina maxima, Bombina Orientalis* and *Bombina variegata* [52], PSKP-1 and PSKP-2 from *Phyllomedusa sauvagii* [17], anntoxin from *Hyla annectans* [20], anntoxin S-1 and anntoxin S-2 from *Hyla simplex* [53]. A kunitz-type trypsin inhibitor isolated from the skin secretions of *Dyscophus guineti*, a species which apparently does not produce classical antimicrobial peptides, was proposed to play a key role as an anti-infective agent [18,54].

Aprotinin, a serine protease inhibitor containing a single Kunitz-type domain, has been used since 1960s to treat acute pancreatitis and later was implemented as a hemostatic agent in cardiac surgery after demonstration of its capacity to inhibit activation of endothelial cells by thrombin and further downstream inflammatory responses in *vitro* via protection of the high-affinity thrombin receptor protease-activated receptor 1 (PAR1) [55]. Also, aprotinin has demonstrated capability to inhibit intracellular signaling via p42/44 mitogen-activated protein kinase (MAPK) and Egr-1, as well as interleukin-6 (IL-6) secretion due PAR1 activation by thrombin [56]. PAR1 activation by trypsin, thrombin and matrix metalloproteinase-1 mediates adverse events, such as proinflammatory responses, angiogenesis, cell invasion, and neurodegeneration; thus, antagonism of PAR1 may have broad therapeutic significance [45].

In addition to its ability to inhibit trypsin, Kunitz-like PIs such as anntoxin from *H. annectans* has been identified as an inhibitor of neuronal tetrodotoxin-sensitive (TTX-S) voltage-gated sodium channels (VGSC) with an IC_{50} value of 3.4 μM in rat dorsal root ganglion neurons, proposing an antinociceptive application for anntoxin based on VGSCs role in electrical signaling in almost all kinds of excitable tissues [20]. Furthermore, anntoxin has shown anti-inflammatory effects in a dose-dependent relationship in a model of carrageenan-induced edema of mice through the inhibition of COX-2 and TNF-α levels (Up to 20% and 50% respectively at 2.5 mg/kg body weight) [57].

2.3 Current strategies for the isolation and identification of peptides and proteins from amphibian origin.

From an evolutionary point of view, tetrapod vertebrates included in the Amphibia class are of interest due to their biphasic life stages. This has likely led to the development of highly specialized and diverse molecules aimed for their protection from microorganisms, parasites, predators and physical factors. In the 1980s amphibian skin secretions began to draw attention as one of the most abundant sources of diverse bioactive molecules in nature. Characterization of the peptides in the skin secretions of the African clawed frog, *Xenopus laevis,* led to the discovery of molecules with unique chemical properties, biosynthesis pathways and potential clinical applications [58–60]. Since then, bioactive components of amphibian skin secretions have been extensively studied, aiding the exploration of the structures and biological functions of bioactive molecules from natural sources that could serve as scaffolds for development of new therapeutic agents.

In the post-genomic era, the field of proteomics has experienced a rapid growth driven by the need to identify new biomarkers, targets for drug delivery and potential therapeutic drugs. This interest has driven the progressive development and refinement of the methodology used to study the proteomic identity and profile of cells and tissues. In the following lines, a brief description of the most commonly used techniques in the field of protein characterization such as sample preparation, different types of polyacrylamide gel electrophoresis (*i.e.,* 1D and 2D- Tris-glycine and Tris-Tricine-PAGE), Liquid Chromatography (*i.e.,* ion exchange, reverse-phase, hydrophobic interaction), Mass Spectrometry (*i.e.,* Electrospray ionization Ion-Trap, Matrix-assisted laser desorption/ionization Quadrupole-Time-of-Flight) and cDNA cloning are presented.

2.3.1 Sample preparation

Before purification of a peptide or protein from tissue can be achieved, the molecule of interest must be efficiently solubilized, preferably in its biologically active form, however there is no "universal solvent" that can accomplish this. Homogenization or recovery medium must extract the peptide from tissue in high yield while simultaneously inactivating proteolytic enzymes in the tissue that would otherwise cause a rapid degradation, *e.g.*, for neutral and cationic molecules that are thermally unstable such as proteins that contain multiple disulfide bonds, homogenization in acidified ethanol (ethanol/0.7 M HCl; 3:1 vol/vol) at 0ºC is recommended [61]. This solvent is particularly favorable with very hydrophobic neuropeptides such as neurokinin B and with membrane-active α-helical antimicrobial peptides commonly found in amphibian skin [62]. On the other hand, for neutral and cationic peptides that are relatively hydrophilic and thermally stable, boiling in 1 M acetic acid is recommended. Nonetheless, this solvent is inefficient in the case of acidic peptides, such as gastrin and CCK-8, and so in this case, boiling water is the procedure of choice [63]. In the case of bioactive peptide and proteins whose physicochemical properties are completely unknown, preliminary experiments must be carried out using different extraction procedures to determine which is the most efficient in solubilizing biological activity that characterizes the peptide.

In proteomic research, after recovery of a crude extract for analysis, samples must be conditioned to be suitable for the analytical and downstream processing methodologies, since crude extracts may contain materials that bind irreversibly to expensive HPLC columns, resulting in a rapid deterioration of their resolving power and reproducibility. Consequently, concentration and partial purification of peptides and proteins from initial extracts on Sep-Pak C18 cartridges prior to analytical applications are strongly advised. This procedure also removes salts and acid from the extraction supernatant, which may also damage HPLC columns and interfere with PAGE and MS. Peptides and proteins that occur in soluble form in biological fluids such as plasma, urine, snake venoms and amphibian skin secretions can be concentrated directly on Sep-Pak cartridges without the need for a solvent extraction step. The capacity of Sep-Pak C18 cartridges to isolate peptides and proteins depends on several factors including the total volume and the hydrophobicity of the peptides and proteins. Overloading will result in sample breakthrough and loss of molecules of interest, however it is possible to increase isolation capacity by using multiple cartridges connected in series [61]. Avoidance of sample dilution is one of the main advantages of using C18 cartridges for sample preparation over the use of dialysis cartridges. On the other hand, C18 cartridges are preferred over the use of rotary evaporators and freeze-drying process

since through these techniques only sample concentration is achieved but impurities are also retained.

2.3.2 Polyacrylamide Gel-based protein separation

Glycine-SDS-PAGE (also known as Laemmli-SDS-PAGE [64]) and Tricine-SDS-PAGE, based on glycine-Tris and Tricine-Tris buffer systems, respectively, are the commonly used SDS electrophoretic techniques for separating proteins. The acrylamide gels used are often characterized by the total percentage concentration (%T) of both monomers (acrylamide and the crosslinker bisacrylamide) and the percentage concentration of the crosslinker (%C) relative to the total concentration. For simplicity, it is commonly abbreviated *i.e.* 12%T, 3%C gels as 12% gels. Together, Laemmli-SDS-PAGE and Tricine-SDS-PAGE cover the protein mass range 1-500 kDa. Tricine-SDS-PAGE is used preferentially for the optimal separation of proteins <30 kDa, and Laemmli-SDS-PAGE for proteins > 30 kDa. The different separation characteristics of the two techniques are directly related to the strongly differing pK (acid dissociation logarithmic constant) values of the functional groups of Glycine and Tricine that define their electrophoretic mobilities as trailing ions relative to the electrophoretic mobilities of proteins [65]. Uniform acrylamide Tricine-SDS gels cover narrow mass ranges – for example, 10% gels cover the range 1-100 kDa ad 16% gels cover the range 1-70 kDa – and offer high resolution, especially for the small protein and peptide range. Doubling the crosslinker concentration by using 16% T, 6% C gels and including 6 M urea in these gels increases the resolution of small proteins further. These uniform acrylamide Tricine-SDS gels are almost exclusively used to separate very small proteins and peptides. Uniform high-acrylamide Laemmli gels cannot be used to access the small protein range because the stacking limit in the Laemmli system is too high, and small proteins usually appear as smearing band near the gel front. In a less convenient way, however, the small protein and peptide range can be accessed by making use of gradient gels that continuously *destack* proteins according to decreasing mass during electrophoresis (*i.e.,* 8-16% and 10-27% acrylamide gels for the ranges 6-250 kDa and 2-200 kDa, respectively).

A common separation step in proteomic research is two-dimensional polyacrylamide gel electrophoresis (2D-PAGE), based on an orthogonal approach applied to separate proteins according to their isoelectric point and molecular weight in a high-resolution able to yield focused spots of protein, which can be cut out and the protein-containing gel plug is then digested with trypsin for further structure characterization. At the very beginning of the 1970s, two high-performance electrophoretic separations of proteins were available: i) zone electrophoresis of

proteins in the presence of SDS, as described in its almost final form by Laemmli [64], a technique that instantly became very popular and ii) denaturing isoelectric focusing, as described for example by Gronow and Griffith [66]. As these two techniques used completely independent separation parameters (molecular mass and isoelectric point, respectively) it is not surprising that it was soon tried to couple them. The first successful report in 1974 [67] got almost unnoticed, because the difficult method of sample inclusion in the isoelectric focusing (IEF) gel was used [68]. 2D-PAGE has the capacity to separate, visualize and quantify several thousand of proteins in a single gel from a complex biological sample, *i.e.* allowing the large-scale analysis of protein expression differences. Gel-to-gel variability has been largely improved thanks to the use of immobilized pH gradient (IPG) strips and robust staining protocols. But even now, IEF in the alkaline region is considered a challenge to separate basic proteins by 2-DE and at the beginning of the proteomic era, most of gel-based proteomic studies were performed in the acidic range.

Basic proteins are difficult to separate in the first dimension, isoelectric focusing, for several reasons. At pH above 8, polymerized acrylamide gel is unstable, and can degrade, therefore it is very important to use only fresh strips stored at a correct temperature. Degradation of acrylamide can be visualized when the plastic part of the dry strip glues to the acrylamide gel part, with a tendency to twist [69]. Another common issue when electro-focusing in the basic pH region is the presence of hydroxide ions in the IPG-strips causing electro-osmotic pumping from the cathode towards the anode with the result that water present in the cathodic paper wick is pumped into the IPG-strip, leading to a gap characterized by a zone of streaking and poorly focused proteins close to the cathode. This gap can be avoided by the use of solutions containing urea in the cathodic electrode wick [69]. Finally, at basic pH, it is mandatory to keep the redox status for cysteines using reducing agents such as dithiothreitol (DTT) to limit unspecific oxidation of protein thiol groups. However, since DTT is a weak acid, it is transported out of the basic part of the IPG strip during focusing. This migration of DTT towards the anode during IEF at basic pH results in depletion of DTT at the cathode leading to reformation of intra- and inter-molecular disulfide bridges due to the oxidation of sulfhydryl groups [68], causing proteins within the sample to become less soluble, leading to horizontal streaking within the gels and thus poor resolution of the basic proteins [70]. Different approaches such as sample application methods (anodic cup-loading, in gel rehydration, or paper-bridge loading), and use of *destreak* solutions as the combination of isopropanol and glycerol in the rehydration buffer have been reported to improve the focusing of proteins in the alkaline range in IPG strips [71].

Protein bands containing a minimum of 0.2 µg of protein are suitable for Coomassie staining. The staining intensities can be used to estimate the molar ratios of the protein subunits of multiprotein complexes, except the very hydrophobic subunits that stain very poorly [65].

2.3.3 High Performance Liquid Chromatography

The past five to six decades have seen a remarkable reduction in the amount of time and effort required for the purification and characterization of biologically active molecules from animal tissues and other natural sources. During the 1950s and 1960s, such processes required industrial-scale facilities and astounding planning. For example, the laboratory of Jorpes and Mutt [72] processed more than 10,000 hog duodena to purify the gastrointestinal hormone secretin, and the laboratories of Guillemin [73] and Schally [74] extracted approximately 500,000 sheep and pig hypothalami, respectively, to isolate and characterize thyrotropin-releasing hormone. In contrast to these major achievements, a somewhat more trivial, but nevertheless, illustrative accomplishment, in 2001 the laboratory of Conlon purified and characterized the structure of neuropeptide Y (NPY) from the whole brain of the amphibian *Typhlonectes natans*, starting with only 270 mg of tissue in a procedure that took only 1 week [61,75].

Clearly, there have been important advances in the methodology of peptide and protein purification, and probably the most significant of these is the introduction of reverse-phase high performance liquid chromatography (RP-HPLC). Prior to the development of this technique, purification protocols involved highly inefficient procedures with low recoveries, such as selective precipitations and adsorption of materials on diatomaceous earths, coupled with low-resolution separation techniques, such as ion-exchange and gel permeation chromatography. Reversed-phase HPLC came into routine laboratory use in the late 1970s and combines high resolving power and recovery with relative ease and speed of operation [76]. Most small peptides and proteins (molecular mass <10,000 Da) are recovered from the RP-HPLC columns in high yield, particularly from those employing wide-pore silica packing materials; columns of 5 µm particle size and 300 Å pore size [61].

To purify a protein to apparent homogeneity from a complex mixture, some strategies involve sequential chromatographic columns containing different silica-based packing materials; for example, initial chromatography could be carried out on a preparative (2.2 cm x 25 cm) or a semipreparative (1.0 cm x 25 cm) n-octadecyl (C-18) column followed by chromatography on analytical (0.46 cm x 25 cm) n-butyl (C4) and diphenyl columns. This sequence of column use is recommended because the capacity of columns decreases in the order C18 > C4 > diphenyl [77].

C-18 columns usually provide excellent resolution for small (M_r < 5,000 Da), relatively hydrophilic peptides, but recovery and peak shape may not be optimal for larger, more hydrophobic proteins. In this case, the performance of C4 and diphenyl columns will be superior. Purification to near homogeneity (generally >98% purity) is accomplished by a final chromatography on an analytical (0.46 cm x 25 cm) C-18 or (0.21 cm x 25 cm) C-18 microbore column [61]. Purity can be assessed from a symmetrical peak measured at two absorbance wavelengths (214 and 280 nm) and by electrospray or MALDI-TOF mass spectrometry. Absorbance at 214 nm will detect all components that contain a -CONH- peptide bond, whereas absorbance at 280 nm will detect only peptides that contain a tryptophan and/or tyrosine residue [78].

Reversed-phase HPLC of peptides and proteins is carried out in the presence of an organic modifier and an ion-pairing reagent. For laboratory-scale separations, acetonitrile is the organic modifier of choice since this reagent has low absorbance at 214 nm and relatively high volatility for easy removal under reduced pressure. Gradient elution conditions are almost always used to facilitate peak sharpness, although isocratic elution may be necessary to resolve complex mixtures. Trifluoroacetic acid (TFA) is the most commonly used ion-pairing reagent at a final concentration of 0.12% (vol/vol) in the aqueous solvent, usually HPLC-grade water, and 0.10% (vol/vol) in the organic solvent. Like acetonitrile TFA has acceptable UV absorbance characteristics and is easily removed under reduced pressure. The use of TFA increases the sharpness and symmetry of peaks and may increase peptide solubility. Alternative ion-pairing reagents might be considered in a situation in which two peptides prove very difficult to resolve. In these cases, heptafluorobutyric (HFBA), at a final concentration of 0.05% (vol/vol), may be used in a final chromatography step instead of TFA [79]. Under these conditions, proteins are separated primarily based on hydrophobicity, and the retention times of peptides with less than 30-40 amino acid residues of known composition may be predicted with a high degree of accuracy [80].

Although reversed-phase HPLC can be used for the purification of peptides with a wide range of physicochemical properties, the technique has some limitations. Extremely hydrophilic peptides may bind only very weakly or not at all to the columns, and extremely hydrophobic peptides and proteins may be recovered only in low yield. In this case, two-dimensional separations based on orthogonal chemistries (*i.e.,* gel filtration followed by ion exchange chromatography steps, or ion exchange chromatography steps) are often considered. Such approaches are now playing an important role in “top-down proteomics” [81]. A range of columns based on polystyrene-divinylbenzene copolymer beads, derivatized for anion- or cation-exchange chromatography, are

available that are chemically stable in the pH range 1-13. It should be noted that the use of an organic solvent such as acetonitrile may result in irreversible denaturation of proteins and loss of biological activity. Similarly, the organic solvent may produce solubility problems that, in a worst-case scenario, can result in precipitation of material in the column with drastic loss of performance.

2.3.4 Mass spectrometry

The introduction of chemical protein sequencing by Peer Edman in the 1950s was a milestone in the development of protein research [82]. This method relies on the identification of amino acids that have been chemically cleaved in a stepwise fashion from the amino terminus of the protein [83]. At the beginning, LC was used for identification of Edman degradation products, gradually MS was introduced as alternative method to LC with optical detection. This was achieved in combination with early soft ionization techniques such as chemical ionization [84], field desorption [85], and fast atom bombardment [86]. Later, the progressive refinement of MS/MS techniques permitted the analysis of proteolytic peptides creating the basis for peptide sequencing by MS [87]. Within the last three decades, protein sequence determination by MS/MS became more and more powerful, a development driven mainly by the improvements of LC techniques in combination with Electrospray Ionization (ESI) and latter with Matrix-assisted Laser Desorption/Ionization (MALDI). The advantages of MS/MS techniques with respect to speed, sensitivity, and applicability to complex peptide mixture gradually led to the replacement of Edman techniques by LC-MS/MS. As a result, MS-based proteomic has emerged as the method of choice for the identification of proteins *via* database-supported interpretation of MS data using searches engines such as MASCOT [88], SEQUEST [89], X! TANDEM [90], or OMSSA [91].

Although all amino acid sequence combinations are theoretically possible, only a portion of these protein sequences are realized in nature, therefore a short peptide sequence is already highly protein-specific [87]. Proteomic research has taken advantage of this feature through the development of databases of probability-based annotated peptides MS/MS spectra leading to protein identification at high level of confidence from fragmentary sequence information [92]. Even though database-supported protein identification is very effective, it rules out the recognition of all peptides not present in the reference database. Despite the continuously growing sequence databases, *de novo* sequence of proteins, (peptide sequence prediction from MS data without assistance of a linear sequence database), is essential in several analytical situations such as in analyses of protein sequence variants of their spliced isoforms or in protein analysis from

organisms with unsequenced genomes. In addition, *de novo* sequencing is essential for analysis of peptides containing non-proteinic or modified amino acids.

Both, MS/MS and LC performance influences the utility of *de novo* sequencing mainly because the significance of peptide MS/MS data depends on the purity of the peptide ions selected for fragmentation. The introduction of soft ionization techniques enabled the efficient generation of intact peptide ions which can be selected as precursors for subsequent activation and detection of their fragment ions. For digested-peptides sequencing, positive ionization mode is generally used due to its higher sensitivity and since MS/MS spectra of protonated peptides contain a wealth of sequence-specific fragment ions [87]. Currently, most of peptide *de novo* sequencing has been performed using Collision-activated Dissociation (CID). In low energy CID, activation of molecular ions is achieved by collisions with inert gas molecules (He, N_2, Ar) contained in a separate collision cell or as bath gas in an ion trap. In CID, the translational energy of the ions is partially converted into internal vibrational energy which then induces peptide fragmentation. Acceleration of the precursor ions in the collision zone by a potential difference (collision off set) intensifies the fragmentation and leads to more second (or higher order) fragments, due to repeated collisions during the ions travel through the collision cell. Moderate collision offset values are most favorable for sequencing in terms of absolute fragment ion intensity and background level. For unmodified peptides, activation of protonated molecules leads primarily to backbone fragmentations, resulting in structure-specific fragments [83].

The reliability of peptide sequencing improves with increasing accuracy of the mass measurement, since the exact mass contains information about the elemental composition. Currently, several instrument types such as Fourier-transform ion cyclotron resonance (FT-ICR) and Orbitrap are available, providing MS analysis with a resolution in the range of 100,000-500,000 with mass accuracies in the range of 2-0.2 ppm. Such extreme mass accuracy has led to the development of composition-based *de novo* sequencing. This two-step procedure starts with calculation of a set of possible amino acid compositions based on the highly accurate mass value for a peptide molecular ion and its fragment ions. Based on the calculation of all mass value-compatible amino acid compositions, a database containing all permutations is generated. This database is then used for assignment of the MS/MS spectra [93].

Engines for *de novo* sequencing have undergone continuous improvement as tools for database-supported spectra interpretation [94]. Currently, all results provided by automated *de novo* sequencing should be checked manually. Since proteins of organisms with unknown genomes

often show sequence homologies to functionally related homologs in other already completely sequenced organisms, sequence databases are helpful to support the *de novo* sequencing results obtained from unknown proteins. In practice, peptide sequence candidates must be subjected to homology-based search programs such as Basic Local Alignment Tool (BLAST) to identify similarities to sequences present in databases. Bioinformatic tools are of high interest for further advancement of *de novo* peptide sequencing [95].

Shotgun proteomics, also termed bottom-up proteomics, focuses on the analysis of protein mixtures after enzymatic digestion of the proteins into peptides. On the other hand, top down proteomics focuses on the MS analysis derived from the fragmentation of complete (undigested) proteins [96]. In bottom-up proteomics, complete protein sequence may be obtained by MS alone by the implementation of different proteases. Each protease generates different sets of peptides so that overlapping sequences may be found, and longer continuous sequences can be obtained. In general, a sequence overlap of three amino acids is enough for stitching of two sequences, since mostly a three amino acid sequence motif is already unique for a protein of intermediate size (20-60 kDa) [87]. The combined used of trypsin (cleavage site at C-terminal of R and K), chymotrypsin (cleavage site at C-terminal of F,Y, L, W and M), AspN (cleavage site at N-terminal of D), GluC (cleavage site at C-terminal of D), LysC (cleavage site at C-terminal of K), LysN (cleavage site at N-terminal of K) and ArgC (cleavage site at C-terminal of R) is beneficial for this purpose due to their different cleavage characteristics at basic, neutral, or acidic sites [97].

Regarding the bottom-up approach, two phenomena that may cause errors in the primary sequence prediction should be considered. First, residues rearrangement processes during ion trap CID have been described [98]; second, protease catalyzed transpeptidation reactions have been observed, leading, *e.g.* to the transfer of terminal residues or to the ligation of originally distant sequence parts [99]. Peptide *de novo* sequencing results can also help to obtain protein sequences via molecular biology approaches. For instance, a cDNA library is constructed, and primers derived from *de novo* sequenced peptides are used for Rapid Amplification of cDNA-ends with polymerase chain reaction (RACE-PCR). Finally, the complete protein sequence can be identified using DNA sequencing.

2.3.5 cDNA cloning

In the past, acquisition of frog skin molecular libraries involved the killing of the frog and extraction of the dissected skin in organic solvents. This procedure was destructive, often requiring several hundreds of specimens, and choice of extraction medium was highly selective in terms of

component solubility. The introduction of the mild transdermal electrical- and norepinephrine-stimulation techniques revolutionized skin secretions acquisition by removing the need for specimen death and at the same time, by producing a more defined and molecularly complete secretion suitable for granular-gland secretory proteomic analyses [14]. After a full release, the granular gland needs to be totally regenerated before skin secretions can be released again, a process that can take longer than 3 weeks [100]. However, molecular-biological studies related to cloning of cDNA encoding granular-gland peptides and proteins still required killing of specimens and library construction from large amounts of excised skin. As with the original peptide extraction technology, this approach suffered from the two inherent disadvantages of specimen death and non-selective cDNA library construction, in addition to the fact that the granular glands in most species represent a minor cellular component of total skin.

The work of Chen and collaborators was pioneer on the recovery of nucleic acids from the skin secretions and transformed the proteomic research focused on granular glands from amphibians. In addition to the peptides and variety of other bioactive molecules, the granular gland secretions contain poly-adenylated messenger RNAs encoding the propeptides and proteins expressed in the secretions [101]. Since then, RNA has been isolated from skin secretions collected in field and in the laboratory, immediately preserved, often by snap freezing and lyophilization [100].

After recovery of skin secretions, mRNA can be isolated through different methodologies such as the use of oligo (dT) residues covalently coupled to the surface of magnetic beads to facilitate mRNA isolation [102]. The primary structures of novel proteins and peptides partially identified with MS could be confirmed by molecular cloning of their biosynthetic precursors using degenerate primers designed from the amino acid sequence predicted by the *de novo* algorithm. Rapid amplification of cDNA ends (RACE) can be used to identify full-length sequences of a gene if only part of its sequence is known; either amplifying the 5’ or the 3’ ends of genes. RACE primarily utilizes Reverse Transcriptase-Polymerase Chain Reaction (RT-PCR) and PCR to amplify the ends of transcripts starting with mRNA and cDNA, respectively [103]. For 3’RACE, oligo(dT) primers with adaptor tails are commonly used in the RT-PCR step. In the cDNA amplification step, gene specific primers (GSPs) or degenerate primers with adaptor tails are used to extend from the unknown 5’ end of the message back to the known poly(A) 3’ region that will be primed by the adaptor-tailed oligo(dT). Later, the PCR product can be purified and cloned for further sequencing and confirmation of the protein sequence can be obtained.

Chapter 3

3. Methodology

To accomplish the specific objectives, test the hypothesis defined in **Chapter 1** and according to the current strategies for the isolation and identification of peptides and proteins from amphibian origin described in **Chapter 2,** the methodology summarized in **Figure 3.1** is detailed in the following **Chapter 3.**

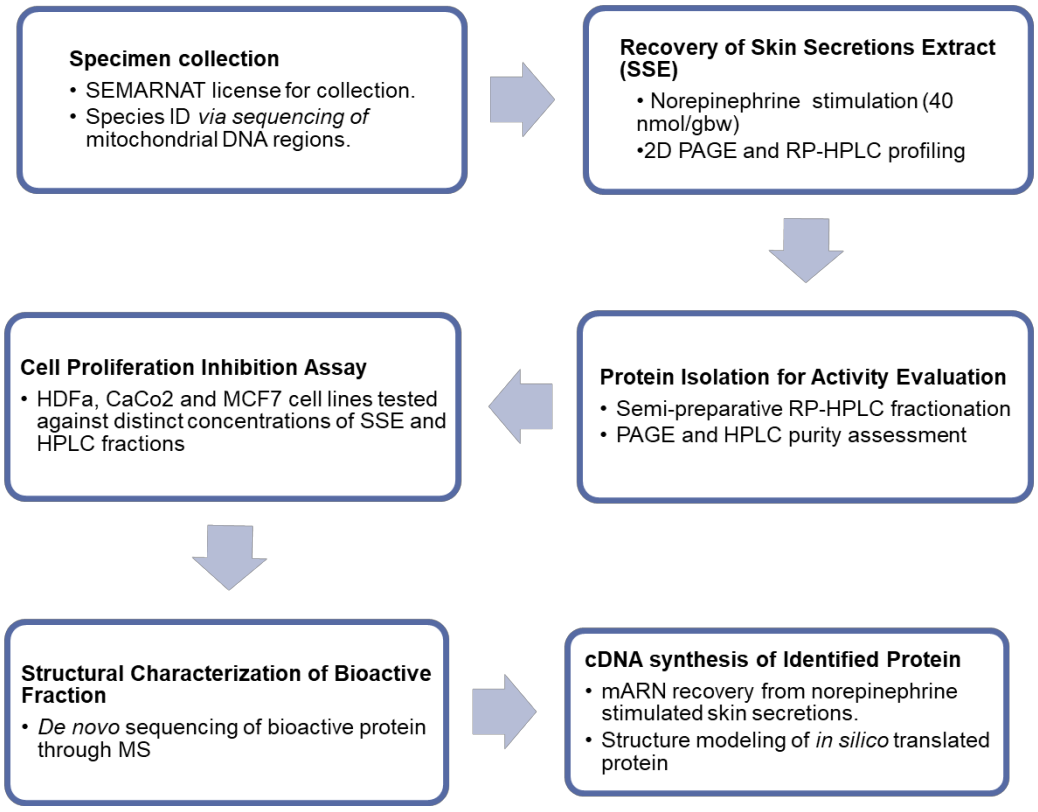

Figure 3.1. Methodology followed during the course of this research.

3.1 Collection and identification of *D. arenicolor*

Adult *D. arenicolor* of both sexes (n=13, weight range 4-7 g) were collected from rocks near water bodies at Reserva de la Biosfera de Sierra Gorda, under SEMARNAT permission (SGPA/DGVS/06751/15). All specimens were kept in groups of 4 individuals in a 60 cm x 30 cm x 50 cm fish tank with soil, rocks and water, temperature in each terrarium was maintained between 20ºC to 25ºC with a heat mat, photoperiod was set to 12 h light and vitamin-

supplemented live crickets were fed *ad libidum*. Species identification was determined through PCR amplification, sequencing and BLAST of mitochondrial DNA regions previously reported as useful markers for differential identification of *D. arenicolor* species [38]. Total genomic DNA was extracted from freeze-dried skin using the NucleoSpin® Tissue kit (Machinery-Nagel, Düren, Germany). PCR was performed with ExTaq DNA Polymerase (TaKaRa Bio Inc., Kusatsu, Shiga, Japan), primers MVZ-59^{F} (5'-ATAGCACTGAAAAYGCTDAGATG-3') and tRNAVal^{R} (5'-GGTGTAAGCGARAGCTTTKGTTAAG-3') [104] to amplify a portion of the mitochondrial 12S rDNA and tRNA-Val genes, using the following thermocycler protocol: initial denaturation of 3 min at 95ºC; 30 cycles comprised by denaturation for 10 s at 98ºC, annealing for 30 s at 53ºC, extension for 70 s at 72ºC; and a final extension for 5 min at 72ºC. Products were visualized with a 0.7% agarose gel, purified using a Wizard SV Gel and PCR Clean-up System (Promega Corporation, Madison, WI, USA), cloned into a pGEM-T vector system (Promega Corporation, Madison, WI, USA) and sequenced at Instituto de Biotecnología de la UNAM (Cuernavaca, Mexico). All obtained sequences were subjected to online BLAST searches against Gen-Bank for identification and to check for possible contamination.

3.2 Recovery of Skin Secretions Extract

To promote release of skin secretions, frogs were stimulated by injecting 40 nmol/grams body weight norepinephrine bitartrate salt (Sigma-Aldrich, St. Louis, MO, USA) dissolved in sterile 200 µL water at two sites into dorsal lymph sacs. Skin secretions were collected by placing the stimulated frog in a covered glass beaker with 40 mL of collection buffer, 25 mM NaCl and 25 mM ammonium acetate, pH 7.0, [105,106] for 15 min. After removing the frog, collected skin secretions were acidified with hydrochloric acid (1% v/v) and centrifuged 30 min at 5000xg. Supernatants were immediately desalted and concentrated using Sep-Pak C-18 cartridges (Waters Associates, Milford, MA, USA) as previously described [61]. Concentrated and desalted protein solution was named as Skin Secretions Extract (SSE). Protein concentration was determined using Microplate BCA^{TM} Protein Assay Kit (Thermo Scientific, Rockford, IL, USA). After norepinephrine stimulation and recovery of SSE, none of the frogs tested showed any distress related to this process. This protocol was reviewed and approved by the Institutional Committee for the Use and Care of Lab Animals of Tecnológico de Monterrey (Comité Institucional para el Cuidado y Uso de Animales de Laboratorio (CICUAL) del Tecnológico de Monterrey) under the protocol number 2015-007.

3.3 SSE Characterization by Reverse-Phase HPLC and 2D-PAGE

RP-HPLC profile of SSE was assessed to determine sample complexity by injecting 20 µg of skin secretions into a XBridge Peptide BEH C-18 column (4.6 mm i.d. x 250 mm, 5 µm) connected to an Agilent 1200 HPLC-UV System (Agilent, Santa Clara, CA, USA). Elution was conducted at 0.75 mL/min employing solutions A (water:TFA 99.9:0.1 v/v) and B (ACN:water:TFA 70.0:29.9:0.1, v/v/v) using a linear gradient from 0% to 100% solution B over 85 min. Absorbance was monitored at 214 nm and 280 nm. Absorbance spectra (190 nm to 600 nm) of most abundant peaks were analyzed as a preliminary identification step.

To evaluate the protein composition of the skin secretions, 150 µg of SEE were loaded into a 7 cm immobilized pH gradient (IPG) strip (3-10L). Isoelectric focusing (IEF) was carried out on an Ettan IPGphorTM 3 (GE Healthcare, Uppsala, Sweden). After completion of the IEF, reduction and alkylation steps as per manufacturer instructions, IPG strips were placed on home casted 10% SDS/Tricine-PAGE [65]. Second dimension electrophoresis was performed in a Mini-PROTEAN Tetra Cell (Bio-Rad, Hercules, CA, USA). Gels were stained overnight with GelCode™ Blue Stain Reagent (Thermo Scientific, Rockford, IL, USA). Gels were rinsed with water several times over 6 h to remove background before being scanned in a GE Image Scanner III (GE Healthcare Bio-Sciences AB, Uppsala, Sweden)

3.4 Protein Isolation for Activity Evaluation

For activity screening assays to identify bioactive fractions, SSE were separated into a Zorbax SB-C18 (Agilent, Santa Clara, CA, USA) semi-preparative column (9.4 mm i.d. x 250 mm, 5 µm) connected to an Agilent 1100 HPLC-UV system (Agilent, Santa Clara, CA, USA) equipped with a fraction collector. Mobile phase system was the same as described for SSE characterization by RP-HPLC. Fractionation was performed using the following method: a linear gradient from 10% to 25% of solution B from 0 to 5 min at a flow rate of 1.5 mL/min, linear gradient to 30% of solvent B from 5 to 10 min at a flow rate of 1.5 mL/min, linear gradient to 50% of solvent B from 10 to 25 minutes at a flow rate of 2.5 mL/min, and a linear gradient to 100% of solvent B from 25 to 30 min at a flow rate of 3 mL/min. Total method time was 35 min. Fractions with same retention time were pooled and evaporated in a GeneVac EZ-2 series (Genevac Ltd, Ipswich, UK); protein quantification was performed as describe in the Recovery of Skin Secretions Extract section. Purity of fractions collected was assessed using HPLC and 10% SDS/Tricine-PAGE.

3.5 Cell Proliferation Inhibition by SSE and HPLC-purified fractions

To evaluate the potential effect on the inhibition of cell proliferation, SSE and HPLC-purified fractions were tested at different concentrations (2 µg/mL, 4 µg/mL, 8 µg/mL, 16 µg/mL, 32 µg/mL, 64 µg/mL and 128 µg/mL) by triplicate in two independent experiments at different time periods in normal human dermal fibroblasts (HDFa, ATCC® PCS-201-012), human epithelial cells from colorectal adenocarcinoma (Caco-2, ATCC® HTB-37) and human epithelial cells from breast adenocarcinoma (MCF7, ATCC® HTM-22). Cells were cultured in DMEM medium containing 5% fetal calf serum in flat-bottomed 96-well microtiter trays at $5x10^4$ cells per well at 37ºC in a humidified incubator with 5% CO_2. After 24 hours of incubation, culture media was removed and fresh media containing SSE or HPLC-purified fractions was added to each well and incubated for 48 h at 37ºC in a humidified incubator with 5% CO_2. To estimate proliferation of viable cells, 20 µL of phenazine methosulfate 3-(4,5-dimethyl thiazole-2-yl)-2,5-diphenyl tetrazolium bromide mix-based (MTS) CellTiter 96® AQueous One Solution Cell Proliferation Assay (Promega Corporation, Madison, WI, USA) were added to each well and after 45 min incubation at 37ºC, absorbance at 490 nm was recorded using a 96-well plate reader. Percentage of viable treated cells was calculated in relation to untreated controls (viability percentage = treated cells Optical Density/ untreated cells Optical Density x 100%) [107].

3.6 Structural Characterization of Bioactive Protein

3.6.1 In-gel digestion of bioactive proteins

Isolated fractions were solubilized in sodium dodecyl sulfate (SDS) and resolved in a 12% Tricine-SDS-PAGE. Gel was stained with colloidal Coomassie Blue and protein bands were cut and destained in 50% acetonitrile containing 25 mM ammonium bicarbonate (ABB).

In-gel digestion of proteins was performed as previously described [108], with minor modifications. Briefly, gel bands were cut in 1-mm^2 cubes and proteins were reduced in 10 mM dithiothreitol in 25 mM ABB at 60 ºC for 1 h. Proteins were subsequently alkylated with 55 mM iodoacetamide in 25 mM ABB at room temperature for 45 min protected from the light. Gel cubes were then dehydrated with ACN in two washes of 1 min/each and dried during 5 min in the speedvac. Tryptic digestion of proteins was performed at 37 ºC overnight by the addition of 10 ng/µL of sequencing grade trypsin prepared in 25 mM ABB. Tryptic digested peptides were extracted from the gel cubes twice with 50% ACN, 5% acetic acid during 15 min with vigorous vortexing. Subsequently, two rounds of extraction were performed with 50% ACN, 5% formic acid (FA) for 15 min/each. The obtained supernatants were combined and dried in the speedvac. Dried peptides were

resuspended in 3% ACN, 0.1% formic acid (FA) for their subsequent analysis by liquid chromatography mass spectrometry.

3.6.2 Liquid chromatography mass spectrometry analysis of bioactive proteins

Primary structure of the bioactive proteins was characterized by MS as previously described [109,110] with minor modifications.

Analysis of peptides was performed using a QExactive mass spectrometers coupled with a Dionex UltiMate 3000 UHPLC system from Thermo Fisher Scientific Inc. (Bremen, Germany). Peptide separation was performed using a reverse-phase EASY-SPRAY LC column (75 µm ID × 15cm, 3 µm particle size, Thermo Scientific Inc.) maintained at 35°C and working at 300 nl/min. Eluents A (0.1% FA) and B (90% ACN, 0.1% FA) were used to establish the following 60-min gradient: 7-18% B for 30 min, 18–32% B for 15 min, 32–50% B for 4 min, 50–90% B for 1 min, 90-5% B for 0.1 min, 5% B for 7.9 min, 5-7% B for 2 min. Spray was generated using a Thermo Scientific EASY-Spray source at 1.75 kV. QExactive mass spectrometer was set to positive mode for data acquisition with Xcalibur 3.0.63 software (Thermo Fisher Scientific Inc., Bremen, Germany) software alternating between full Fourier transform-mass spectrometry (FT-MS) (350−1600m/z, resolution 75000, with 1 µscan per spectrum) and FT-MS/MS (resolution 35000, with 1 µscan per spectrum). Fragmentation of the 10 most intense precursors with charge >+2 and isolated within a 2 Da window was performed using a normalized collision energy of 28%. A threshold of 500 counts was enabled. For Full FT-MS and FT-MS/MS automatic gain control was set to 3×10^6 and 2×10^5, respectively.

3.6.3 Bioinformatics and data analysis

The raw MS/MS data were processed using PEAKS software version 7.5 (Bioinformatics Solutions, Waterloo, Canada) for the *de novo* sequencing of peptides [94]. In parallel data were searched using PEAKS software against a tailored database containing all anuran mRNA (648,884) and protein (425,093) entries available in the National Center for Biotechnology Information (NCBI). For the de novo sequencing of peptides, local confidence was considered as the confidence (%) that a particular amino acid was present in the de novo peptide at a particular position. The sum of the total confidence scores (0 to 1) from each amino acid in the peptide sequence divided by the number of amino acids is presented to be ALC used to assess the accuracy of the interpretation. The database search was performed as previously described [111], allowing a precursor ion tolerance of 10 ppm, a fragment tolerance of 0.05 Da MS/MS and a false

discovery rate of 1% at peptide level. Carbamidomethylation at Cys residues was set as a fixed modification.

3.7 Identified Protein cDNA Synthesis

To identify the DNA sequence for the encoded protein analyzed by MS, cDNA synthesis was performed using mRNA isolated from skin secretions as template for reverse-transcription. After neuroendocrine stimulation, skin secretions were recovered by directly rubbing the stimulated skin with a sterile tip and immediately transferred into a sterile polypropylene tube containing 1 mL of lysis/binding buffer provided by the Dynabeads® mRNA purification kit (Ambion, Carlsbad, CA, USA). Polyadenylated mRNA was isolated as per manufacturer's instructions.

First strand cDNA synthesis was carried out using the 3'RACE CDS Primer A from SMARTer RACE 5'/3' kit (Clontech, UK) and the Improm-II Reverse Transcriptase (Promega Corporation, Madison, WI, USA). 3'-RACE PCR was performed using a universal primer mix (UPM), supplied with the SMARTer RACE 5'/3' kit, a degenerate sense primer (RAnx1: 5'-GAARACWTCTGTKGTKTTYYTGG-3') and high fidelity polymerase TaKaRa Ex Taq (Clontech, UK) with the following program: initial denaturation step: 60 s at 94 ºC; 35 cycles: denaturation 30 s at 94ºC, primer annealing for 30 s at 56ºC, extension for 180 s at 72ºC. The resulting PCR fragment (416 bp) were purified with a Wizard SV Gel and PCR Clean-Up System (Promega Corporation, Madison, WI, USA), cloned using a pGEM-T vector system (Promega Corporation, Madison, WI, USA) and sequenced at Instituto de Biotecnología de la UNAM (Cuernavaca, Mexico). All sequences obtained were subjected to online BLAST (https://blast.ncbi.nlm.nih.gov/Blast.cgi) searches against Gen-Bank for identification and to check for possible contamination. cDNA was confirmed by *in silico* translation of sequenced PCR products and further alignment against digested peptides with highest ALC. Signal peptide of the sequenced cDNA was predicted in the SignalP 4.1 server (http://www.cbs.dtu.dk/services/SignalP/) [112].

3.8 Structural Modeling of Arenin

After confirmation of the correlation between the cDNA generated with the mRNA recovered from the skin secretions of *D. arenicolor* and the MS analysis performed to fraction's c protein, a 3D model of the in silico translated protein was generated using the SWISS MODEL server (https://swissmodel.expasy.org/) [113,114]. Protein model generated was downloaded and customized with the molecular visualization software UCSF Chimera [115]. A structural

comparison between the identified *D. arenicolor*'s skin secreted protein and anntoxin, the protein used as template for modeling (PDB: 2kcr) [20], was performed in order to detect conformational differences.

3.9 Statistical analysis

Results are expressed as the mean ± SE. Statistical analysis was carried out with the statistical software JMP version 14.1.0. One way-analysis of variance (ANOVA) was used to analyze the variation between groups. Tukey's test was used to identify significantly different means. Results were considered significant if $p \leq 0.05$. Significantly different means are identified with different significance letters.

Chapter 4

4. Results and Discussion

Results obtained according to the methodology described in **Chapter 3** are presented in **Chapter 4** along with the discussion generated from the observations made over the course of this study.

4.1 Collection and identification of *D. arenicolor*

All specimens utilized in this study were collected in one night at the same location according to their call and morphological characteristics such as size (between 4 and 7 cm SVL), skin (green or gray with dark spots) and leg color (yellow or light orange). Further molecular identification was carried out as described in the collection and identification methodology section. PCR products (GenBank: MG554648) amplified from total DNA extracted from freeze-dried skin of collected frogs using MVZ-59^{F} and tRNAVal^{R} primers resulted in a 1,012 base pair fragment corresponding to partial sequences of 12S ribosomal RNA and tRNA-Val genes of *D. arenicolor,* formerly known as *Hyla arenicolor*, when searched against the nr/nt database from GenBank using local NCBI-BLASTn software (v2.7.1+). Alignment of the 1,012 bp fragment with four sequences that showed high similarity is in Appendix **Figure A.1** and **Table A.6** shows identity percentage of the sequence obtained from this study with other Hylid sequences deposited in GenBank**.**

4.2 Recovery of Skin Secretions Extract

Following the methodology described in the Recovery of the Skin Secretion Extract (SSE) section, average total soluble protein recovered in SSE was 90±15 µg per gram body weight. None of the frogs tested showed any health complication after release from skin secretions recovery and norepinephrine stimulation.

4.3 SSE Characterization by Reverse-Phase HPLC and 2D-PAGE

According to the methodology described for the SSE characterization by 2D gel electrophoresis, 76 spots were stained (**Figure 4.1**), revealing the absence of peptides or oligopeptides below 10 kDa, a low content of proteins between 10 and 20 kDa with very well defined spots at pH 3 and pH 7 around 10 kDa, a high content of proteins between 20 to 37 kDa with a higher density between pH 4 and pH 6 and a low content of proteins between 37 and 75 kDa with all of the proteins between pH 3 and 7.

Following the RP-HPLC method described in the Materials and Methods section, analysis of SSE (**Figure 4.2.A**) revealed 3 main peaks when the Diode Array Detector was set to 214 nm for detection of peptide bond (–CONH–) [61]. Compounds with retention times at 22.3 min (*Fraction c*), 30.2 min (*Fraction d*) and 36.2 min (*Fraction f*) were the most abundant species across all specimens tested. Minor variations on the relative signal of these compounds between SSE of different individuals were observed, meanwhile the elution profile pattern maintained reproducible along this study.

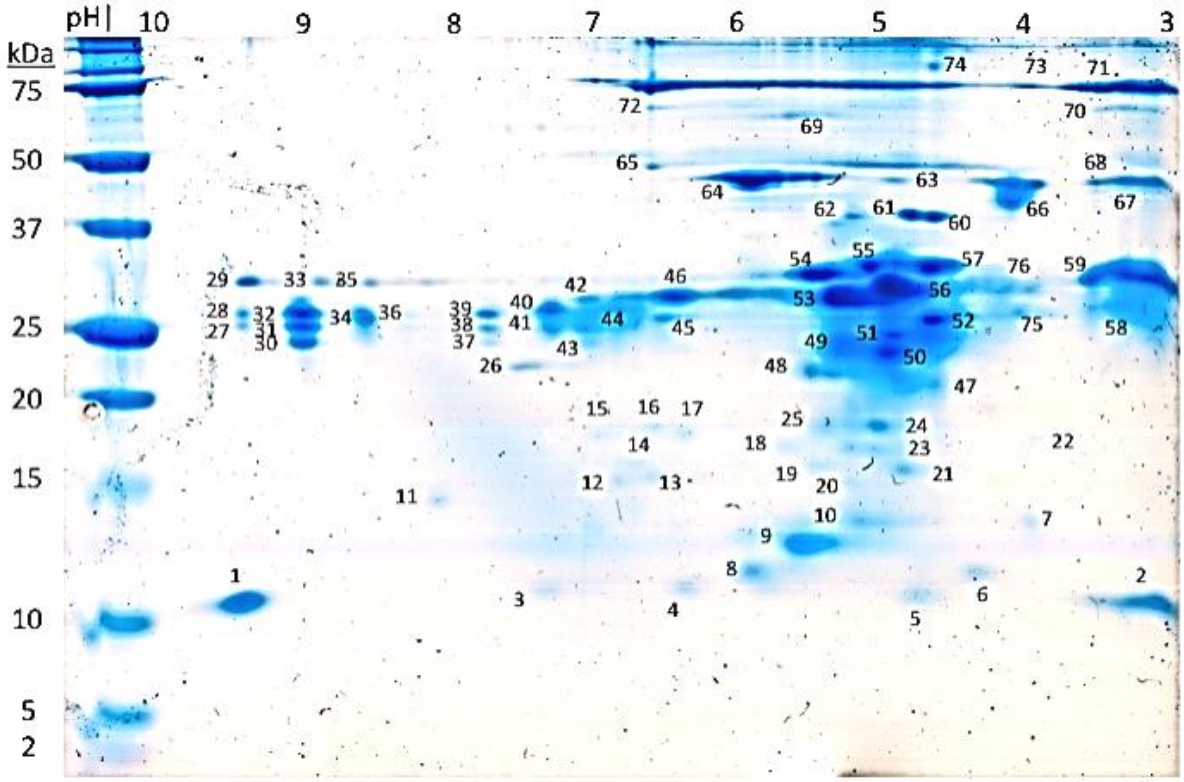

Figure 4.1. Tricine-2D-PAGE of the SSE of *D. arenicolor*

150 µg of SSE analyzed by 2D-Tricine PAGE yielded 76 spots stained with Colloidal Coomassie Blue.

Skin anti-predator defense systems of many anurans are enriched with various types of compounds including biogenic amines, bufogenines, bufotoxins, alkaloids, peptides and proteins. Of these various compounds, biologically active peptides of 12 to 48 amino acids have been the most studied molecules in amphibian skin secretions with over 2000 peptides classified in more than 100 families including *i.e.* myotropical peptides, opioid peptides, angiotensins, neuropeptides, antioxidant peptides, wound-healing peptides, antimicrobial peptides, immunomodulatory peptides, insulin-release peptide, and other peptides [17]. However, there are many reports of

anurans lacking peptides (12-48 amino acids long) in their skin secretions [26] such as the Tomato Frog *Dyscophus guineti* (Microhylidae) [54] or *Pipa Carvalhoi* [25] that display a Kunitz-like protease inhibitor polypeptide and kynurenic acid, respectively, as major constitutive components in each species skin secretions. In the Hylidae family, at least 30 species have been suggested to lack peptides [116].

4.4 Protein isolation for activity evaluation

Based on the RP-HPLC fractionation method described in the protein isolation section, 3 fractions eluting at 10.5 min *(Fraction c)*, 13.6 min *(Fraction d)* and 22.1 min *(Fraction f)* were the most abundant species, promoting its purification. Fractions with the same retention time were pooled and analyzed through Tricine-PAGE and RP-HPLC (**Figure 4.2**) employing the method described in the SSE characterization section.

RP-HPLC analysis revealed that fractions *c*, *d* and *f* corresponded to the 214 nm signals detected at 22.3 min **(Figure 4.2.B)**, 30.2 min **(Figure 4.2.C)** and 36.2 min **(Figure 4.2.D)** respectively. Tricine-PAGE showed the correlation between the purified fractions and their apparent molecular weight. Fractions *c* and *d* yielded the lowest bands between the molecular marker bands of 10 kDa and 15 kDa, where the band produced by fraction *c* resolved slightly above the band displayed by fraction *d*. Fraction *f* showed a strong 214 nm signal at 36.2 min in RP-HPLC analysis, however it was not possible to detect this fraction through Tricine-PAGE stained either with silver nitrate or colloidal Coomassie Blue.

Although most amphibian skin secretions analysed through RP-HPLC display a complex profile with various peaks and similar intensities, *D. arenicolor*'s SSE reverse-phase chromatogram (**Figure 4.2.A**) show few peaks with similar intensities contrasting with the number of spots with relatively similar intensity in 2D-PAGE (**Figure 4.1**). Even though the resolution difference between 2D-PAGE and RP-HPLC profiles and the amount of sample analysed by each method was largely different (150 ug of SSE for Tricine-2D-PAGE and 20 ug of SSE for analytical RP-HPLC), skin secretions from other amphibians have also been reported to present RP-HPLC profiles of reduced complexity, such as the case with *Pipa Carvalhoi* [25] and *Rana tigerina* [117].

Based on our findings, skin secretions of *D. arenicolor* are highly rich in proteins with an apparent molecular weight between 20 and 37 kDa (**Figure 4.1**). However, *D. arenicolor* skin secretions do not contain any of the typical 12 to 48 amino acid-long peptides described in other members of the Hylidae family.

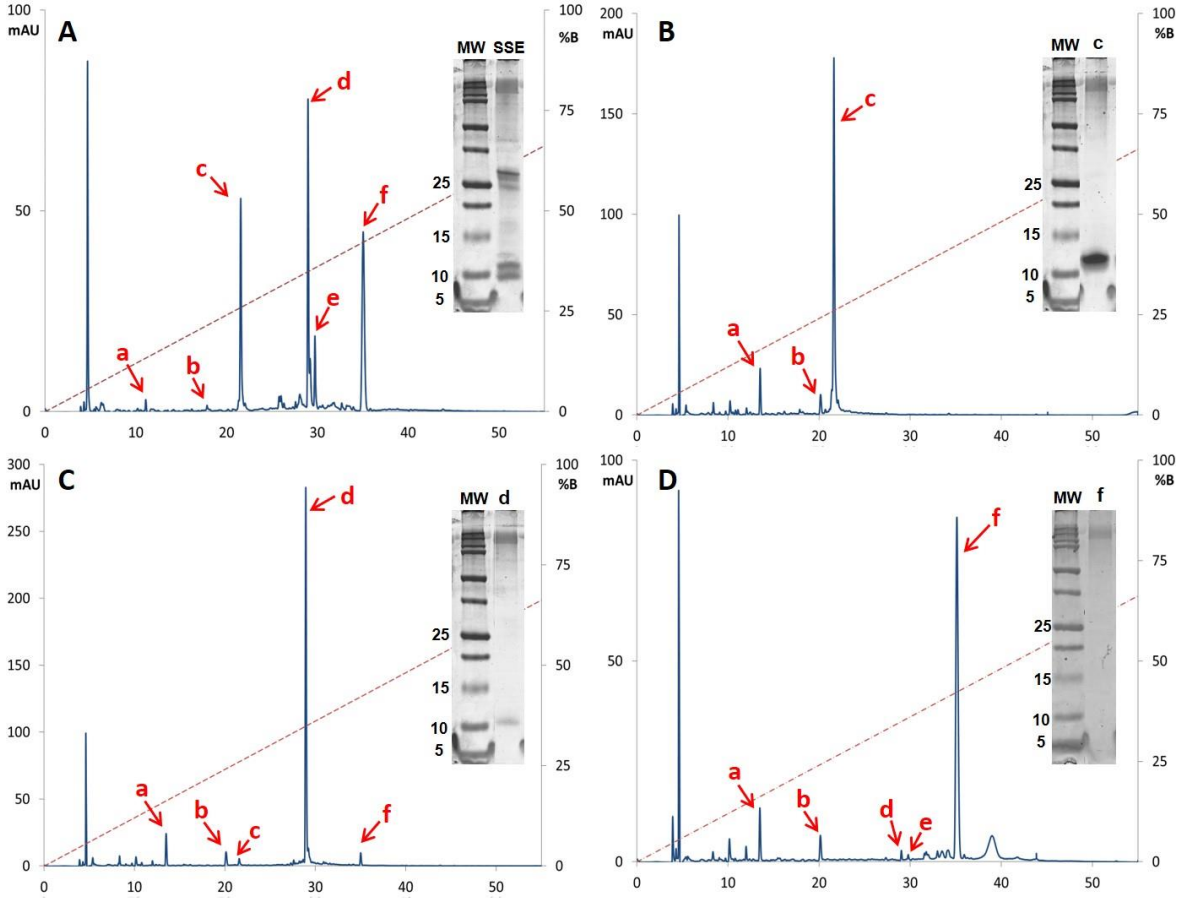

Figure 4.2. Chromatograms and Tricine SDS-PAGE of the most abundant fractions recovered after SSE semi-preparative RP-HPLC fractionation

(A) Skin secretion extracts with recovered fractions indicated by letters a, b, c, d, e and f. **(B)** *Fraction c* had a retention time of 22.3 min and an apparent molecular weight around 12 kDa, **(C)** *Fraction d* showed correlation with the 214 nm signal at 30.2 min and an apparent molecular weight around 11 kDa. **(D)** *Fraction f* showed 214 nm signal at 36.2 min, however it was not possible to correlate this fraction with any Tricine-PAGE band. The red dotted line represents the mobile phase composition for elution in relation to solvent B. Mw: Molecular Weight marker; mAU: milli-Absorbance Units.

4.5 Cell Proliferation Inhibition by SSE and HPLC-purified fractions

At the beginning of our research we were interested in the antimicrobial potential of skin secretions of *D. arenicolor* based on ethnopharmacology studies pointing out its use in MTM activities for treatment of skin infections [8,22]. To explore this suggested antimicrobial property, *E. coli, S. mutans* and *S. aureus* cultures were subjected to microdilution assays to test its susceptibility against HPLC fractions and SSE at 5, 10 and 50 µg/mL (data not shown). Although there is a small antimicrobial effect produced by the HPLC fractions or SSE over *E. coli, S. mutans* or *S. aureus*, it is not a significant response that could suggest that the main purpose of the skin

secretions of *D. arenicolor* is protection against microorganisms. Moreover, the lack of classical antimicrobial peptides suggests that this species has developed skin secretions focused primarily, but not exclusively, in defense against non-microbial threats as suggested with *Dyscophys guineti* [18].

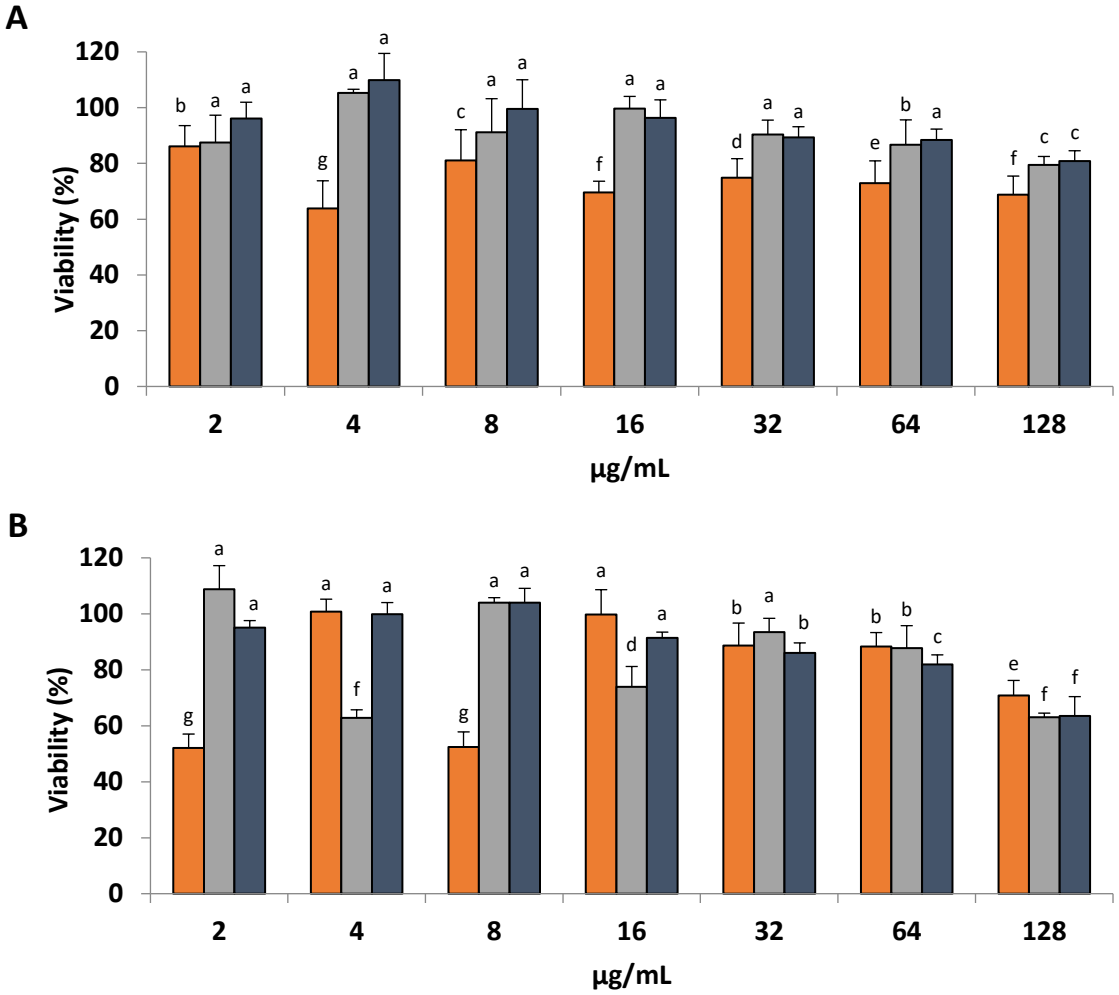

Figure 4.3. Cell proliferation assay.

Viability of (■) HDFa, (■) Caco-2 and (■) MCF7 cells cultured with different concentrations of (**A**) SSE and (**B**) HPLC fraction c is presented as a percentage of the formazan signal recorded at 490 nm compared to untreated cells. According to the Tukey's test performed, significantly different means are identified with different significance letters.

As described in the methodology section, in order to estimate proliferation of HDFa, Caco-2 and MCF7 cells in the presence of SSE and HPLC fractions at 2 µg/mL, 4 µg/mL, 8 µg/mL, 16 µg/mL, 32 µg/mL, 64 µg/mL and 128 µg/mL, a colorimetric method based on bioreduction of tetrazolium into formazan by cells was selected. Results in **Figure 4.3** are presented as a viability percentage calculated in relation to untreated cells representing 100% viability.

Interestingly, and contrary to what we were expecting, a continuous dose-response relationship was not observed in none of the cell lines tested with both the SSE and the most abundant HPLC fraction (*fraction c*, **Figure 4.2.B**). Cells treated with SSE showed a discontinuous trend (**Figure 4.3.A**). HDFa cells cultured in the presence of SSE showed its highest viability of 86.12% ± 4.30 at 2 µg/mL, at 4 µg/mL cell viability decreased to its lowest value of 63.87% ± 5.71, then increased to 81.07% ± 6.36 at 8 µg/mL, dropped to 69.55% ± 2.35 at 16 µg/mL, increased at 32 µg/mL to 74.86% ± 3.94, decreased to 72.97% ± 4.58 at 64 µg/mL and continue decreasing to 68.82% ± 3.84 at 128 µg/mL.

Caco-2 cells treated with SSE at 2 µg/mL presented a viability of 87.45% ± 5.69 that increased to 105.25% ± 0.78 at 4 µg/mL, then decreased to 91.16% ± 6.95 at 8 µg/mL, increased to 99.61% ± 2.55 at 16 µg/mL, decreased to 90.36% ± 2.99 at 32 µg/mL, continued decreasing to 86.64% ± 5.17 at 64 µg/mL and reached its lowest viability of 79.49% ± 1.73 at 128 µg/mL

SSE effect on MCF7 cells was very similar to the response caused by HPLC fraction *c* also on MCF7 cells. At 2 µg/mL of SSE, MCF7 cell viability was 96.11% ± 3.36, at 4 µg/mL a 9.84% ± 5.55 surpass on the viability compared to untreated cells was observed, cell viability at 8 µg/mL decreased to 99.5% ± 6.06 and continued decreasing up to 80.80% ± 2.16 at 128 µg/mL.

HDFa cells treated with fraction *c* (**Figure 4.3.B**) at 2 µg/mL and 8 µg/mL showed a significant reduction in viability, 52.1% ± 2.86 and 52.46% ± 3.08 respectively, while the viability of HDFa cells treated with 4 µg/mL of fraction c was almost the same as the viability of untreated cells. A continuous decline in HDFa cells viability was observed as fraction c concentration increased from 16 µg/mL to 128 µg/mL.

Caco-2 cells treated with 2 µg/mL of fraction c outperformed the viability of untreated cells by 8.8% ± 4.86, for 4 µg/mL viability dropped to 63.87% ± 5.71, at 8 µg/mL increased to 103.96% ± 1.05, dropped at 16 µg/mL to 73.95% ± 4.17, increased at 32 µg/mL to 93.47% ± 2.84, decreased to 87.72% ± 4.65 at 64 µg/mL and finally reached its lower viability of 63.09% ± 0.83 at 128 µg/mL.

A less discontinuous trend was observed for MCF7 cells treated with fraction *c*, although cells viability at 2 µg/mL was 95.09% ± 1.44, increased to 99.88% ± 2.39 at 4 µg/mL continued increasing to 103.96% ± 2.97 at 8 µg/mL, a tendency shift took place at 16 µg/mL with 91.46% ± 1.16 MCF7 cells viability and continued decreasing until 63.5% ± 2.16 at 128 µg/mL of fraction c.

Tukey's test compares simultaneously all pairs of means of every other treatment based on a studentized t-distribution and identifies any difference between two means that is greater than the expected standard error. In this context *i.e.,* although at 2 µg/mL of SSE, the histogram and error bars appear similar between HDFa and Caco-2, letters are different due to the quotient of the means comparisons divided by the standard error of the sum of the means is greater than the critical value obtained from the distribution at the confidence interval set. Indirectly and due to the nature of the cytotoxic assay, letter *a* could be related to 100% viability, however this is not completely true since the Tukey's test is not based on a reference value.

Regarding *fractions d* and *f*, even though both fractions appear as abundant as *fraction c* in the RP-HPLC chromatogram (**Figure 4.2.A**), when total soluble protein from *d* and *f* fractions were quantified, yields were very low in contrast with *fraction c.* Thus, sample quantity limited the design of activity assay for both fractions.

While screening the effect of the skin secretions of *D. arenicolor* and (*fraction c*) in normal human fibroblasts, colon cancer and breast cancer cells (**Figure 4.3**), a variable dose-response relationship was observed in the 3 cell lines. At low concentration of SSE and fraction cn (2, 4, 8 and 16 µg/mL) is difficult to establish a trend in Caco-2 and HDFa cells, in the other hand MCF7 cells maintain a less variable trend that is clearer with fraction c alone, suggesting a role impacting cell proliferation. Based on the switches in cell proliferation caused by fraction c from 2 µg/mL to 4 µg/mL and then at 8 µg/mL in HDFa and Caco-2 cells, an opposed discrete dose-dependent effect could be distinguished between these cell lines where fibroblasts viability its near to half its maximum value at the same fraction c concentration (2µg/mL) at which colon cancer cells exceeds the viability displayed by the non-treated cells. This effect is inverted at 4 µg/mL of fraction c where fibroblast cells shows a viability almost the same as the non-treated cells and colon cancer cells are at its lowest viability. Once again, inversion of this effect is observed at 8 µg/mL and 16 µg/mL of fraction c. At higher concentrations of fraction c (32, 64 and 128 µg/mL) viability inversion is still noticeable but less drastic. This effect is not produced by SSE, since the viability of HDFa cells was lower than Caco-2 and MCF7 cells in all the concentrations tested, suggesting that skin secretions from *D. arenicolor* are more toxic to normal cells than to adenocarcinoma cells at the concentrations assessed. Overall, the response observed by the increasing concentrations of fraction c and SSE on HDFa, Caco-2 and MCF7 cells could be described as an effect with high variability at low doses that is gradually stabilized into a viability reduction trend at increasing concentrations.

Hormesis is a dose-response phenomenon characterized by low-dose stimulation and high-dose inhibition, independent of biological model and endpoint, as well as chemical class and physical agent [118]. The hormetic dose-response has been shown to describe the fundamental features of several dozen receptor systems, thus affecting a vast array of biological endpoints [119], suggesting that hormetic dose-responses may represent the first comprehensive quantitative estimation of biological plasticity [120]. Some examples of systems displaying a hormetic dose-response behavior include the work presented by Bogen and collaborators [121] where human keratinocytes (HEK001) cells exposed to low-doses of arsenite (As^{III}) displayed variable viability responses across the low-range of concentrations of As^{III} tested (0.25, 0.50, 1, 2, 3, 4 μM). Also, a number of cell lines displaying an hormetic dose-response when treated with a wide range of agents including antineoplastic drugs, nonneoplastic drugs, endogenous agonists and phytocompounds have been thoroughly described [122]. A molecular tactic proposed to explain hormetic dose-response relationships involves the presence of two receptors subtypes, one with high affinity and the other with low affinity for the agonist but with notably more capacity. Such an arrangement typically may lead to a biphasic dose-response, with the high-affinity receptor activated at low concentrations and the lower affinity/high-capacity receptor becoming dominant at higher concentrations [122]. Thus, it is proposed that the behavior observed in the viability of HDFa, Caco-2 and MCF7 cells cultured in the presence of increasing concentrations of fraction c and SSE displays an hormetic-like multiphasic dose-response relationship that may be regulated by more than two receptor subtypes.

4.6 Structural Characterization of Bioactive Fraction

Following the methodology described to elucidate the primary structure of the bioactive proteins in the SSE of *D. arenicolor*, several sequences were predicted using PEAKS-assisted *de novo* sequencing combined with the use of a tailored database containing all anuran mRNA and Protein entries available in NCBI. From the *de novo* sequencing analysis of fraction c, tryptic-digested peptide sequence SSFTYYYYDK (**Figure 4.4**) was predicted with high average local confidence (ALC) (>95%). A similarity sequence analysis using BLASTp showed 80% identity with a protein named anntoxin, first described in the skin secretions of *Hyla annectans* [20] and later on *Hyla simplex* [53]. Other peptides with lower ALC and matching different regions of the anntoxins were also predicted accounting for 79.31% of the full sequence (**Figure A.5**). The anntoxin region Y^{36}RGXGGNGNRFK^{47} was not proposed by the *de novo* algorithm.

When analyzed through Tricine-PAGE, *fraction d* (**Figure 4.2.C**) showed a faint band meanwhile *fraction f* (**Figure 4.2.D**) did not show any band at all. *Fraction d* analysis through MS and the *de novo* sequencing algorithm yielded some candidate peptides with ALC>80% that did not match with any other protein or peptide in the databases used. However, it was not possible to obtain any peptide with a high ALC from fractions *d* and *f* through the *de novo* sequencing strategy due to the reduced genomic and transcriptomic information available on anurans. Based on the predicted peptides, it is possible that fraction *d* is a protein which primary structure has none or low homology with any other anuran protein or peptide previously described. Meanwhile, due to its absorption at 214 nm, it is likely that fraction *f* has a proteinic nature, however this only would be confirmed through evidence at mRNA level. Although it was not possible to identify *fractions d* and *f* proteins, it is of our interest to fully characterize both fractions in future research.

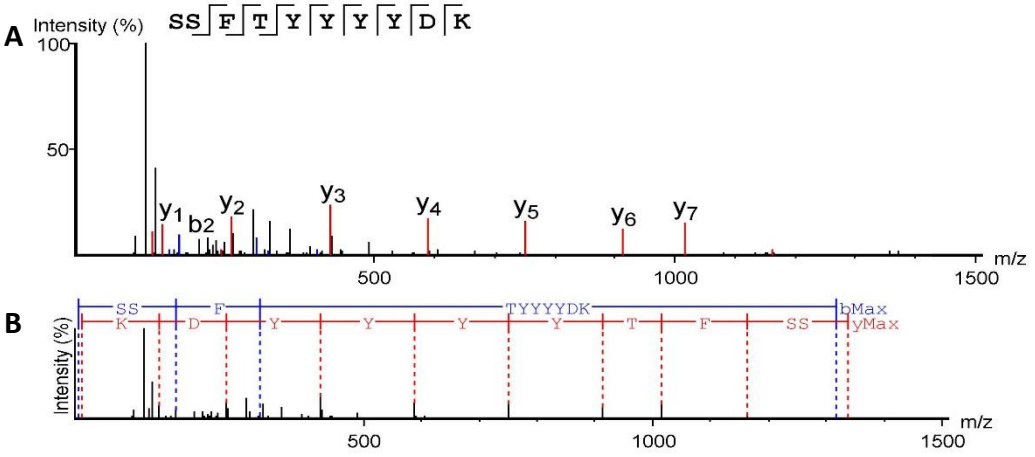

C

#	b	b-H2O	b-NH3	b (2+)	Seq	y	y-H2O	y-NH3	y (2+)	#
1	88.04	70.03	71.01	44.52	S					10
2	175.07	157.06	158.04	88.04	S	1249.54	1231.53	1232.51	625.27	9
3	322.14	304.13	305.11	161.57	F	1162.50	1144.50	1145.48	581.75	8
4	423.19	405.18	406.16	212.09	T	1015.45	997.43	998.41	508.22	7
5	586.25	568.24	569.22	293.63	Y	914.40	896.38	897.37	457.70	6
6	749.31	731.30	732.29	375.16	Y	751.33	733.32	734.30	376.16	5
7	912.38	894.37	895.35	456.69	Y	588.27	570.26	571.24	294.63	4
8	1075.44	1057.43	1058.41	538.22	Y	425.20	407.19	408.18	213.10	3
9	1190.47	1172.46	1173.44	595.73	D	262.14	244.13	245.11	131.57	2
10					K	147.08	129.10	130.09	74.06	1

Figure 4.4. *De novo* sequence prediction of the most abundant trypsin-digested peptide from fraction c.

(**A**) Annotated spectrum of peptide SSFTYYYDK showing identified b (blue signal) and y (red signal) ions. (**B**) Alignment of the spectrum with the fragment ions generated from the peptide, bMax: is the most intense peak in the spectrum corresponding to b ions series (blue uppercase letter and lines); yMax: is the most intense peak in the spectrum corresponding to y ions series (red uppercase letter and lines). (**C**) Predicted b and y ions match table with the calculated mass of possible fragment ions; spectrum matching b ions are highlighted in blue and spectrum matching y ions are highlighted in red, #: identifies the order of the ions identified in the spectrum according to each ion series.

4.7 Identified Protein cDNA Synthesis

From the *de novo* sequencing of the most abundant trypsin-digested peptide from fraction c, SSFTYYYYDK, further BLASTp and partial homology correlation with the anntoxins from *H. annectans* and *H. simplex*, a degenerate 5' primer, denominated RAnx1, was designed based on the amino acid sequence KTSVVFL from the signal peptide sequence of the previously characterized anntoxins. 3'RACE PCR reactions that employed the UPM as 3' primer and degenerate RAnx1 as the 5' primer yielded a 378 bp product, encompassing a signal peptide, a mature peptide and a poly A signal (**Figure 4.5**). BLASTn of this PCR product showed overall nucleotide sequence similarity of 87% between *H. annectans'* anntoxin and the cDNA amplified with RAnx1 and UPM primers from the mRNA recovered from the skin secretions of *D. arenicolor.* cDNA alignment of the reverse-transcribed mRNA isolated from the skin secretions of *D. arenicolor* with anntoxins from *H. annectans* and *H. simplex* is presented in Appendix Figure A.12. Signal peptide was predicted just before the residue Ala^{22} using the SignalP 4.1 server and its nucleotide sequence showed 95% similarity with the signal peptide sequence of *H. annectans'* anntoxin. Meanwhile, the 58 amino acids of the mature protein encoded by the PCR product showed a 93% identity with the anntoxin from *H. annectans* and 82% with the anntoxin S1 from *H. simplex.* The following amino acids were unique in the protein from the skin secretions of *D. arenicolor* when aligned with *H. annectans* and *H. simplex* anntoxins: Glu^{6} Ser^{16} Tyr^{20} and Lys^{28}. Mature protein encoded by the cDNA generated from the skin secretions of *D. arenicolor* has been named **arenin** by our research group. Complete cDNA sequence was deposited in GenBank under the accession number MH898942.

Further BLASTp revealed that, as the anntoxins from *H. annectans* and *H. simplex*, arenin could have a Kunitz/Bovine pancreatic trypsin inhibitor (BPTI) domain, usually indicative of serine protease inhibitory activity. A possible trypsin interaction site *ku* [46] was also identified, comprised by the residues $Lys^{13}Gly^{14}Ser^{15}Ser^{16}Ser^{17}Thr^{19}$.

Interestingly, this polypeptide that was fractionated from the SSE of *D. arenicolor* through RP-HPLC (*fraction c*), further resolved through Tricine-PAGE (**Figure 4.2.B**), in-gel digested and analyzed through MS; showed in PAGE analysis of the skin secretions of *D. arenicolor* (**Figure 4.2.A**) and in PAGE analysis of *fraction c* (**Figure 4.2.B**), bands corresponding to arenin with an apparent molecular weight between 10 and 15 kDa. Nonetheless, after *in silico* translation of its full cDNA, calculated molecular weight of the mature polypeptide based on its amino acid sequence resulted in 6,578 Da. The difference between the calculated and the observed

molecular weight could be explained through the formation of a homodimer between two arenin molecules, since the role of the Kunitz type domain in the formation of homodimers has been suggested previously [123]. An alternative hypothesis may be that this molecular weight shift is due to the presence of post-translational modifications such as glycosylation, methionine oxidation, tyrosine-sulfation, and/or carboxyterminal amidation. Even though these features may be found in Kunitz-like proteins from plants [124], these post-translational modifications have not been associated to amphibian Kunitz-like polypeptides. However, these features have been found in peptides and proteins from the skin secretions of other frogs [125], raising the possibility that arenin may contain them. Therefore, it is possible that arenin could be glycosylated such as the foetal human brain amyloid protein precursor that contains a Kunitz domain that has been described to present N- and O-glycosylations [126]. Yet, these hypotheses should be tested through structural analysis of the purified protein.

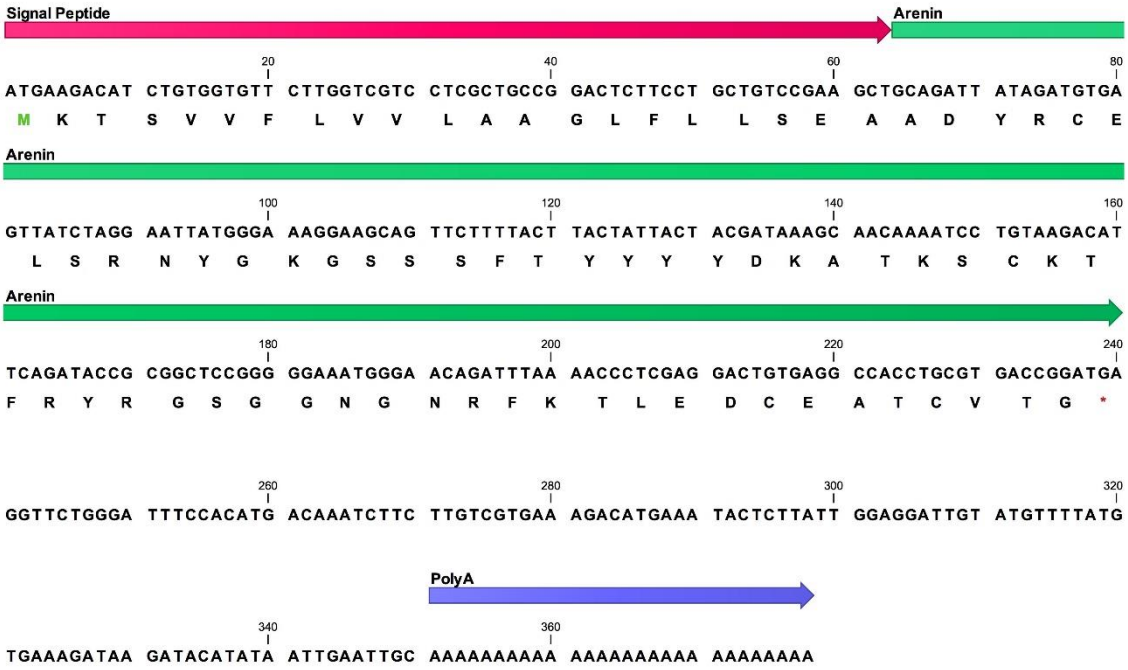

Figure 4.5. Full cDNA sequence encoded arenin isolated from *D. arenicolor* skin secretions

(■) Encoded and translated signal peptide, (■) nucleotide and amino acid sequences of the mature polypeptide arenin, (■) Poly A signal. Green residue indicates translation initiation codon. Red asterisk indicates translation stop codon.

4.8 Structural modeling of arenin

The 3D model of arenin (**Figure 4.6**) generated based on the solution structure of anntoxin from *H. annectans* suggests that arenin keeps a very similar structure maintaining the two disulfide

bonds Cys^{5}-Cys^{55} and Cys^{30}-Cys^{51} due to the proximity between the sulfhydryl groups of each pair of cysteines, 2 alpha-helix motifs Tyr^{3} to Glu^{6} and Leu^{48} to Cys^{55} and a twisted 2-stranded antiparallel beta sheets Phe^{18} to Asp^{24} and Ser^{29} to Tyr^{35}. In the ribbons model (**Figure 4.6.A and 4.6.B**), the possible trypsin interaction site *ku* [46], $Lys^{13}Gly^{14}Ser^{15}Ser^{16}Ser^{17}Thr^{19}$, can be recognized as an outer loop in purple.

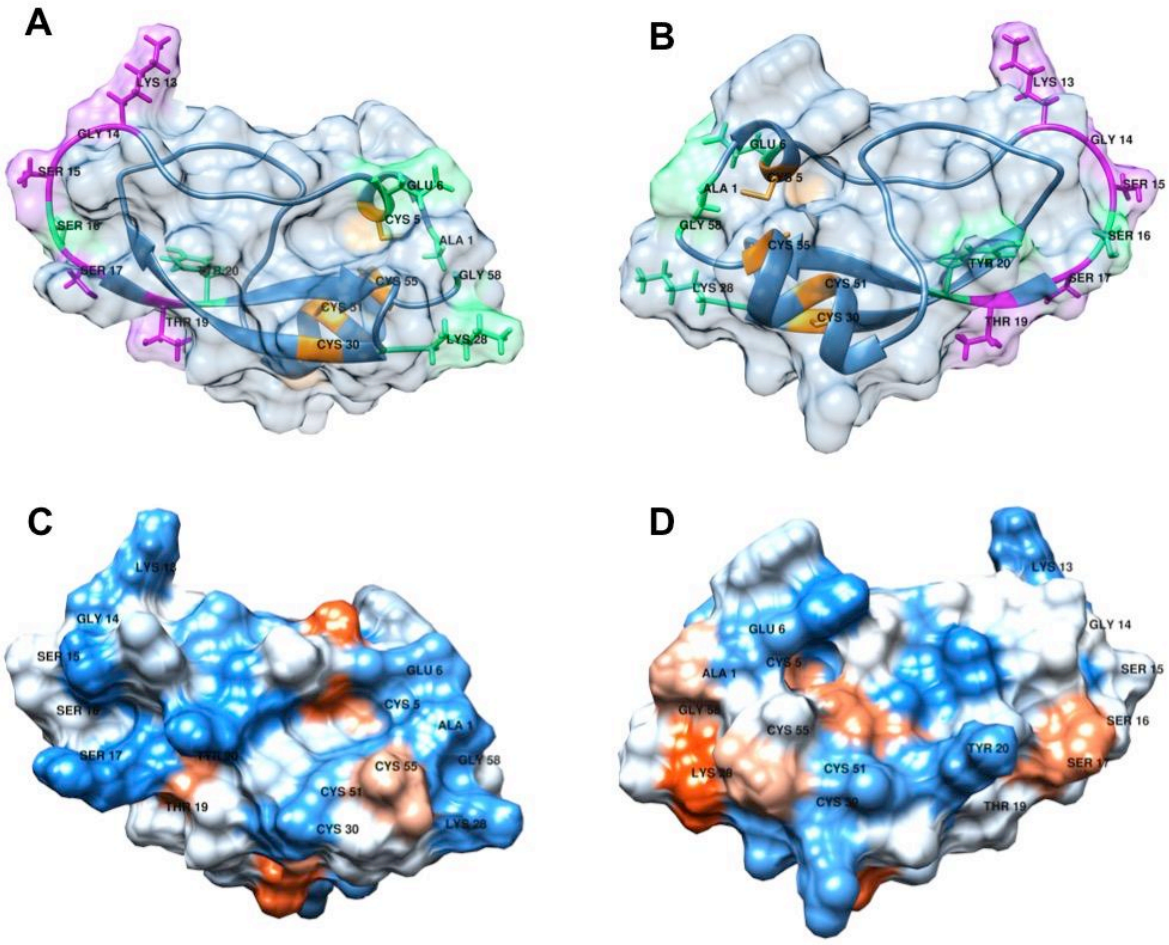

Figure 4.6. 3D model of arenin from *D. arenicolor* skin secretions

(**A**) Front and (**B**) back ribbon model of arenin, Unique amino acids Glu^{6} Ser^{16} Tyr^{20} and Lys^{28} are highlighted in green, amino acids $Lys^{13}Gly^{14}Ser^{15}Ser^{16}Ser^{17}Thr^{19}$ possibly constitutes the trypsin interaction site *ku* and are highlighted in purple, amino acids Cys^{5}-Cys^{55} and Cys^{30}-Cys^{51} involved in the formation of disulfide bonds are highlighted in orange. (**C**) Front and (**D**) back polarity model prediction of arenin, blue zones represent polar residues, red zones non-polar residues and white zones neutral residues.

Polarity prediction model (**Figure 4.6.C and 4.6.D)** and amino acid composition of arenin suggests it has few hydrophobic zones, implying a proclivity to solubilize in aqueous solutions.

This is in accordance with the RP-HPLC solvent composition of 26.87% ± 0.06 acetonitrile (ACN) that prompted the elution of arenin.

Protease inhibitors (PIs) and proteases are ubiquitous molecules in nature involved in a plethora of fundamental functions. In amphibian skin secretions, PIs are known to play a key role on inhibiting the catalytic activity of proteolytic enzymes in charge of the processing of peptide precursors [44]. However, in amphibians lacking defensive peptides, these molecules could play a key role in immunity as a protection against extrinsic proteases produced by invading microorganisms [43]. Generally, proteases are classified based on the catalytic amino acid within their active site (aspartic acid, threonine, cysteine, serine protease) or according to the cofactor essential for catalytic activity (metalloproteases). Similarly, protein based PIs are commonly classified based on three defined structural motifs: Kunitz, Kazal and Bowman-Birk [45].

In amphibians, Kunitz-like PIs have been found in the skin secretions of various toads, ranid and hylid frogs, Kazal inhibitors in Phyllomedusinae frogs and Bowman-Birk inhibitors in ranid frogs [44]. According to the 3D model predicted for arenin (**Figure 4.6**), its structure resembles a typical Kunitz-type fold constituted by a twisted antiparallel β-sheets hairpin (residues Phe^{18}-Tyr^{35}) an α-helix (Leu^{48}-Cys^{55}), and a short 3_{10} helix (residues Tyr^{3}-Glu^{6}) in the N terminus [44]. Amphibian Kunitz-like PIs differ from typical Kunitz PIs in the number of disulfide bonds, since the former contains 2 disulfide bonds (Cys^{5}-Cys^{55} and Cys^{30}-Cys^{51} in arenin), meanwhile typical Kunitz PIs are characterized by the presence of 3 disulfide bonds [17,44].

However, even though they share 93% sequence homology, comparing the 3D model of arenin with the NMR crystallography of anntoxin from *H. annectans*, differences in the amino acid sequence could impact arenin's structure and therefore its activity. Substitution of anntoxin Gln^{7} by Glu^{6} in arenin may stabilize the short 3_{10} helix hosting the Cys^{5} residue that makes a disulfide bond with Cys^{55}, this shift may provide more stability between the 3_{10} helix and the α-helix. In anntoxin, Gly^{17} is localized in the most exposed area of the reactive loop that constitutes the trypsin interaction site (*ku* domain). In arenin Gly^{17} is substituted by Ser^{16} that may reduce the flexibility of the loop, this may decrease the selectivity of the protease inhibition activity, and at the same time, as Ser could accept or donate protons, its specific activity could be enhanced. At first glance, Asn^{21} substitution by Tyr^{20} in arenin may have little impact in overall protein stability-activity since both amino acids are polar, however the size and proximity of tyrosine's aromatic ring to the functional groups of Phe^{18}, Tyr^{35}, Arg^{44} and Lys^{46}, may reduce the flexibility of the reactive loop by stabilizing the twisted antiparallel β-sheets hairpin by hydrogen bonds with these

4 residues. Ser^{29} substitution by Lys^{28} may decrease protein solubility in water, since the hydroxyl group in Ser is more soluble in water than the amine in Lys.

Aside from their anti-protease activity, PIs have been associated with other underlying properties such as contribution in the termination of inflammatory processes through modulation of cytokine expression, signal transduction and tissue remodeling [45], playing a key role in the etiology and treatment of human pathologies such as cancer, inflammation and hemorrhage [44]. As consequence of these bioactivities, PIs have been suggested as useful tools to study pathological processes along with the design of highly-specific drugs [127]. Amphibian Kunitz-like PIs have exhibited inhibition of tetrodotoxin-sensitive (TTX-S) voltage-gated sodium channel (VGSC) suggesting its application as analgesics when delivered at low concentrations [57].

Protease activated receptors (PAR) originally discovered in platelets, endothelial cells and fibroblasts, are seven-transmembrane-spanning receptors coupled to G proteins. PAR activation through protease hydrolyzation at a specific cleavage site in the extracellular N terminus of the receptor exposes a new N-terminal domain, which binds and activates the receptor initiating intracellular signals involved in responses such as platelet activation, vascular functions, inflammation, angiogenesis, neurodegeneration, proliferation, cell migration and even nociception [56,128]. Thrombin, trypsin, and human mast-cell tryptase have been found to activate the 4 PARs cloned thus far (PAR-1, PAR-2, PAR-3 and PAR-4) [129]. In theory, arenin could act as PARs antagonist through the inhibition of the proteases involved in PARs activation. This could explain the response observed at high concentration of arenin and SSE, but not the discrete effect at low concentration. It is possible that arenin could interact directly or indirectly with other cell membrane receptors additionally to PAR in a multi-targeted fashion dependent of arenin concentration according to the hormetic model hypothesis. Transcriptomic, proteomic and metabolomic analysis at different concentrations of arenin could shed light in the mechanism underlying the variable response noticed in our study.

Chapter 5

5. Conclusions and Future Work

Based on the results presented in **Chapter 4**, the main objectives of this dissertation, including the isolation, identification and characterization of a bioactive molecule from the skin secretions of *D. arenicolor,* was achieved through cDNA sequence and amino acid primary structure description of the novel Kunitz-like polypeptide **arenin**. The effect of arenin (fraction c, in this study) was tested on three cell lines (one normal cell line and two adenocarcinoma cell lines) to investigate its potential activity and further applications.

This work demonstrates the lack of peptides of 12-48 amino acid long in the skin secretions of *D. arenicolor*. At the same time, we present the full cDNA of the third gene-encoded Kunitz-like protein from a hylid amphibian skin secretions, a 58 amino acid polypeptide named arenin, one of the major components in the skin secretion of *D. arenicolor*. The absence of typical defensive peptides in the skin secretions of *D. arenicolor*, the high abundance of arenin in SSE and its homology with anntoxin, a proven neurotoxic, suggest that arenin could play a major role in predator defense, supporting the hypothesis that this family of polypeptides may act as a first-line of defense against predators. Moreover, the lack of classical antimicrobial peptides aids the notion that due to selective pressure, this species has developed skin secretions focused primarily, but not exclusively, in defense against non-microbial threats, but rather predatory defense. This hypothesis could be supported by the demonstration of the lethal toxicity induced through the administration of high concentrations (0.05 to 3 mg/kg body weight) of anntoxin, that shares 93% homology with arenin, to potential predators such as insect, snake, bird and mouse [20]. Also, reduced or none antimicrobial activity has been observed in other Kunitz-like proteins [44]. A definitive conclusion regarding the role of the skin of *D. arenicolor* in zootherapy practices cannot be inferred from the data presented in this dissertation. In addition to the experimental approaches and results presented in this work, further research should be explored to determine the molecular mechanisms that could explain the usage of the skin of *D. arenicolor* to treat skin injuries in traditional medicine.

As mentioned in the Results and Discussion chapter, the experimental molecular weight of arenin as estimated by Tricine-PAGE and 2D-Tricine-PAGE is between 10 and 15 kDa, however, the *in silico* theoretical molecular weight of arenin is 6,578 Da. Although the Kunitz domain has been associated to the formation of dimers, there is no evidence supporting this feature in the anntoxins

from *H. annectans* and *H. simplex*. An alternative hypothesis to explain the inconsistency between the observed and theoretical molecular weight of arenin might be since post-translational modifications have been observed in other peptides and proteins from the skin secretions of amphibians, thus, it is possible that arenin could display them. Nonetheless, modifications of this kind have not been described in homologous proteins from *H. annectans* and *H. simple*x. Further research aimed to confirm these hypotheses is needed to enlighten the effect behind the molecular weight differences observed.

Structural characterization of arenin through MS and further BLASTp of the predicted trypsin-digested peptide SSFTYYYYDK, suggested the presence of the Kunitz/Bovine Pancreatic Trypsin Inhibition domain. Identification of arenin's encoded mRNA, *in silico* translation and BLASTp of the full amino acid sequence confirmed the occurrence of the Kunitz domain. Even though the trypsin inhibitory activity has been demonstrated in the Kunitz-like polypeptides from *H. annectans* and *H. simplex*, evaluation of the potential protease inhibition activity of arenin and comparison against the activity displayed by its homologous proteins must be addressed.

Based on the results observed by culture of HDFa, Caco-2 and MCF cell lines with different concentrations of arenin (fraction c), it is proposed that arenin may induce a hormetic-like multiphasic dose-response in the proliferation of normal and cancerous cells, partially through the protection of Protease-activated receptors (PARs). Arenin's hormetic behavior suggests a multitargeted effect through interaction with more than two receptor subtypes involved in distinct signaling pathways. It is possible that at low concentrations of arenin, a selective stimulation-inhibition of receptors occurs, this effect could be mediated by intermediary molecules, not directly with specific receptors. Nonetheless, further research focused on transcriptomics, metabolomics and proteomics changes is needed to confirm this hypothesis. Elucidation of the mechanism of action behind the dose-response relationship observed in HDFa, Caco-2 and MCF7 cells cultured with low concentrations of arenin may contribute to the development of new strategies aimed to cancer treatment.

As a recommendation for future research involving isolation of proteins and peptides from animal sources, special attention should be addressed to the amount of sample available. When possible, in-house breeding of wild specimens must be a priority to establish a continuous sample source.

Since its genesis, this work was conceived to serve as a research scaffold aimed to the investigation of animal derived proteins and peptides. This research line is focused on the

development and design of drugs based on the discovery of bioactive molecules isolated from nature. The scope expected from this research line will involve isolation, structural characterization, bioactivity identification, molecular mechanism elucidation, heterologous expression and bioactivity engineering of peptides and proteins. Some of topics intended to be covered by this research line are:

- Development, implementation and standardization of additional bioactivity assays – different cell lines, model organisms and molecular biomarkers capable to provide information that suggests qualitative and quantitative changes – to increase the span of activity screening to be able to improve the identification of potential applications of animal derived peptides and proteins. Expanding available activity assays will provide further analysis tools aimed to fully characterize proteins and peptides avoiding overlooking of potential promising candidates for drug design.

- Study of the potential synergistic effect of arenin in co-administration with other anti-proliferative compounds will aid the understanding of the effect observed on cell proliferation in this research. Due to the nature of the response observed primarily in HDFa and Caco-2 cells, further research focused to elucidate the interaction between arenin and human cell lines could help to understand not only the role of this Kunitz-like polypeptide in cell proliferation, but also could hint novel molecular mechanism behind cancer pathogenesis.

- Identify non-protein bioactive compounds in the skin secretions of *D. arenicolor* and develop the platform. Although the main research line is focused on bioactive proteins and peptides, strategies for the isolation of low molecular weight compounds from animal sources will be implemented to broaden the potential pharmacological actions to be studied.

- Design and development of a heterologous expression system and purification process of arenin and molecules alike to facilitate bioactivity studies. A critical step in the development of this research line is the implementation of recombinant technologies, since through this approach biomolecules of interest could be overproduced aiding the availability of sample for bioactivity assays. As a result, isolation and purification techniques aimed to improve the recovery yield of these products must be addressed.

- To improve arenin's bioactivity and further protein and peptide discovery, identified and characterized through this research line, protein engineering strategies must be exploited and implemented. Even though nature still has a lot to teach us, strategies such as synthetic amino acid shuffling or rational protein engineering could improve a particular trait such as protein affinity, stability or specificity enhancing its overall activity or any other feature of interest.

As consequence of the establishment of this research line, it is anticipated to provide a research direction for future graduate students and continued contributions to the advancement of knowledge in the life sciences.

Appendix

Abbreviations and acronyms

Table A.1. Abbreviations

ABB	Ammonium bicarbonate
ACN	Acetonitrile
ALC	Average Local Confidence
BLAST	Basic Local Alignment Sequence Tool
BPTI	Bovine pancreatic trypsin inhibitor
FA	Formic Acid
FT-MS	Fourier transform-mass spectrometry
IEF	Isoelectric focusing
IPG	Immobilized pH gradient
MS	Mass spectrometry
MTM	Mexican Traditional Medicine
MTS	Phenazine methosulfate 3-(4,5-dimethyl thiazole-2-yl)-2,5-diphenyl tetrazolium bromide mix-based
PAR	Protease activated receptor
PIs	Protease inhibitors
SDS	Sodium dodecyl sulfate
SSE	Skin Secretions Extract
TEAB	Triethylammonium bicarbonate
TFA	Trifluoroacetic acid
TTX-S	Tetrodotoxin-sensitive
VGSC	Voltage-gated sodium channel

Primers used

Table A.2. Primers used for species identification

Primer name	Sequence 5' to 3'	Reference
MVZ-59a	ATAGCACTGAAAAYGCTDAGATG	[104]
tRNAVala	GGTGTAAGCGARAGCTTTKGTTAAG	[104]

Table A.3. Primers used for screening of antimicrobial peptides

Primer name	Sequence 5' to 3'	Reference
ATGprimer	ATGTTCACCTTGAAGAATC	[130]
Degenera1	GAWYYAYYHRAGCCYAAADATG	[130]
RevATG	AGATGATTTCCAATTCCAT	[130]
NMU-F	GAYGARGARGTICARGTICC	[101]
NMU-R	AAACCCGCTGATCTCCTTCCATT	[101]
DermaS1deg	GGCTTYCCTGAAGAAATCTC	[131]
5UTRPhyllo	ACTTTCYGAWTTRYAAGMSCARABATG	[132]

Table A.4. Primers used for sequencing of PCR products cloned into pGEM-T easy vector

Primer name	Sequence 5' to 3'	Reference
Universal primer M13 Forward (-20)	GTAAAACGACGGCCAGT	[133]
Universal primer M13 Reverse (-48)	AGCGGATAACAATTTCACACAGG	[133]

Table A.5. Degenerated primers used as 5' GSP for second strand cDNA synthesis

Primer name	Sequence 5’ to 3'	Coding Region
RmlSP	ATGAAAACATCTGTGGTGTTTCTGG	MKTSVVFL
RccSP	ATGAARACNWSNGTNGTNTTYYTNG	MKTXVVFX
RNterAnnt	GAARACWTCTGTKGTKTTYYTGG	KTSVVFL
RATGp	ATGTTCACCTTGAAGAATC	MFTLKN
RATG2	ATGTTYACNHTNAARAARWSNYTNY	MFT(L/M)KKSLL
RAnnS2	CAGGACTACAGGTGCCAGCTGCTCGC	QDYRCQLL
RAnnD	GACYAYAGGTGCVRNCTGWBHGC	D(H/Y)RC(N/G/Q)L(S/I)R
RNterHe2	GCWGAYTAYAGRTGYGARYTG	ADYRCEL
RNterHe2.1	GCWGAYTAYHGNTKYGARYTG	ADY(R/C)(C/F)EL
RA3	CTGGCAGTGGTGGGAACTTGTCTG	LAVVGTCL
RA3d	YTNGCNGTNGTNGGNACNTGYYTN	XAVVGTCX

Alignment of mtDNA sequences

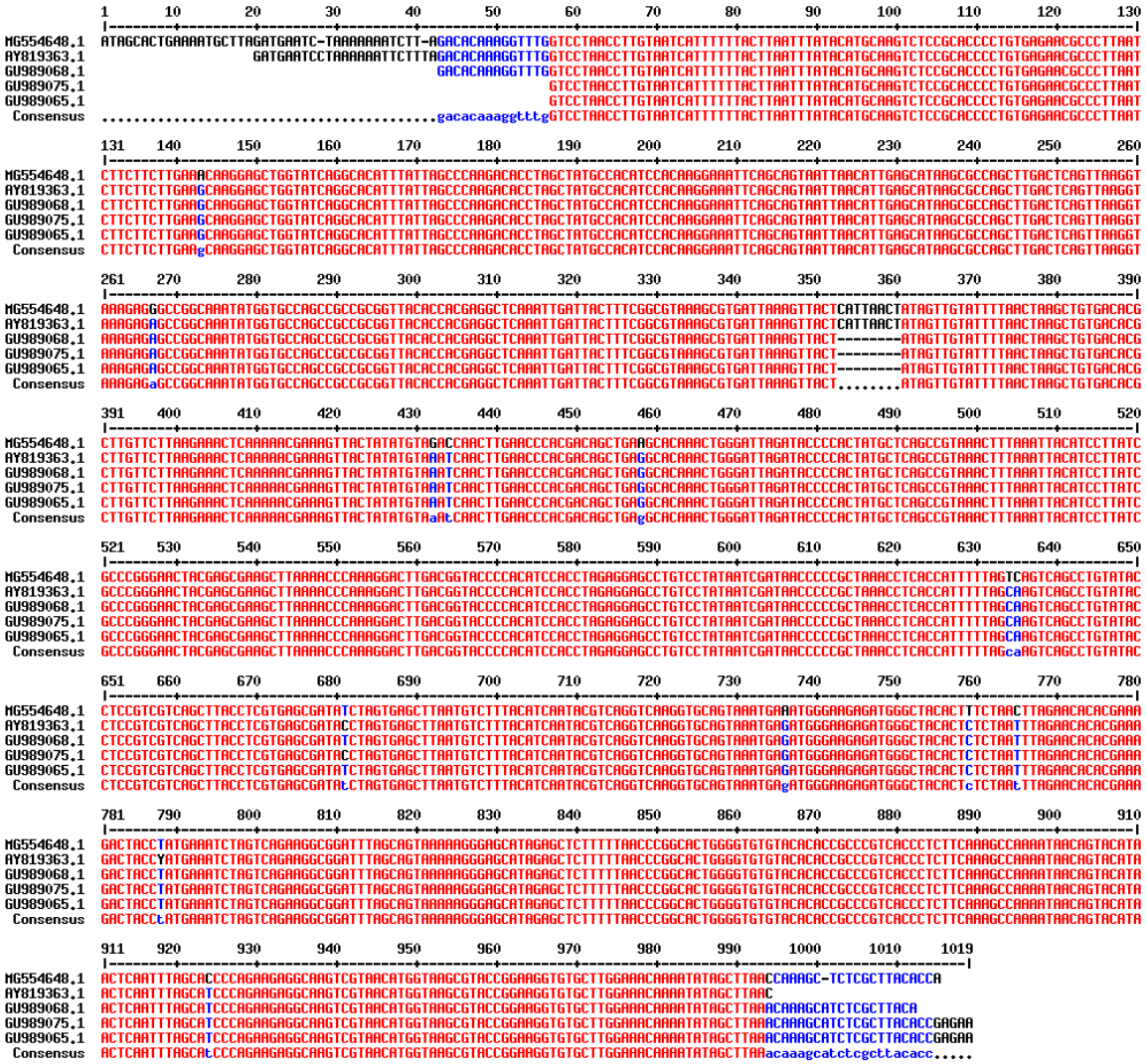

Figure A.1. mtDNA alignment.

mtDNA deposited in GenBank under accession number **MG554648.1** that was amplified from Total DNA isolated from freeze-dried skin of one of the specimens collected for this research (latitude 20.7021887, longitude -99.6251929) was aligned with the following sequences obtained from NCBI Nucleotide database: *Hyla arenicolor* tRNA-Phe gene, partial sequence (**AY819363.1**), *Hyla arenicolor* voucher KEK HAR11 12S ribosomal RNA gene (**GU989068.1**), *Hyla arenicolor* voucher KEK HAR51 12S ribosomal RNA gene (**GU989075.1**), *Hyla arenicolor* voucher KEK HAR49 12S ribosomal RNA gene (**GU989065.1**)

Species	GenBank	coverage	Identity	Locality collected
D. arenicolor	GU989068.1	0.97	0.98	Lower Workman Creek, AZ
D. arenicolor	AY819363.1	0.96	0.98	Chiricahua, AZ
D. arenicolor	GU989075.1	0.96	0.98	Rucker Canyon Road, AZ
D. arenicolor	GU989065.1	0.96	0.98	Houston Mesa, AZ
D. arenicolor	EF566960.1	0.96	0.98	Coconino, AZ
D. arenicolor	AY843603.1	0.94	0.99	Houston Creek, AZ
D. eximia	EF566957.1	0.97	0.95	Jalisco, MX
D. chrysoscelis	EF566948.1	0.97	0.96	San Saba, TX
Hyla tsinlingenesis	KU601448.1	0.99	0.92	China
Hyla annectans	KM271781.1	0.99	0.92	China

Table A.6. Similarity results of MG554648 subjected to BLAST.

MG554648 is the GenBank sequence code for the PCR product amplified from Total DNA isolated from freeze-dried skin of one of the specimens collected for this research (latitude 20.7021887, longitude -99.6251929) from the skin corresponding to partial sequences of partial 12S rDNA and tRNA-Val genes from different D. arenicolor isolates and

Cell Proliferation Assay

	SSE				*HPLC fraction x*				*HPLC fraction y*			
	1	2	3	4	5	6	7	8	9	10	11	12
A	SSE dilutions tested by triplicate			C+	HPLC fraction x dilutions tested by triplicate			C+	HPLC fraction y dilutions tested by triplicate			C+
B												
C												
D												
E												
F												
G	C-				C-				C-			

Figure A.2. Cell proliferation assay plate layout.

C- stands for negative control composed by 100 µL of DMEM/F12 10%. **C+** stands for positive control, in this case, comprised by untreated cells seeded at 5,000 cells/well cultured, after 24 h medium was removed and 100 µL fresh DMEM/F12 10% were added. **SSE or HPLC fraction dilutions tested by triplicate** corresponds to the treated cells**;** 5,000 cells/well were cultured for 24 h, medium was removed and SSE or HPLC fractions were diluted at assay concentrations, as shown in figures **A.3.** and **A.4**, in 100 µL of fresh DMEM/F12 10% were added to each well.

Fraction tested **c**									
						Per assay			
[stock]	4824.56	**µg/mL**	**Code**	**[1X] tested**		**µL**	**V_{from}**	**V_{DMEM} (µL)**	**V_{total} (µL)**
Cell Lines	3	n	A	128	µg/mL	47.994	Stock	1761.006	1809
Replicates/Dilution	3	wells	B	64	µg/mL	904.5	A	904.5	1809
Dilutions tested	7		C	32	µg/mL	904.5	B	904.5	1809
V_{total}/well	100	µL	D	16	µg/mL	904.5	C	904.5	1809
V/Dilution (per strain)	300	µL	E	8	µg/mL	904.5	D	904.5	1809
V/Dilution (n strains)	900	µL	F	4	µg/mL	904.5	E	904.5	1809
V_{stock}/assay	47.994	µL	G	2	µg/mL	904.5	F	904.5	1809
V_{stock} after assay	2.006	µL						7188.006	

Figure A.3. Example of cell proliferation assay dilution calculations for fraction c.

Fraction tested **SSE**									
						Per assay			
[stock]	2846.22	**µg/mL**	**Code**	**[1X] tested**		**µL**	**V_{from}**	**V_{DMEM} (µL)**	**V_{total} (µL)**
Cell Lines	3	n	A	128	µg/mL	81.354	Stock	1727.646	1809
Replicates/Dilution	3	wells	B	64	µg/mL	904.5	A	904.5	1809
Dilutions tested	7		C	32	µg/mL	904.5	B	904.5	1809
V_{total}/well	100	µL	D	16	µg/mL	904.5	C	904.5	1809
V/Dilution (per strain)	300	µL	E	8	µg/mL	904.5	D	904.5	1809
V/Dilution (n strains)	900	µL	F	4	µg/mL	904.5	E	904.5	1809
V_{stock}/assay	81.354	µL	G	2	µg/mL	904.5	F	904.5	1809
V_{stock} after assay	18.646	µL						7154.646	

Figure A.4. Example of cell proliferation assay dilution calculations for SSE.

MS characterization of arenin

In silico translation of arenin is as follows:

ADYRCELSRNYGKGSSSFTYYYYDKATKSCKTFRYRGSGGNGNRFKTLEDCEATCVTG

Underlined residues were identified through MS analysis of in-gel trypsin digested fraction c, residues highlighted in green were not identified. Peptides described in **Table A.7**. were identified through MS:

Table A.7. Digested Peptides of arenin identified through MS analysis.

	ALC (%)	m/z	z	Area	Sequence
P1	80	541.5797	3	3.74E+06	adycfELSRNYGK
P2	99	668.7899	2	1.08E+07	SSFTYYYYDK
P3	92	594.2738	3	3.78E+07	agSSFTYYYYDKATK
P4	91	640.8006	4	3.46E+06	ytacaYYYYDKATKSCKTFR
P5	94	678.2761	2	6.61E+07	TLEDCEATCTR

Alignment of these peptides compared to the full *in silico*-translated sequence of arenin is presented in **Figure A.5.**

```
CLUSTAL O(1.2.4) multiple sequence alignment

P4          --------------ytacaYYYYDKATKSCKTFR------------------------  20
P5          ----------------------------------------------TLEDCEATCTR-  11
P1          adycfELSRNYGK--------------------------------------------  13
Arenin      ADYRCELSRNYGKGSSSFTYYYYDKATKSCKTFRYRGSGGNGNRFKTLEDCEATCVTG  58
P2          ---------------SSFTYYYYDK--------------------------------  10
P3          -------------SGSSFTYYYYDKATK----------------------------  15
```

Figure A.5. Alignment of the peptides predicted by the *de novo* algorithm and *in-silico* translated sequence of arenin.

Residues highlighted in blue were not identified by the *de novo* algorithm of the software PEAKS.

The annotated spectrum with alignment, ion table and error map of each peptide *de novo* predicted by the software PEAKS are presented in **Figures A.6.** through **A.10.**

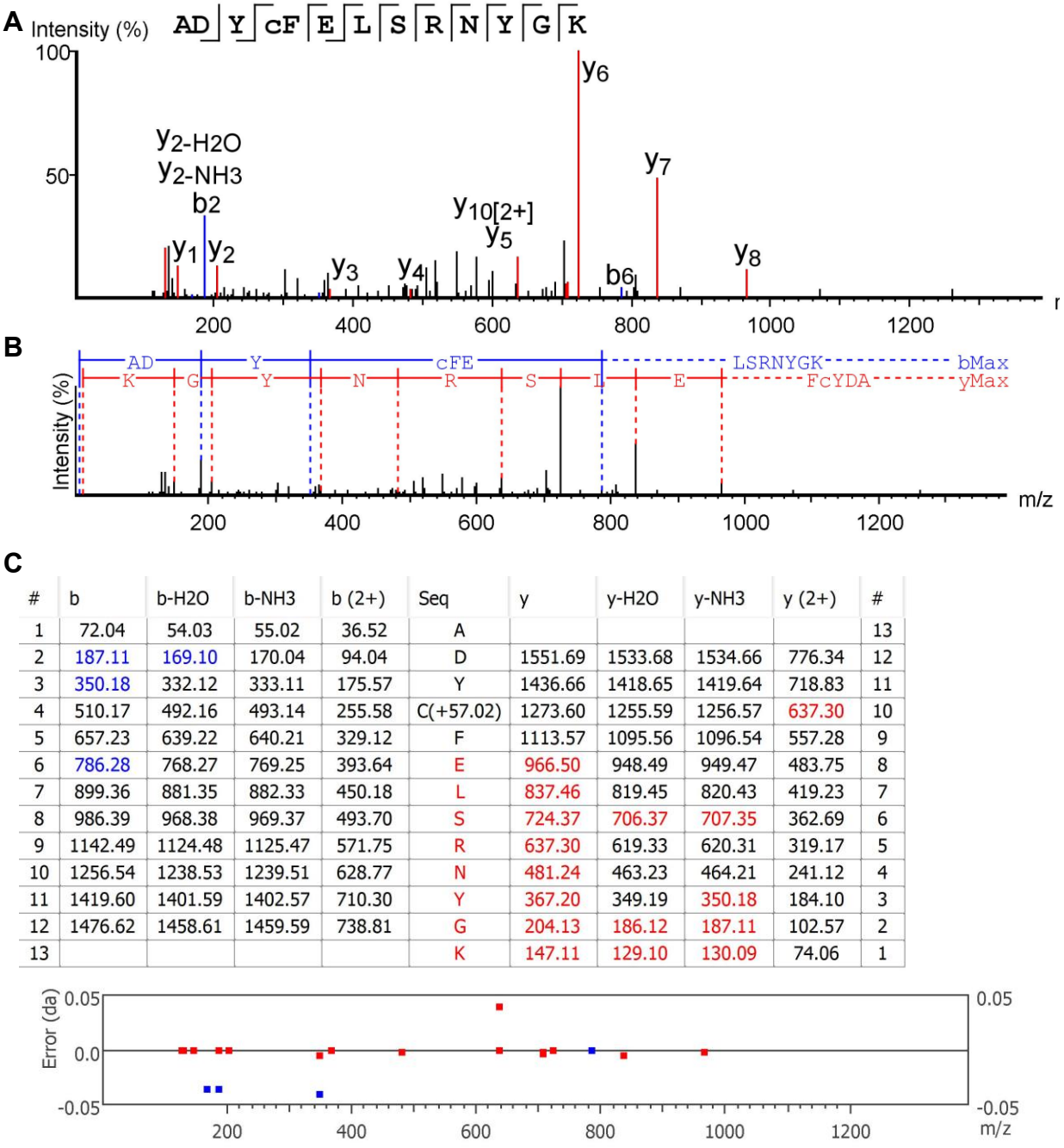

#	b	b-H2O	b-NH3	b (2+)	Seq	y	y-H2O	y-NH3	y (2+)	#
1	72.04	54.03	55.02	36.52	A					13
2	187.11	169.10	170.04	94.04	D	1551.69	1533.68	1534.66	776.34	12
3	350.18	332.12	333.11	175.57	Y	1436.66	1418.65	1419.64	718.83	11
4	510.17	492.16	493.14	255.58	C(+57.02)	1273.60	1255.59	1256.57	637.30	10
5	657.23	639.22	640.21	329.12	F	1113.57	1095.56	1096.54	557.28	9
6	786.28	768.27	769.25	393.64	E	966.50	948.49	949.47	483.75	8
7	899.36	881.35	882.33	450.18	L	837.46	819.45	820.43	419.23	7
8	986.39	968.38	969.37	493.70	S	724.37	706.37	707.35	362.69	6
9	1142.49	1124.48	1125.47	571.75	R	637.30	619.33	620.31	319.17	5
10	1256.54	1238.53	1239.51	628.77	N	481.24	463.23	464.21	241.12	4
11	1419.60	1401.59	1402.57	710.30	Y	367.20	349.19	350.18	184.10	3
12	1476.62	1458.61	1459.59	738.81	G	204.13	186.12	187.11	102.57	2
13					K	147.11	129.10	130.09	74.06	1

Figure A.6. Annotated spectrum with alignment, ion table and error map of the peptide ADYCFELSRNYGK (P1).

(**A**) Annotated spectrum of peptide **ADYCFELSRNYGK** showing identified b and y ions. (**B**) Alignment of the spectrum with the fragment ions generated from the peptide. (**C**) Predicted b and y ions match table with the calculated mass of possible fragment ions. Identified b ions are highlighted in blue and identified y ions are highlighted in red.

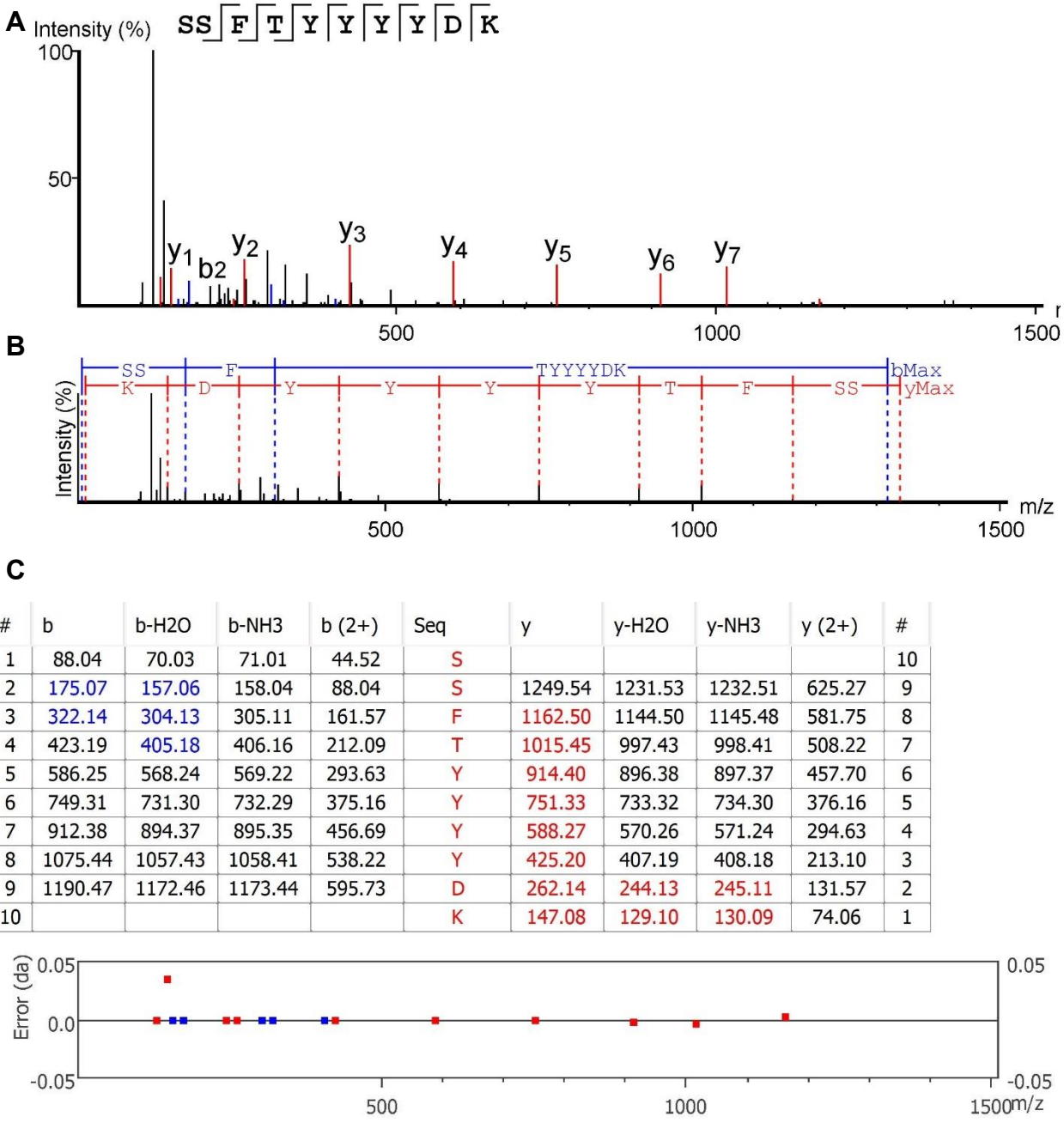

#	b	b-H2O	b-NH3	b (2+)	Seq	y	y-H2O	y-NH3	y (2+)	#
1	88.04	70.03	71.01	44.52	S					10
2	175.07	157.06	158.04	88.04	S	1249.54	1231.53	1232.51	625.27	9
3	322.14	304.13	305.11	161.57	F	1162.50	1144.50	1145.48	581.75	8
4	423.19	405.18	406.16	212.09	T	1015.45	997.43	998.41	508.22	7
5	586.25	568.24	569.22	293.63	Y	914.40	896.38	897.37	457.70	6
6	749.31	731.30	732.29	375.16	Y	751.33	733.32	734.30	376.16	5
7	912.38	894.37	895.35	456.69	Y	588.27	570.26	571.24	294.63	4
8	1075.44	1057.43	1058.41	538.22	Y	425.20	407.19	408.18	213.10	3
9	1190.47	1172.46	1173.44	595.73	D	262.14	244.13	245.11	131.57	2
10					K	147.08	129.10	130.09	74.06	1

Figure A.7. Annotated spectrum with alignment, ion table and error map of the peptide SSFTYYYYDK (P2).

(**A**) Annotated spectrum of peptide **SSFTYYYDK** showing identified b and y ions. (**B**) Alignment of the spectrum with the fragment ions generated from the peptide. (**C**) Predicted b and y ions match table with the calculated mass of possible fragment ions. Identified b ions are highlighted in blue and identified y ions are highlighted in red.

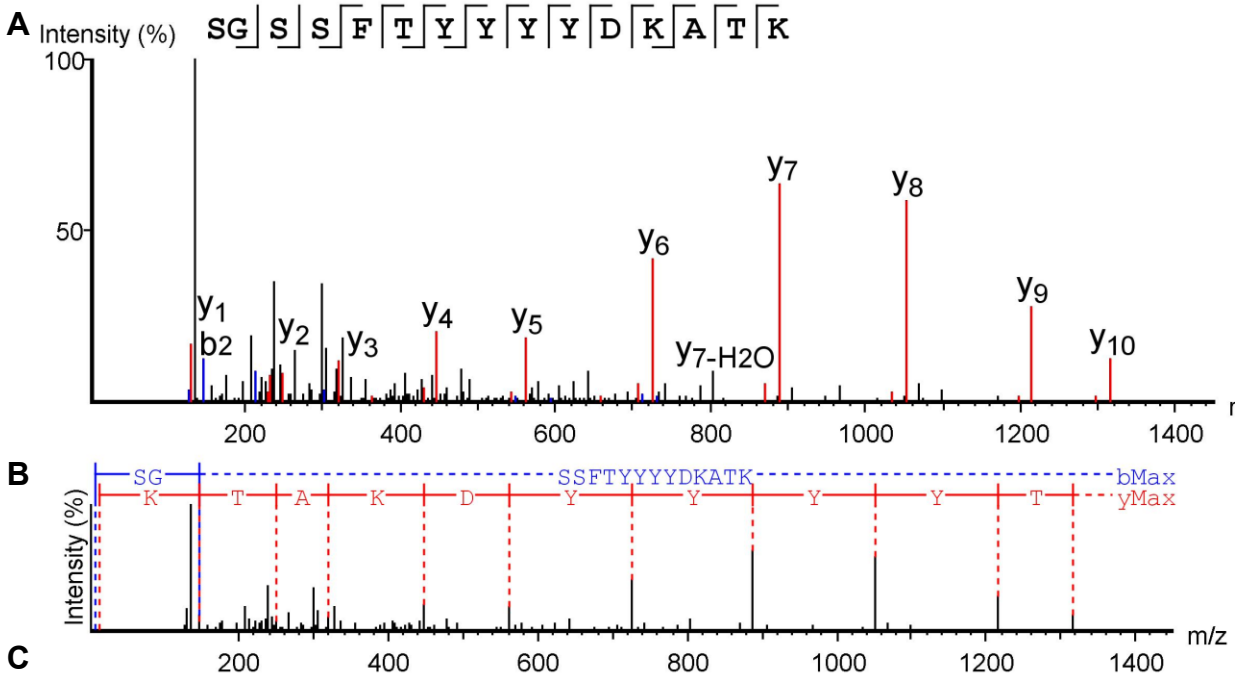

#	b	b-H2O	b-NH3	b (2+)	Seq	y	y-H2O	y-NH3	y (2+)	#
1	88.04	70.03	71.01	44.52	S					15
2	145.06	127.05	128.03	73.03	G	1693.77	1675.76	1676.75	847.39	14
3	232.09	214.08	215.07	116.55	S	1636.75	1618.74	1619.73	818.88	13
4	319.13	301.11	302.10	160.06	S	1549.72	1531.71	1532.69	775.36	12
5	466.19	448.18	449.17	233.60	F	1462.69	1444.68	1445.66	731.85	11
6	567.24	549.23	550.21	284.12	T	1315.62	1297.61	1298.59	658.26	10
7	730.30	712.29	713.29	365.65	Y	1214.58	1196.57	1197.57	607.79	9
8	893.37	875.36	876.34	447.18	Y	1051.51	1033.50	1034.51	526.25	8
9	1056.43	1038.42	1039.40	528.72	Y	888.45	870.44	871.42	444.72	7
10	1219.49	1201.48	1202.47	610.25	Y	725.38	707.37	708.36	363.20	6
11	1334.52	1316.51	1317.49	667.76	D	562.32	544.31	545.29	281.66	5
12	1462.62	1444.61	1445.59	731.85	K	447.29	429.28	430.27	224.15	4
13	1533.65	1515.64	1516.63	767.33	A	319.20	301.19	302.17	160.10	3
14	1634.70	1616.69	1617.67	817.85	T	248.16	230.15	231.11	124.58	2
15					K	147.08	129.10	130.09	74.06	1

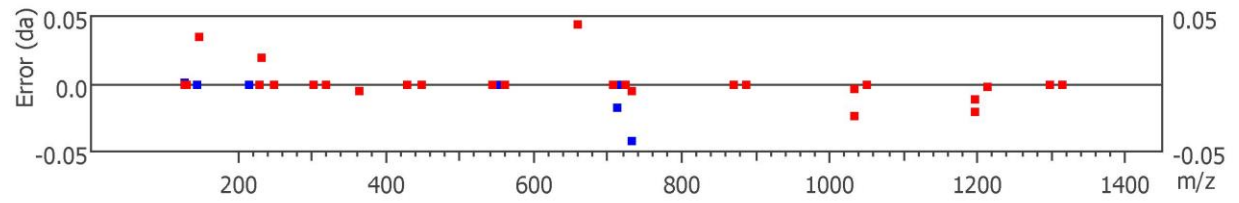

Figure A.8. Annotated spectrum with alignment, ion table and error map of the peptide SGSSFTYYYYDKATK (P3).

(**A**) Annotated spectrum of peptide **SGSSFTYYYYDKATK** showing identified b and y ions. (**B**) Alignment of the spectrum with the fragment ions generated from the peptide. (**C**) Predicted b and y ions match table with the calculated mass of possible fragment ions. Identified b ions are highlighted in blue and identified y ions are highlighted in red.

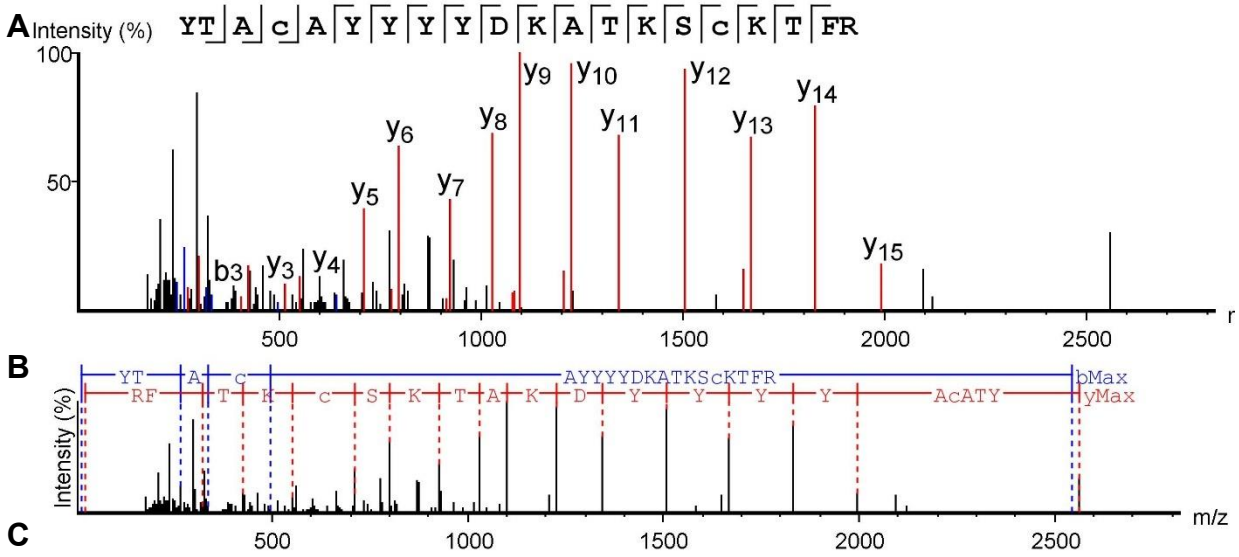

#	b	b-H2O	b-NH3	b (2+)	Seq	y	y-H2O	y-NH3	y (2+)	#
1	164.07	146.06	147.04	82.54	Y					20
2	265.12	247.11	248.09	133.06	T	2397.10	2379.09	2380.07	1199.05	19
3	336.15	318.14	319.15	168.58	A	2296.05	2278.04	2279.03	1148.53	18
4	496.19	478.18	479.16	248.59	C(+57.02)	2225.02	2207.00	2207.99	1113.01	17
5	567.22	549.21	550.20	284.11	A	2064.98	2046.97	2047.96	1032.99	16
6	730.29	712.28	713.26	365.64	Y	1993.94	1975.94	1976.92	997.47	15
7	893.35	875.34	876.32	447.18	Y	1830.88	1812.87	1813.86	915.94	14
8	1056.41	1038.40	1039.39	528.71	Y	1667.81	1649.81	1650.79	834.41	13
9	1219.48	1201.47	1202.45	610.24	Y	1504.75	1486.75	1487.73	752.88	12
10	1334.50	1316.49	1317.48	667.75	D	1341.70	1323.68	1324.67	671.35	11
11	1462.60	1444.59	1445.57	731.80	K	1226.67	1208.66	1209.64	613.83	10
12	1533.64	1515.63	1516.61	767.32	A	1098.57	1080.57	1081.55	549.79	9
13	1634.68	1616.67	1617.66	817.84	T	1027.53	1009.52	1010.51	514.27	8
14	1762.78	1744.77	1745.75	881.89	K	926.48	908.48	909.46	463.74	7
15	1849.81	1831.80	1832.78	925.41	S	798.39	780.38	781.37	399.70	6
16	2009.84	1991.83	1992.81	1005.42	C(+57.02)	711.36	693.35	694.33	356.18	5
17	2137.94	2119.93	2120.91	1069.47	K	551.33	533.32	534.30	276.13	4
18	2238.98	2220.97	2221.96	1119.99	T	423.24	405.18	406.21	212.12	3
19	2386.05	2368.04	2369.03	1193.53	F	322.19	304.13	305.16	161.59	2
20					R	175.12	157.11	158.09	88.06	1

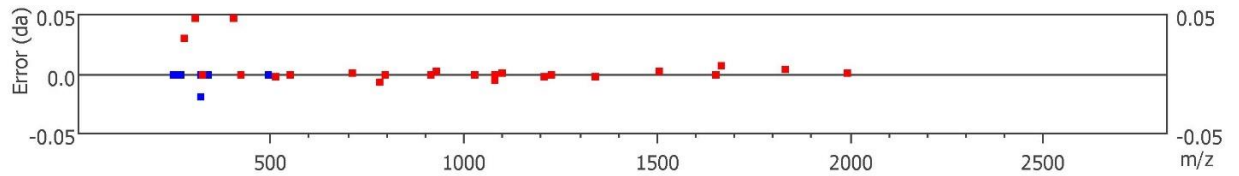

Figure A.9. Annotated spectrum with alignment, ion table and error map of the peptide ytacaYYYYDKATKSCKTFR (P4).

(**A**) Annotated spectrum of peptide **ytacaYYYYDKATKSCKTFR** showing identified b and y ions. (**B**) Alignment of the spectrum with the fragment ions generated from the peptide. (**C**) Predicted b and y ions match table with the calculated mass of possible fragment ions. Identified b ions are highlighted in blue and identified y ions are highlighted in red.

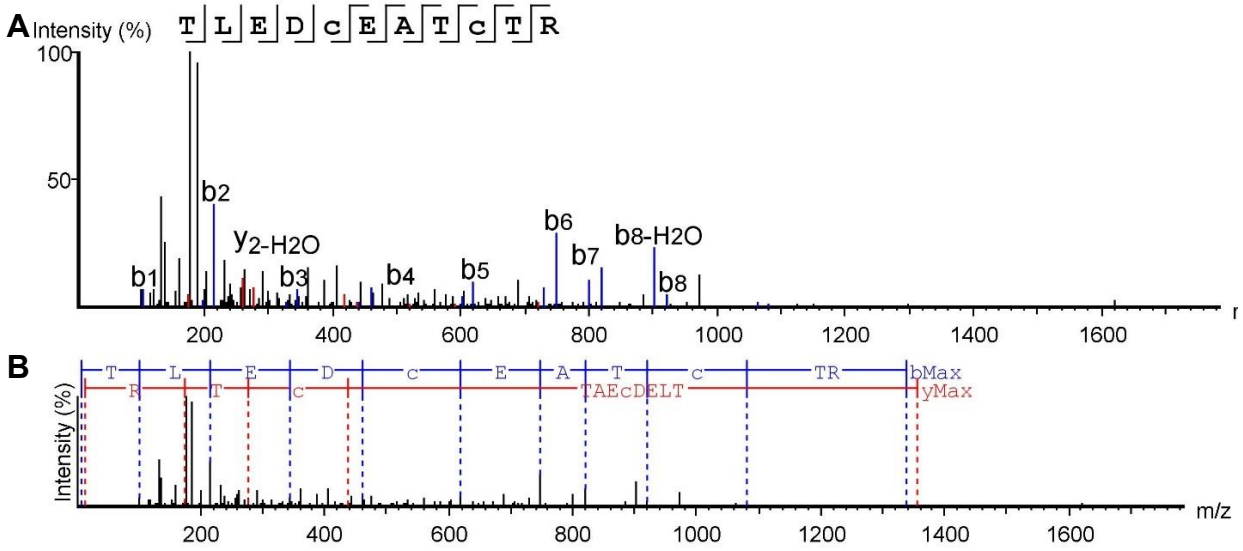

C

#	b	b-H2O	b-NH3	b (2+)	Seq	y	y-H2O	y-NH3	y (2+)	#
1	102.06	84.04	85.03	51.53	T					11
2	215.14	197.13	198.11	108.07	L	1254.51	1236.50	1237.48	627.75	10
3	344.18	326.17	327.13	172.59	E	1141.42	1123.41	1124.40	571.21	9
4	459.21	441.20	442.18	230.10	D	1012.38	994.37	995.36	506.69	8
5	619.24	601.23	602.21	310.12	C(+57.02)	897.36	879.34	880.33	449.18	7
6	748.28	730.27	731.27	374.64	E	737.32	719.31	720.28	369.16	6
7	819.32	801.31	802.29	410.16	A	608.28	590.26	591.24	304.64	5
8	920.36	902.36	903.34	460.68	T	537.24	519.22	520.22	269.12	4
9	1080.39	1062.38	1063.37	540.70	C(+57.02)	436.18	418.17	419.17	218.60	3
10	1181.45	1163.43	1164.42	591.24	T	276.16	258.15	259.14	138.58	2
11					R	175.12	157.11	158.09	88.06	1

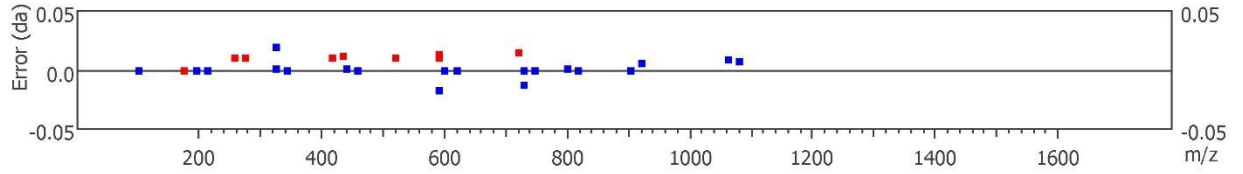

Figure A.10. Annotated spectrum with alignment, ion table and error map of the peptide TLEDCEATCTR (P5).

(**A**) Annotated spectrum of peptide **TLEDCEATCTR** showing identified b and y ions. (**B**) Alignment of the spectrum with the fragment ions generated from the peptide. (**C**) Predicted b and y ions match table with the calculated mass of possible fragment ions. Identified b ions are highlighted in blue and identified y ions are highlighted in red.

cDNA synthesis

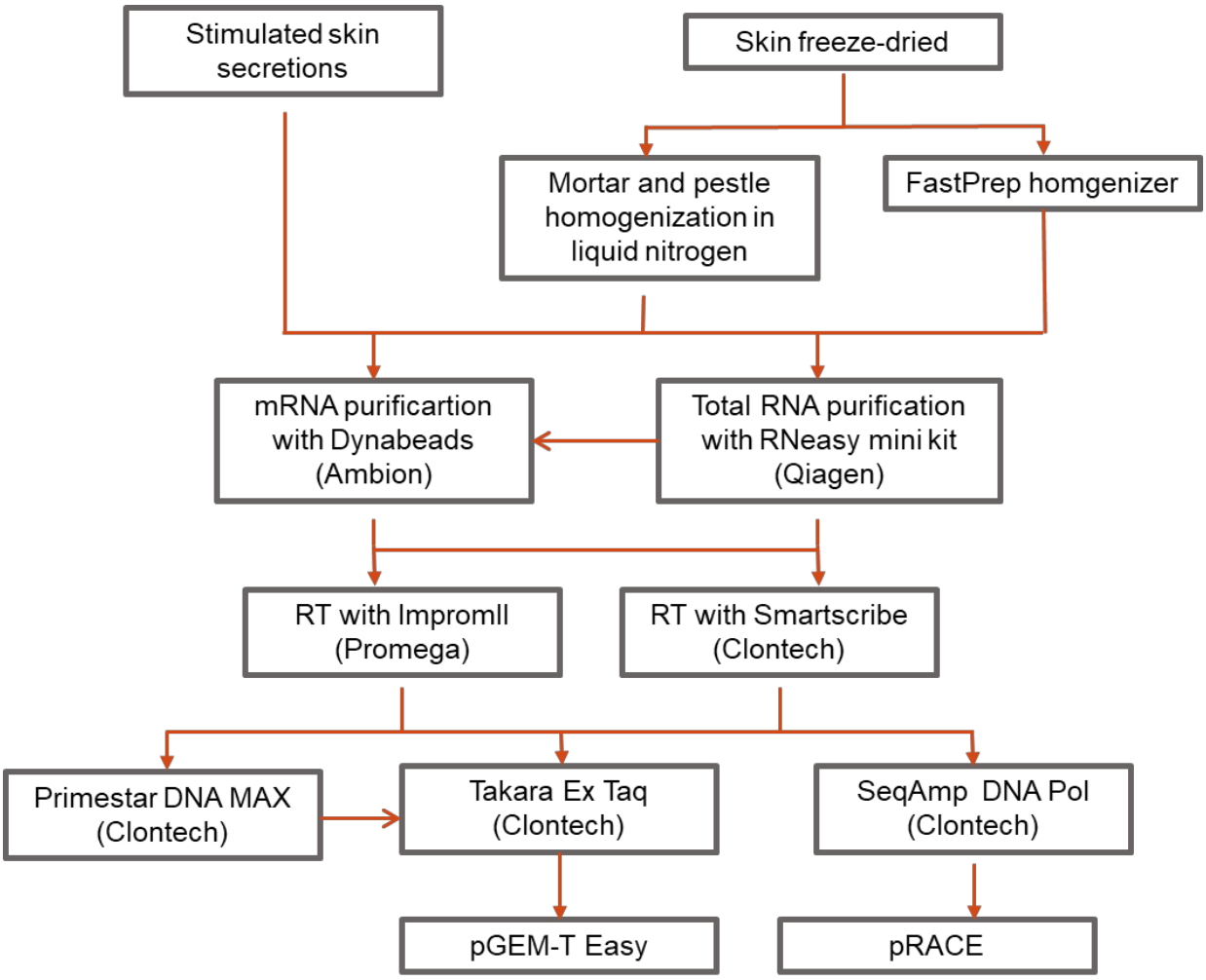

Figure A.11. Flow diagram cDNA synthesis.

During the course of this research, as part of the standardization of the methodology, different strategies for the mRNA isolation and cDNA synthesis were explored, being the most successful the mRNA recovery from stimulated skin secretions, following mRNA purification with Dynabeads, first strand synthesis using Improm II Reverse-Transcriptase, 3'RACE PCR amplification using Primestar DNA MAX (High Fidelity polymerase that produces blunt-end amplicons), amplification of PCR product suitable for cloning using Takara Ex Taq (High Fidelity polymerase that A-tails amplicons) and cloning into pGEM-T Easy for further sequencing using M13 primers.

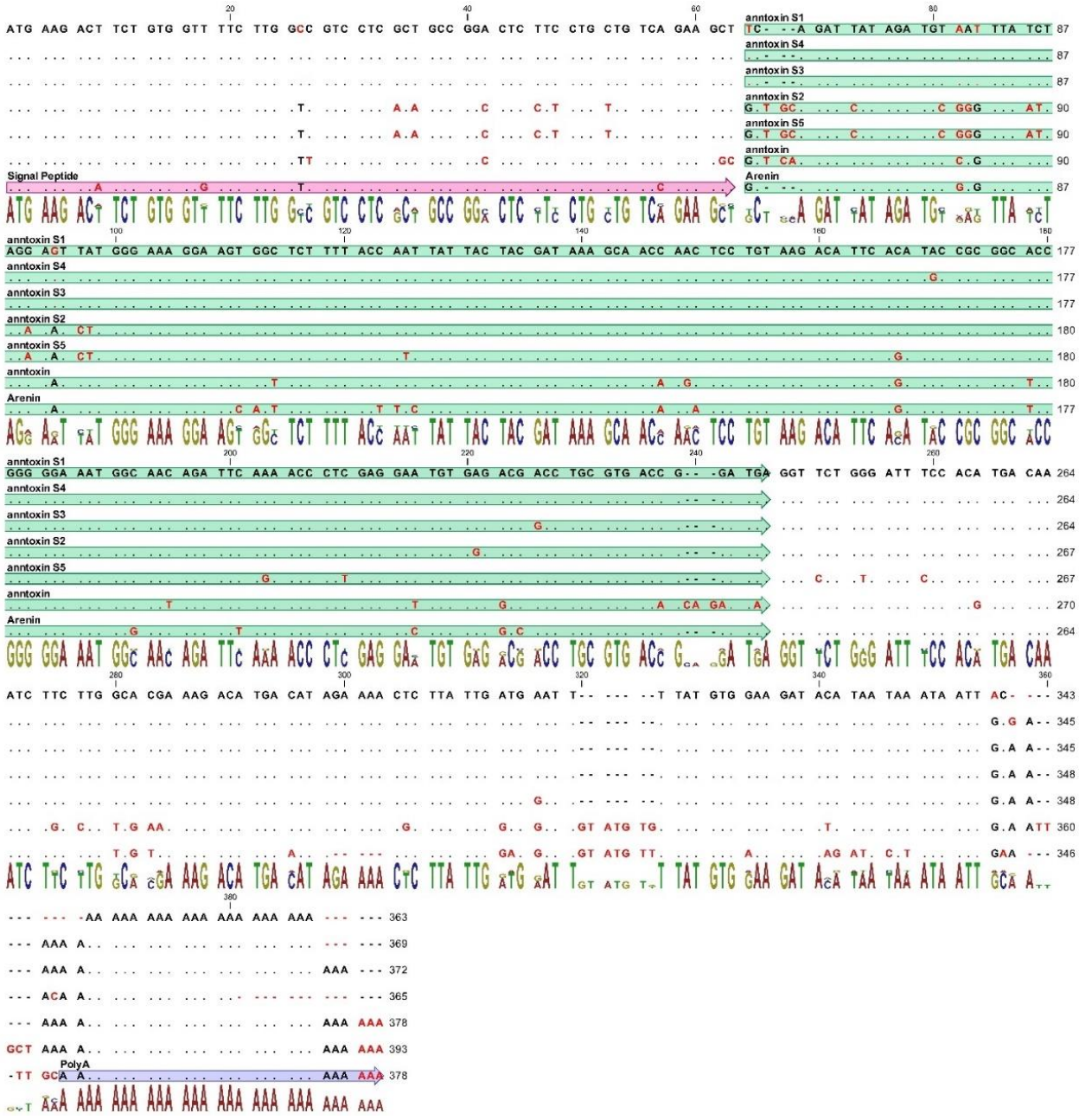

Figure A.12. Arenin cDNA alignment with *H. annectans* and *H. simplex* anntoxins.

Arenin cDNA deposited in GenBank under accession number **MH898942** and aligned with the following sequences obtained from NCBI Nucleotide database: *Hyla annectans* anntoxin mRNA complete cds (**FJ598043.1**), *Hyla simplex* anntoxin S1 mRNA complete cds (**HM747291.1**), *Hyla simplex* S2 mRNA complete cds (**HM747294.1**), *Hyla simplex* S3 mRNA complete cds (**HM747292.1**), *Hyla simplex* S4 mRNA complete cds (**HM747293.1**) and *Hyla simplex* S5 mRNA complete cds (**HM747295.1**).

Bibliography

1. Souza, S. P.; Begossi, A. Whales, dolphins or fishes? The ethnotaxonomy of cetaceans in São Sebastião, Brazil. *J. Ethnobiol. Ethnomed.* **2007**, *3*, 9, doi:10.1186/1746-4269-3-9.
2. Alves, R. R. N.; Rosa, I. L. Why study the use of animal products in traditional medicines? *J. Ethnobiol. Ethnomed.* **2005**, *1*, 5, doi:10.1186/1746-4269-1-5.
3. Alves, R. R. N.; Alves, H. N. The faunal drugstore: animal-based remedies used in traditional medicines in Latin America. *J. Ethnobiol. Ethnomed.* **2011**, *7*, 9, doi:10.1186/1746-4269-7-9.
4. Yesilada, E. Past and future contributions to traditional medicine in the health care system of the Middle-East. *J. Ethnopharmacol.* **2005**, *100*, 135–137, doi:10.1016/j.jep.2005.06.003.
5. Lev, E.; Amar, Z. Ethnopharmacological survey of traditional drugs sold in the Kingdom of Jordan. *J. Ethnopharmacol.* **2002**, *82*, 131–45.
6. Voultsiadou, E. Therapeutic properties and uses of marine invertebrates in the ancient Greek world and early Byzantium. *J. Ethnopharmacol.* **2010**, *130*, 237–247, doi:10.1016/j.jep.2010.04.041.
7. Jacobo-Salcedo, M. D. R.; Alonso-Castro, A. J.; Zarate-Martinez, A. Folk medicinal use of fauna in Mapimi, Durango, México. *J. Ethnopharmacol.* **2011**, *133*, 902–6, doi:10.1016/j.jep.2010.10.005.
8. Alonso-Castro, A. J.; Carranza-Álvarez, C.; Maldonado-Miranda, J. J.; Del Rosario Jacobo-Salcedo, M.; Quezada-Rivera, D. A.; Lorenzo-Márquez, H.; Figueroa-Zúñiga, L. A.; Fernández-Galicia, C.; Ríos-Reyes, N. A.; de León-Rubio, M. Á.; Rodríguez-Gallegos, V.; Medellín-Milán, P. Zootherapeutic practices in Aquismón, San Luis Potosí, México. *J. Ethnopharmacol.* **2011**, *138*, 233–7, doi:10.1016/j.jep.2011.09.020.
9. Mahawar, M.; Jaroli, D. Traditional zootherapeutic studies in India: a review. *J. Ethnobiol. Ethnomed.* **2008**, *4*, 17, doi:10.1186/1746-4269-4-17.
10. Ferreira, F. S.; Brito, S. V.; Sales, D. L.; Menezes, I. R. A.; Coutinho, H. D. M.; Souza, E. P.; Almeida, W. O.; Alves, R. R. N. Anti-inflammatory potential of zootherapeutics derived from animals used in Brazilian traditional medicine. *Pharm. Biol.* **2014**, *52*, 1403–1410, doi:10.3109/13880209.2014.894091.
11. van der Meer, J.-Y.; Kellenbach, E.; van den Bos, L. J. From Farm to Pharma: An Overview of Industrial Heparin Manufacturing Methods. *Molecules* **2017**, *22*, doi:10.3390/molecules22061025.
12. Hemker, H. C. A century of heparin: past, present and future. *J. Thromb. Haemost.*

2016, *14*, 2329–2338, doi:10.1111/jth.13555.

13. Xi, X.; Li, B.; Chen, T.; Kwok, H. A Review on Bradykinin-Related Peptides Isolated from Amphibian Skin Secretion. *Toxins (Basel).* **2015**, *7*, 951–970, doi:10.3390/toxins7030951.

14. Rollins-Smith, L. A.; Reinert, L. K.; O'Leary, C. J.; Houston, L. E.; Woodhams, D. C. Antimicrobial Peptide defenses in amphibian skin. *Integr. Comp. Biol.* **2005**, *45*, 137–42, doi:10.1093/icb/45.1.137.

15. Clarke, B. T. The Natural History of Amphibian Skin Secretions, Their Normal Functioning and Potential Medical Applications. *Biol. Rev. Camb. Philos. Soc.* **1997**, *72*, 365–379, doi:10.1017/S0006323197005045.

16. Cardoso, M. H.; Berwanger, N.; Dornelles, M.; Soares, M.; Santos, C.; Rocha, M.; Gonçalves, E.; Campos, S.; Luiz, O. Insights into the Antimicrobial Activities of Unusual Antimicrobial Peptide Families from Amphibian Skin. *J. Clin. Toxicol.* **2014**, *04*, doi:10.4172/2161-0495.1000205.

17. Xu, X.; Lai, R. The Chemistry and Biological Activities of Peptides from Amphibian Skin Secretions. *Chem. Rev.* **2015**, *115*, 1760–1846, doi:10.1021/cr4006704.

18. König, E.; Wesse, C.; C. Murphy, A.; Zhou, M.; Wang, L.; Chen, T.; Shaw, C.; Bininda-Emonds, O. R. P. Molecular cloning of the trypsin inhibitor from the skin secretion of the Madagascan Tomato Frog, Dyscophus guineti (Microhylidae), and insights into its potential defensive role. *Org. Divers. Evol.* **2013**, *13*, 453–461, doi:10.1007/s13127-013-0128-4.

19. Daly, J. W.; Witkop, B.; Bommer, P.; Biemann, K. Batrachotoxin. The Active Principle of the Colombian Arrow Poison Frog, Phyllobates bicolor. *J. Am. Chem. Soc.* **1965**, *87*, 124–126, doi:10.1021/ja01079a026.

20. You, D.; Hong, J.; Rong, M.; Yu, H.; Liang, S.; Ma, Y.; Yang, H.; Wu, J.; Lin, D.; Lai, R. The first gene-encoded amphibian neurotoxin. *J. Biol. Chem.* **2009**, *284*, 22079–22086, doi:10.1074/jbc.M109.013276.

21. Lev, E. Traditional healing with animals (zootherapy): medieval to present-day Levantine practice. *J. Ethnopharmacol.* **2003**, *85*, 107–118, doi:10.1016/S0378-8741(02)00377-X.

22. Alonso-Castro, A. J. Use of medicinal fauna in Mexican traditional medicine. *J. Ethnopharmacol.* **2014**, *152*, 53–70, doi:10.1016/j.jep.2014.01.005.

23. Rollins-Smith, L. a; Reinert, L. K.; Miera, V.; Conlon, J. M. Antimicrobial peptide defenses of the Tarahumara frog, Rana tarahumarae. *Biochem. Biophys. Res. Commun.* **2002**, *297*, 361–367, doi:10.1016/S0006-291X(02)02217-9.

24. Bai, B.; Zhang, Y.; Wang, H.; Zhou, M.; Yu, Y.; Ding, S.; Chen, T.; Wang, L.; Shaw, C. Parallel peptidome and transcriptome analyses of amphibian skin secretions using archived frozen acid-solvated samples. *Mol. Biotechnol.* **2013**, *54*, 187–197, doi:10.1007/s12033-012-9551-6.

25. Mariano, D. O. C.; Yamaguchi, L. F.; Jared, C.; Antoniazzi, M. M.; Sciani, J. M.; Kato, M. J.; Pimenta, D. C. Pipa carvalhoi skin secretion profiling: Absence of peptides and identification of kynurenic acid as the major constitutive component. *Comp. Biochem. Physiol. C. Toxicol. Pharmacol.* **2014**, *167C*, 1–6, doi:10.1016/j.cbpc.2014.08.001.

26. König, E.; Bininda-Emonds, O. R. P.; Shaw, C. The diversity and evolution of anuran skin peptides. *Peptides* **2015**, *63*, 96–117, doi:10.1016/j.peptides.2014.11.003.

27. Nguyen, L. T.; Haney, E. F.; Vogel, H. J. The expanding scope of antimicrobial peptide structures and their modes of action. *Trends Biotechnol.* **2011**, *29*, 464–472, doi:10.1016/j.tibtech.2011.05.001.

28. Faivovich, J.; Haddad, C. F. B.; Garcia, P. C. a.; Frost, D. R.; Campbell, J. a.; Wheeler, W. C. Systematic Review of the Frog Family Hylidae, With Special Reference To Hylinae: Phylogenetic Analysis and Taxonomic Revision. *Bull. Am. Museum Nat. Hist.* **2005**, *294*, 1, doi:10.1206/0003-0090(2005)294[0001:SROTFF]2.0.CO;2.

29. Conlon, J. M.; Kolodziejek, J.; Nowotny, N. Antimicrobial peptides from the skins of North American frogs. *Biochim. Biophys. Acta - Biomembr.* **2009**, *1788*, 1556–1563, doi:10.1016/j.bbamem.2008.09.018.

30. Duellman, W. E.; Marion, A. B.; Hedges, S. B. *Phylogenetics, classification, and biogeography of the treefrogs (Amphibia: Anura: Arboranae)*; Auckland, New Zealand, 2016; Vol. 4104; ISBN 9781775579373.

31. Calderon, L.; Stabeli, R. *Changing Diversity in Changing Environment*; Grillo, O., Ed.; InTech: Rijeka, Croatia, 2011; ISBN 978-953-307-796-3.

32. Bevins, C. L.; Zasloff, M. Peptides from frog skin. *Annu. Rev. Biochem.* **1990**, *59*, 395–414, doi:10.1146/annurev.bi.59.070190.002143.

33. Savalli, U. BIO370-Frog Skin Available online: http://www.savalli.us/BIO370/Anatomy/4.FrogSkin.html (accessed on Oct 30, 2018).

34. Goniakowska-Witalińska, L.; Kubiczek, U. The structure of the skin of the tree frog (Hyla arborea arborea L.). *Ann. Anat. - Anat. Anzeiger* **1998**, *180*, 237–246, doi:10.1016/S0940-9602(98)80080-0.

35. Stebbins, R. C. (Robert C. *A field guide to western reptiles and amphibians*; Houghton Mifflin, 2003; ISBN 0395982723.

36. NatureServe Comprehensive Report Species - Dryophytes arenicolor Available online: http://explorer.natureserve.org/servlet/NatureServe?searchName=hyla+arenicolor (accessed on Oct 28, 2018).

37. Hammerson, G.; Santos-Barrera, G. Dryophytes arenicolor (amended version of

2010 assessment). The IUCN Red List of Threatened Species 2017: e.T55396A112711835 Available online: https://www.iucnredlist.org/species/55396/112711835 (accessed on Oct 29, 2018).

38. Klymus, K. E.; Carl Gerhardt, H. AFLP markers resolve intra-specific relationships and infer genetic structure among lineages of the canyon treefrog, Hyla arenicolor. *Mol. Phylogenet. Evol.* **2012**, *65*, 654–667, doi:10.1016/j.ympev.2012.07.028.

39. Klymus, K. E.; Humfeld, S. C.; Marshall, V. T.; Cannatella, D.; Gerhardt, H. C. Molecular patterns of differentiation in canyon treefrogs (Hyla arenicolor): evidence for introgressive hybridization with the Arizona treefrog (H. wrightorum) and correlations with advertisement call differences. *J. Evol. Biol.* **2010**, *23*, 1425–1435, doi:10.1111/j.1420-9101.2010.02008.x.

40. Taylor, J. D. The presence of reflecting platelets in integumental melanophores of the frog, Hyla arenicolor. *J. Ultrasructure Res.* **1971**, *35*, 532–540, doi:10.1016/S0022-5320(71)80009-6.

41. Snyder, G. K.; Hammerson, G. A. Interrelationships between water economy and thermo-regulation in the Canyon tree-frog Hyla arenicolor. *J. Arid Environ.* **1993**, *25*, 321–329, doi:10.1006/JARE.1993.1065.

42. Di Cera, E. Serine proteases. *IUBMB Life* **2009**, *61*, 510–5, doi:10.1002/iub.186.

43. Song, G.; Zhou, M.; Chen, W.; Chen, T.; Walker, B.; Shaw, C. HV-BBI-A novel amphibian skin Bowman-Birk-like trypsin inhibitor. *Biochem. Biophys. Res. Commun.* **2008**, *372*, 191–196, doi:10.1016/j.bbrc.2008.05.035.

44. Chen, X.; Wang, H.; Shen, Y.; Wang, L.; Zhou, M.; Chen, T.; Shaw, C. Kunitzins: Prototypes of a new class of protease inhibitor from the skin secretions of European and Asian frogs. *Biochem. Biophys. Res. Commun.* **2016**, *477*, 302–309, doi:10.1016/j.bbrc.2016.06.062.

45. Shigetomi, H.; Onogi, A.; Kajiwara, H.; Yoshida, S.; Furukawa, N.; Haruta, S.; Tanase, Y.; Kanayama, S.; Noguchi, T.; Yamada, Y.; Oi, H.; Kobayashi, H. Anti-inflammatory actions of serine protease inhibitors containing the Kunitz domain. *Inflamm. Res.* **2010**, *59*, 679–687, doi:10.1007/s00011-010-0205-5.

46. Otlewski, J.; Jelen, F.; Zakrzewska, M.; Oleksy, A. The many faces of protease-protein inhibitor interaction. *EMBO J.* **2005**, *24*, 1303–1310, doi:10.1038/sj.emboj.7600611.

47. Rawlings, N. D.; Morton, F. R.; Kok, C. Y.; Kong, J.; Barrett, A. J. MEROPS: the peptidase database. *Nucleic Acids Res.* **2007**, *36*, D320–D325, doi:10.1093/nar/gkm954.

48. Harvey, A. L. Twenty years of dendrotoxins. *Toxicon* **2001**, *39*, 15–26.

49. Salier, J. P. Inter-alpha-trypsin inhibitor: emergence of a family within the Kunitz-type protease inhibitor superfamily. *Trends Biochem. Sci.* **1990**, *15*, 435–9, doi:10.1016/0968-0004(90)90282-G.

50. Chua, L. M.; Lim, M. L.; Wong, B. S. The Kunitz-protease inhibitor domain in amyloid precursor protein reduces cellular mitochondrial enzymes expression and function. *Biochem. Biophys. Res. Commun.* **2013**, *437*, 642–647, doi:10.1016/j.bbrc.2013.07.022.

51. Sprecher, C. A.; Kisiel, W.; Mathewes, S.; Foster, D. C. Molecular cloning, expression, and partial characterization of a second human tissue-factor-pathway inhibitor. *Proc. Natl. Acad. Sci.* **1994**, *91*, 3353–3357, doi:10.1073/pnas.91.8.3353.

52. Mignogna, G.; Pascarella, S.; Wechselberger, C.; Hinterleitner, C.; Mollay, C.; Amiconi, G. I. N.; Barra, D.; Kreil, G.; Biochimiche, S.; Fanelli, A. R.; Sapienza, U. La BSTI, a trypsin inhibitor from skin secretions of Bombina bombina related to protease inhibitors of nematodes. *Protein Sci.* **1996**, *5*, 357–362, doi:10.1002/pro.5560050220.

53. Wu, J.; Liu, H.; Yang, H.; Yu, H.; You, D.; Ma, Y.; Ye, H.; Lai, R. Proteomic analysis of skin defensive factors of tree frog Hyla simplex. *J. Proteome Res.* **2011**, *10*, 4230–4240, doi:10.1021/pr200393t.

54. Conlon, J. M.; Kim, J. B. A protease inhibitor of the Kunitz family from skin secretions of the tornato frog, Dyscophus guineti (Microhylidae). *Biochem. Biophys. Res. Commun.* **2000**, *279*, 961–964, doi:10.1006/bbrc.2000.4052.

55. Day, J. R. S.; Taylor, K. M.; Lidington, E. A.; Mason, J. C.; Haskard, D. O.; Randi, A. M.; Landis, R. C. Aprotinin inhibits proinflammatory activation of endothelial cells by thrombin through the protease-activated receptor 1. *J. Thorac. Cardiovasc. Surg.* **2006**, *131*, 21–27, doi:10.1016/j.jtcvs.2005.08.050.

56. Day, J. R. S.; Landis, R. C.; Taylor, K. M. Aprotinin and the Protease-Activated Receptor 1 Thrombin Receptor: Antithrombosis, Inflammation, and Stroke Reduction. *Semin. Cardiothorac. Vasc. Anesth.* **2006**, *10*, 132–142, doi:10.1177/1089253206288997.

57. Wei, L.; Dong, L.; Zhao, T.; You, D.; Liu, R.; Liu, H.; Yang, H.; Lai, R. Analgesic and anti-inflammatory effects of the amphibian neurotoxin, anntoxin. *Biochimie* **2011**, *93*, 995–1000, doi:10.1016/j.biochi.2011.02.010.

58. Richter, K.; Egger, R.; Kreil, G. Sequence of preprocaerulein cDNAs cloned from skin of Xenopus laevis. A small family of precursors containing one, three, or four copies of the final product. *J. Biol. Chem.* **1986**, *261*, 3676–3680.

59. Hoffmann, W.; Bach, T. C.; Seliger, H.; Kreil, G. Biosynthesis of caerulein in the skin of Xenopus laevis: partial sequences of precursors as deduced from cDNA clones. *EMBO J.* **1983**, *2*, 111–114.

60. Zasloff, M. Magainins, a class of antimicrobial peptides from Xenopus skin: isolation, characterization of two active forms, and partial cDNA sequence of a precursor. *Proc. Natl. Acad. Sci. U. S. A.* **1987**, *84*, 5449–53, doi:10.1097/00043764-198806000-00004.

61. Conlon, J. M. Purification of naturally occurring peptides by reversed-phase HPLC.

Nat. Protoc. **2007**, *2*, 191–197, doi:10.1038/nprot.2006.437.

62. Conlon, J. M. Measurement of Neurokinin B by Radioimmunoassay. *Methods Neurosci.* **1991**, *6*, 221–231, doi:10.1016/B978-0-12-185261-0.50019-8.

63. Marley, P. D.; Rehfeld, J. F. Extraction techniques for gastrins and cholecystokinins in the rat central nervous system. *J. Neurochem.* **1984**, *42*, 1515–22.

64. LAEMMLI, U. K. Cleavage of Structural Proteins during the Assembly of the Head of Bacteriophage T4. *Nature* **1970**, *227*, 680–685, doi:10.1038/227680a0.

65. Schägger, H. Tricine–SDS-PAGE. *Nat. Protoc.* **2006**, *1*, 16–22, doi:10.1038/nprot.2006.4.

66. Gronow, M.; Griffiths, G. Rapid isolation and separation of the non-histone proteins of rat liver nuclei. *FEBS Lett.* **1971**, *15*, 340–344.

67. MacGillivray, A. J.; Rickwood, D. The heterogeneity of mouse-chromatin nonhistone proteins as evidenced by two-dimensional polyacrylamide-gel electrophoresis and ion-exchange chromatography. *Eur. J. Biochem.* **1974**, *41*, 181–90.

68. Rabilloud, T.; Lelong, C. Two-dimensional gel electrophoresis in proteomics: A tutorial. *J. Proteomics* **2011**, *74*, 1829–1841, doi:10.1016/j.jprot.2011.05.040.

69. Dépagne, J.; Chevalier, F. Technical updates to basic proteins focalization using IPG strips. *Proteome Sci.* **2012**, *10*, 54, doi:10.1186/1477-5956-10-54.

70. Gorg, A. 2-D Electrophoresis. Principles and Methods. *Handbook* **2004**, 163, doi:10.1186/1755-8794-4-24.

71. Luche, S.; Diemer, H.; Tastet, C.; Chevallet, M.; Van Dorsselaer, A.; Leize-Wagner, E.; Rabilloud, T. About thiol derivatization and resolution of basic proteins in two-dimensional electrophoresis. *Proteomics* **2004**, *4*, 551–561, doi:10.1002/pmic.200300589.

72. Mutt, V.; Jorpes, J. E. Contemporary developments in the biochemistry of the gastrointestinal hormones. *Recent Prog. Horm. Res.* **1967**, *23*, 483–503.

73. GUILLEMIN, R.; SAKIZ, E.; WARD, D. N. FURTHER PURIFICATION OF TSH-RELEASING FACTOR (TRF) FROM SHEEP HYPOTHALAMIC TISSUES, WITH OBSERVATIONS ON THE AMINO ACID COMPOSITION. *Proc. Soc. Exp. Biol. Med.* **1965**, *118*, 1132–7.

74. Schally, A. V; Bowers, C. Y.; Redding, T. W.; Barrett, J. F. Isolation of thyrotropin releasing factor (TRF) from porcine hypothalamus. *Biochem. Biophys. Res. Commun.* **1966**, *25*, 165–9.

75. Ebersole, T. J.; Conlon, J. M.; Goetz, F. W.; Boyd, S. K. Characterization and distribution of neuropeptide Y in the brain of a caecilian amphibian. *Peptides* **2001**, *22*, 325–34.

76. Gritti, F.; Guiochon, G. Surface Heterogeneity of Six Commercial Brands of End-Capped C18-Bonded Silica. RPLC Separations. *Anal. Chem.* **2003**, *75*, 5726–5738, doi:10.1021/ac0301752.

77. Soloviev, M. *Peptidomics*; Soloviev, M., Ed.; Methods in Molecular Biology; Humana Press: Totowa, NJ, 2010; Vol. 615; ISBN 978-1-60761-534-7.

78. Kuipers, B. J. H.; Gruppen, H. Prediction of molar extinction coefficients of proteins and peptides using UV absorption of the constituent amino acids at 214 nm to enable quantitative reverse phase high-performance liquid chromatography-mass spectrometry analysis. *J. Agric. Food Chem.* **2007**, *55*, 5445–5451, doi:10.1021/jf070337l.

79. Pearson, J. D.; McCroskey, M. C. Perfluorinated acid alternatives to trifluoroacetic acid for reversed-phase high-performance liquid chromatography. *J. Chromatogr. A* **1996**, *746*, 277–81.

80. Krokhin, O. V.; Ying, S.; Cortens, J. P.; Ghosh, D.; Spicer, V.; Ens, W.; Standing, K. G.; Beavis, R. C.; Wilkins, J. A. Use of Peptide Retention Time Prediction for Protein Identification by off-line Reversed-Phase HPLC−MALDI MS/MS. *Anal. Chem.* **2006**, *78*, 6265–6269, doi:10.1021/ac060251b.

81. Jennifer F. Nemeth-Cawley, *; Bruce S. Tangarone, and; Rouse, J. C. “Top Down” Characterization Is a Complementary Technique to Peptide Sequencing for Identifying Protein Species in Complex Mixtures. **2003**, doi:10.1021/PR034008U.

82. EDMAN, P. A method for the determination of amino acid sequence in peptides. *Arch. Biochem.* **1949**, *22*, 475.

83. Steen, H.; Mann, M. The ABC’s (and XYZ’s) of peptide sequencing. *Nat. Rev. Mol. Cell Biol.* **2004**, *5*, 699–711, doi:10.1038/nrm1468.

84. Fales, H. M.; Nagai, Y.; Milne, G. W. A.; Bryan Brewer, H.; Bronzert, T. J.; Pisano, J. J. Use of chemical lonization mass spectrometry in analysis of amino acid phenylthiohydantoin derivatives formed during edman degradation of proteins. *Anal. Biochem.* **1971**, *43*, 288–299, doi:10.1016/0003-2697(71)90136-9.

85. Schulten, H.-R.; Wittmann-Liebold, B. High resolution field desorption mass spectrometry V: Mixtures of amino acid phenylthiohydantoins and Edman degradation products. *Anal. Biochem.* **1976**, *76*, 300–310, doi:10.1016/0003-2697(76)90288-8.

86. Bradley, C. V; Williams, D. H.; Hanley, M. R. Peptide sequencing using the combination of edman degradation, carboxypeptidase digestion and fast atom bombardment mass spectrometry. *Biochem. Biophys. Res. Commun.* **1982**, *104*, 1223–30.

87. Seidler, J.; Zinn, N.; Boehm, M. E.; Lehmann, W. D. De novo sequencing of peptides by MS/MS. *Proteomics* **2010**, *10*, 634–649, doi:10.1002/pmic.200900459.

88. Perkins, D. N.; Pappin, D. J. C.; Creasy, D. M.; Cottrell, J. S. Probability-based

protein identification by searching sequence databases using mass spectrometry data. *Electrophoresis* **1999**, *20*, 3551–3567, doi:10.1002/(SICI)1522-2683(19991201)20:18<3551::AID-ELPS3551>3.0.CO;2-2.

89. Yates III, J. R.; Eng, J. K.; Clauser, K. R.; Burlingame, A. L. Search of sequence databases with uninterpreted high-energy collision-induced dissociation spectra of peptides. *J. Am. Soc. Mass Spectrom.* **1996**, *7*, 1089–1098, doi:10.1016/S1044-0305(96)00079-7.

90. Craig, R.; Beavis, R. C. TANDEM: matching proteins with tandem mass spectra. *Bioinformatics* **2004**, *20*, 1466–1467, doi:10.1093/bioinformatics/bth092.

91. Geer, L. Y.; Markey, S. P.; Kowalak, J. A.; Wagner, L.; Xu, M.; Maynard, D. M.; Yang, X.; Shi, W.; Bryant, S. H. Open Mass Spectrometry Search Algorithm. *J. Proteome Res.* **2004**, *3*, 958–964, doi:10.1021/pr0499491.

92. Cottrell, J. S. Protein identification using MS/MS data. *J. Proteomics* **2011**, *74*, 1842–1851, doi:10.1016/j.jprot.2011.05.014.

93. Naldrett, M. J.; Zeidler, R.; Wilson, K. E.; Kocourek, A. Concentration and desalting of peptide and protein samples with a newly developed C18 membrane in a Microspin column format. *J. Biomol. Tech.* **2005**, *16*, 421–426.

94. Ma, B.; Zhang, K.; Hendrie, C.; Liang, C.; Li, M.; Doherty-Kirby, A.; Lajoie, G. PEAKS: Powerful software for peptide de novo sequencing by tandem mass spectrometry. *Rapid Commun. Mass Spectrom.* **2003**, *17*, 2337–2342, doi:10.1002/rcm.1196.

95. Shevchenko, A.; Valcu, C.-M.; Junqueira, M. Tools for exploring the proteomosphere. *J. Proteomics* **2009**, *72*, 137–144, doi:10.1016/j.jprot.2009.01.012.

96. Liu, X.; Dekker, L. J. M.; Wu, S.; Vanduijn, M. M.; Luider, T. M.; Tolić, N.; Kou, Q.; Dvorkin, M.; Alexandrova, S.; Vyatkina, K.; Paša-Tolić, L.; Pevzner, P. A. De Novo Protein Sequencing by Combining Top-Down and Bottom-Up Tandem Mass Spectra. *J. Proteome Res.* **2014**, *13*, 3241–3248, doi:10.1021/pr401300m.

97. Giansanti, P.; Tsiatsiani, L.; Low, T. Y.; Heck, A. J. R. Six alternative proteases for mass spectrometry-based proteomics beyond trypsin. *Nat. Protoc.* **2016**, *11*, 993–1006, doi:10.1038/nprot.2016.057.

98. Jesús Yagüe; Alberto Paradela; Manuel Ramos; Samuel Ogueta; Anabel Marina; Fernando Barahona; José A. López de Castro, and; Vázquez*, J. Peptide Rearrangement during Quadrupole Ion Trap Fragmentation: Added Complexity to MS/MS Spectra. **2003**, doi:10.1021/AC026280D.

99. Schaefer, H.; Chamrad, D. C.; Marcus, K.; Reidegeld, K. A.; Blüggel, M.; Meyer, H. E. Tryptic transpeptidation products observed in proteome analysis by liquid chromatography-tandem mass spectrometry. *Proteomics* **2005**, *5*, 846–852, doi:10.1002/pmic.200401203.

100. Robertson, L. S.; Fellers, G. M.; Marranca, J. M.; Kleeman, P. M. Expression analysis and identification of antimicrobial peptide transcripts from six North American frog species. *Dis. Aquat. Organ.* **2013**, *104*, 225–236, doi:10.3354/dao02601.

101. Chen, T.; Farragher, S.; Bjourson, A. J.; Orr, D. F.; Rao, P.; Shaw, C. Granular gland transcriptomes in stimulated amphibian skin secretions. *Biochem. J.* **2003**, *371*, 125–30, doi:10.1042/BJ20021343.

102. Kit, P. Dynabeads ® mRNA Purification Kit. **2012**, 1–2.

103. Yeku, O.; Frohman, M. A. Rapid Amplification of cDNA Ends (RACE). In; Humana Press, 2011; pp. 107–122.

104. Goebel, a M.; Donnelly, J. M.; Atz, M. E. PCR primers and amplification methods for 12S ribosomal DNA, the control region, cytochrome oxidase I, and cytochrome b in bufonids and other frogs, and an overview of PCR primers which have amplified DNA in amphibians successfully. *Mol. Phylogenet. Evol.* **1999**, *11*, 163–199, doi:10.1006/mpev.1998.0538.

105. Conlon, J. M.; Leprince, J. Identification and Analysis of Bioactive Peptides in Amphibian Skin Secretions. In *Peptidomics, Methods in Molecular Biology*; New York, NY, 2010; Vol. 615, pp. 145–157 ISBN 978-1-60761-534-7.

106. Gammill, W. M.; Scott Fites, J.; Rollins-Smith, L. A. Norepinephrine depletion of antimicrobial peptides from the skin glands of Xenopus laevis. *Dev. Comp. Immunol.* **2012**, *37*, 19–27, doi:10.1016/j.dci.2011.12.012.

107. Groot, H.; Muñoz-Camargo, C.; Moscoso, J.; Riveros, G.; Salazar, V.; Kaston Florez, F.; Mitrani, E. Skin micro-organs from several frog species secrete a repertoire of powerful antimicrobials in culture. *J. Antibiot. (Tokyo).* **2012**, *65*, 461–467, doi:10.1038/ja.2012.50.

108. Gallart-Palau, X.; Serra, A.; Lee, B. S. T.; Guo, X.; Sze, S. K. Brain ureido degenerative protein modifications are associated with neuroinflammation and proteinopathy in Alzheimer's disease with cerebrovascular disease. *J. Neuroinflammation* **2017**, *14*, 1–12, doi:10.1186/s12974-017-0946-y.

109. Serra, A.; Hemu, X.; Nguyen, G. K. T.; Nguyen, N. T. K.; Sze, S. K.; Tam, J. P. A high-throughput peptidomic strategy to decipher the molecular diversity of cyclic cysteine-rich peptides. *Sci. Rep.* **2016**, *6*, doi:10.1038/srep23005.

110. Serra, A.; Zhu, H.; Gallart-Palau, X.; Park, J. E.; Ho, H. H.; Tam, J. P.; Sze, S. K. Plasma proteome coverage is increased by unique peptide recovery from sodium deoxycholate precipitate. *Anal. Bioanal. Chem.* **2016**, *408*, 1963–1973, doi:10.1007/s00216-016-9312-7.

111. Serra, A.; Gallart-Palau, X.; Park, J. E.; Lim, G. G. Y.; Lim, K. L.; Ho, H. H.; Tam, J. P.; Sze, S. K. Vascular Bed Molecular Profiling by Differential Systemic Decellularization In Vivo. *Arterioscler. Thromb. Vasc. Biol.* **2018**, *38*, 2396–2409, doi:10.1161/ATVBAHA.118.311552.

112. Nielsen, H. Predicting Secretory Proteins with SignalP. In; Kihara, D., Ed.; Methods in Molecular Biology; Springer New York: New York, NY, 2017; Vol. 1611, pp. 59–73 ISBN 978-1-4939-7013-1.

113. Bertoni, M.; Kiefer, F.; Biasini, M.; Bordoli, L.; Schwede, T. Modeling protein quaternary structure of homo- and hetero-oligomers beyond binary interactions by homology. *Sci. Rep.* **2017**, *7*, 1–15, doi:10.1038/s41598-017-09654-8.

114. Waterhouse, A.; Bertoni, M.; Bienert, S.; Studer, G.; Tauriello, G.; Gumienny, R.; Heer, F. T.; De Beer, T. A. P.; Rempfer, C.; Bordoli, L.; Lepore, R.; Schwede, T. SWISS-MODEL: Homology modelling of protein structures and complexes. *Nucleic Acids Res.* **2018**, *46*, W296–W303, doi:10.1093/nar/gky427.

115. Pettersen, E. F.; Goddard, T. D.; Huang, C. C.; Couch, G. S.; Greenblatt, D. M.; Meng, E. C.; Ferrin, T. E. UCSF Chimera - A visualization system for exploratory research and analysis. *J. Comput. Chem.* **2004**, *25*, 1605–1612, doi:10.1002/jcc.20084.

116. Erspamer, V.; Erspamer, G. F.; Cei, J. M. Active peptides in the skins of two hundred and thirty American amphibian species. *Comp. Biochem. Physiol. Part C, Comp.* **1986**, *85*, 125–137, doi:10.1016/0742-8413(86)90063-0.

117. Sai, K. P.; Jagannadham, M. V; Vairamani, M.; Raju, N. P.; Devi, A. S.; Nagaraj, R.; Sitaram, N. Tigerinins: novel antimicrobial peptides from the Indian frog Rana tigerina. *J. Biol. Chem.* **2001**, *276*, 2701–7, doi:10.1074/jbc.M006615200.

118. Calabrese, E. Hormesis and Pharmacology. *Pharmacology* **2009**, 75–102, doi:10.1016/B978-0-12-369521-5.00005-1.

119. Cornelius, C.; Graziano, A.; Perrotta, R.; Paola, R. Di; Cuzzocrea, S.; Calabrese, E. J.; Calabrese, V. Cellular Stress Response, Hormesis, and Vitagens in Aging and Longevity: Role of mitochondrial “Chi.” *Inflammation, Adv. Age Nutr.* **2014**, 309–321, doi:10.1016/B978-0-12-397803-5.00026-5.

120. Calabrese, E. J.; Mattson, M. P. Hormesis provides a generalized quantitative estimate of biological plasticity. *J. Cell Commun. Signal.* **2011**, *5*, 25–38, doi:10.1007/s12079-011-0119-1.

121. Bogen, K. T.; Arnold, L. L.; Chowdhury, A.; Pennington, K. L.; Cohen, S. M. Low-dose dose-response for reduced cell viability after exposure of human keratinocyte (HEK001) cells to arsenite. *Toxicol. Reports* **2017**, *4*, 32–38, doi:10.1016/j.toxrep.2016.12.003.

122. Calabrese, E. J. Cancer biology and hormesis: human tumor cell lines commonly display hormetic (biphasic) dose responses. *Crit. Rev. Toxicol.* **2005**, *35*, 463–582.

123. Ben Khalifa, N.; Tyteca, D.; Courtoy, P. J.; Renauld, J. C.; Constantinescu, S. N.; Octave, J. N.; Kienlen-Campard, P. Contribution of Kunitz protease inhibitor and transmembrane domains to amyloid precursor protein homodimerization. *Neurodegener. Dis.* **2012**, *10*, 92–95, doi:10.1159/000335225.

124. Rustgi, S.; Boex-Fontvieille, E.; Reinbothe, C.; von Wettstein, D.; Reinbothe, S. The complex world of plant protease inhibitors: Insights into a Kunitz-type cysteine protease inhibitor of Arabidopsis thaliana. *Commun. Integr. Biol.* **2018**, *11*, e1368599, doi:10.1080/19420889.2017.1368599.

125. Pinkse, M.; Evaristo, G.; Pieterse, M.; Yu, Y.; Verhaert, P. MS approaches to select peptides with post-translational modifications from amphibian defense secretions prior to full sequence elucidation. *EuPA Open Proteomics* **2014**, *5*, 32–40, doi:10.1016/J.EUPROT.2014.11.001.

126. Godfroid, E.; Octave, J. N. Glycosylation of the amyloid peptide precursor containing the Kunitz protease inhibitor domain improves the inhibition of trypsin. *Biochem. Biophys. Res. Commun.* **1990**, *171*, 1015–21.

127. Christeller, J. T. Evolutionary mechanisms acting on proteinase inhibitor variability. *FEBS J.* **2005**, *272*, 5710–5722, doi:10.1111/j.1742-4658.2005.04975.x.

128. Vergnolle, N.; Ferazzini, M.; D'Andrea, M. R.; Buddenkotte, J.; Steinhoff, M. Proteinase-activated receptors: Novel signals for peripheral nerves. *Trends Neurosci.* **2003**, *26*, 496–500, doi:10.1016/S0166-2236(03)00208-X.

129. Rezaie, A. Protease-activated receptor signalling by coagulation proteases in endothelial cells. *Thromb. Haemost.* **2014**, *112*, 876–882, doi:10.1160/th14-02-0167.

130. Conlon, J. M.; Iwamuro, S.; King, J. D. Dermal cytolytic peptides and the system of innate immunity in anurans. *Ann. N. Y. Acad. Sci.* **2009**, *1163*, 75–82, doi:10.1111/j.1749-6632.2008.03618.x.

131. König, E.; Clark, V. C.; Shaw, C.; Bininda-Emonds, O. R. P. Molecular cloning of skin peptide precursor-encoding cDNAs from tibial gland secretion of the Giant Monkey Frog, Phyllomedusa bicolor (Hylidae, Anura). *Peptides* **2012**, *38*, 371–376, doi:10.1016/j.peptides.2012.09.010.

132. Chen, T.; Li, L.; Zhou, M.; Rao, P.; Walker, B.; Shaw, C. Amphibian skin peptides and their corresponding cDNAs from single lyophilized secretion samples : Identification of novel brevinins from three species of Chinese frogs §. **2006**, *27*, 42–48, doi:10.1016/j.peptides.2005.06.024.

133. Tannich, E.; Tümmler, M.; Arnold, H. H.; Lingelbach, K. Deletion mutagenesis in M13 by polymerase chain reaction using universal sequencing primers. *Anal. Biochem.* **1990**, *188*, 255–258, doi:10.1016/0003-2697(90)90602-6.

Published papers

Hernández-Pérez, J.; Serra, A.; Sze, S.K.; Conway, P.L.; Schlundt, J.; Benavides, J. Identification of Arenin, a Novel Kunitz-Like Polypeptide from the Skin Secretions of *Dryophytes arenicolor*. *Int. J. Mol. Sci.* **2018**, *19*, 3644.

https://www.mdpi.com/1422-0067/19/11/3644

International Journal of
Molecular Sciences

MDPI

Article

Identification of Arenin, a Novel Kunitz-Like Polypeptide from the Skin Secretions of *Dryophytes arenicolor*

Jesús Hernández-Pérez [1], Aida Serra [2], Siu Kwan Sze [2], Patricia L. Conway [3,4], Jørgen Schlundt [3,4] and Jorge Benavides [1,*]

1 School of Engineering and Science, Tecnologico de Monterrey, Av. Eugenio Garza Sada 2501 Sur, C.P. 64849 Monterrey, N.L., Mexico; a00799272@itesm.mx
2 School of Biological Sciences, Nanyang Technological University, 60, Nanyang Drive, Singapore 637551, Singapore; aserramaq@ntu.edu.sg (A.S.); sksze@ntu.edu.sg (S.K.S.)
3 Nanyang Technological University Food Technology Centre (NAFTEC), Nanyang Technological University (NTU), Singapore 637459, Singapore; pconway@ntu.edu.sg (P.L.C.); jschlundt@ntu.edu.sg (J.S.)
4 School of Chemical and Biomedical Engineering, Nanyang Technological University (NTU), 62 Nanyang Drive, Singapore 637459, Singapore
* Correspondence; jorben@itesm.mx; Tel.: +52-81-8358-2000 (ext. 4821)

Received: 20 October 2018; Accepted: 17 November 2018; Published: 19 November 2018

Abstract: Amphibian skin secretions are enriched with complex cocktails of bioactive molecules such as proteins, peptides, biogenic amines, alkaloids guanidine derivatives, steroids and other minor components spanning a wide spectrum of pharmacological actions exploited for centuries in folk medicine. This study presents evidence on the protein profile of the skin secretions of the canyon tree frog, *Dryophytes arenicolor*. At the same time, it presents the reverse-phase liquid chromatography isolation, mass spectrometry characterization and identification at mRNA level of a novel 58 amino acids Kunitz-like polypeptide from the skin secretions of *Dryophytes arenicolor*, arenin. Cell viability assays performed on HDFa, CaCo2 and MCF7 cells cultured with different concentrations of arenin showed a discrete effect at low concentrations (2, 4, 8 and 16 μg/mL) suggesting a multi-target interaction in a hormetic-like dose-response. Further work is required to investigate the mechanisms underlying the variable effect on cell viability produced by different concentrations of arenin.

Keywords: amphibians; skin secretions; *Dryophytes arenicolor*; Kunitz-like polypeptide; cytotoxicity

1. Introduction

Amphibians were the first group of vertebrates to make the transition from water to land [1] and over millions of years have been developing a multifunctional skin that is morphologically and biochemically adapted to accomplish both general physiological and more specific survival roles, such as chemical defense against predators [2,3].

Skin secretions synthesized and stored in highly specialized granular glands contain complex cocktails of bioactive molecules such as proteins, peptides, biogenic amines, alkaloids guanidine derivatives, steroids and other minor components spanning a wide spectrum of pharmacological actions exploited for centuries in folk medicine [4–7].

Due to vast amphibian biodiversity, diverse applications and an enormous array of bioactive molecules that have not been described yet, frog and toad (Anurans) skin secretions continue drawing attention as source of novel biologically active molecules [4,8]. Although peptides of 10 to 48 residues long comprise the majority of biomolecules described in literature [8], a considerable number of species from distinct families have been described to lack peptides in their skin secretions [9–12].

Hylidae is one of the largest families of anurans with over 870 species recognized and is considered a rich source of amphibian bioactive peptides. The vast majority of the bioactive peptides and proteins described belong to the subfamilies Pelodryadinae and Phyllomedusinae even though the subfamily Hylinae has the widest distribution and the most species [13,14]. From the hylinae subfamily, the *Hyla* genus, recently divided into Old World (*Hyla*) and New World (*Dryophytes*) subgenera [15], comprises 35 species from which antimicrobial peptides, neuropeptides, wound-healing peptides, antinociception peptides, protease inhibitor peptides, tryptophyllins and caeruleins have been described [8].

Based on the evidence of the presence of bioactive peptides in amphibian skin secretions and taking advantage of the enormous biodiversity in Mexico, we selected a member of the Hylidae family that has been mentioned in ethnopharmacological studies as an ingredient used in Mexican Traditional Medicine (MTM) practices [16,17], to study its skin secretions. Here, we present the first report about the characterization of the skin secretion of *Dryophytes arenicolor*, formerly known as *Hyla arenicolor* [15], a frog with an atypical skin secretion profile due to the absence of low molecular weight peptides and a preliminary activity characterization of its most abundant fraction.

2. Results

2.1. Collection and Identification of D. arenicolor

All specimens utilized in this study were collected in one night at the same location according to their call and morphological characteristics such as size, skin and leg color. Further molecular identification was carried out as described in the collection and identification methodology section. Polymerase chain reaction (PCR) products (GenBank: MG554648) amplified from total DNA extracted from freeze-dried skin of collected frogs using MVZ-59^{F} and tRNAVal^{R} primers resulted in a 1012 bp fragment corresponding to partial sequences of 12S ribosomal RNA and tRNA-Val genes of *D. arenicolor*, formerly known as *Hyla arenicolor*, when searched against the nr/nt database from GenBank using local NCBI-BLASTn software (v2.7.1+).

2.2. Recovery of Skin Secretions Extract

Following the methodology described in the Recovery of the Skin Secretion Extract (SSE) section, average total soluble protein recovered in SSE was 90 $\pm$ 15 μg per gram body weight. None of the frogs tested showed any health complication after release from skin secretions recovery and norepinephrine stimulation.

2.3. Skin Secretion Extract (SSE) Characterization by 2D Polyacrylamide Gel Electrophoresis (2D-PAGE) and Reverse-Phase High-Performance Liquid Chromatography (HPLC)

According to the methodology described for the SSE characterization by 2D gel electrophoresis, 76 spots were stained (Figure 1), revealing the absence of detection of peptides or oligopeptides below 10 kDa, a low content of proteins between 10 and 20 kDa with very well defined spots at pH 3 and pH 7 around 10 kDa; a high content of proteins between 20 to 37 kDa with a higher density between pH 4 and pH 6; and a low content of proteins between 37 and 75 kDa with all of the proteins between pH 3 and 7.

Following the reversed-phase high-performance liquid chromatography (RP-HPLC) method described in the Materials and Methods section, analysis of SSE (Figure 2A) revealed more than 30 peaks when the diode array detector was set to 214 nm for detection of peptide bond (–CONH–) [18]. Compounds with retention times at 22.3 min (Fraction c), 30.2 min (Fraction d) and 36.2 min (Fraction f) were the most abundant species across all specimens tested. minor variations on the relative signal of these compounds between SSE of different individuals were observed, meanwhile the elution profile pattern was maintained reproducible along this study.

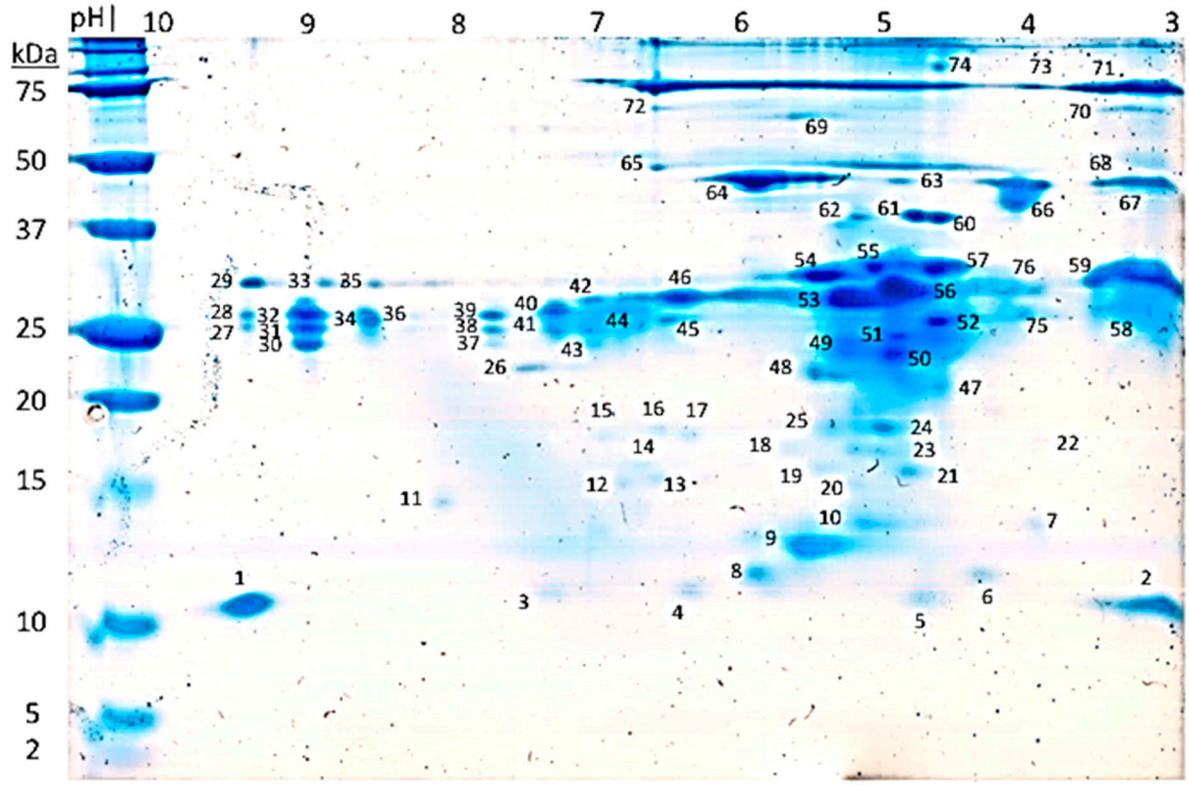

Figure 1. *D. arenicolor*'s skin secretions extract (SSE) Tricine-2D polyacrylamide gel electrophoresis (2D-PAGE). 150 µg of SSE analyzed by Tricine-2D-PAGE yielded 76 spots stained with Colloidal Coomassie Blue.

2.4. Protein Isolation for Activity Evaluation

Based on the RP-HPLC fractionation method described in the protein isolation section, 3 fractions eluting at 10.5 min (Fraction c), 13.6 min (Fraction d) and 22.1 min (Fraction f) were the most abundant species, promoting its purification. Fractions with the same retention time were pooled and analyzed through Tricine-polyacrylamide gel electrophoresis (PAGE) and RP-HPLC (Figure 2) employing the method described in the SSE characterization section.

RP-HPLC analysis revealed that fractions c, d and f corresponded to the 214 nm signals detected at 22.3 min (Figure 2B), 30.2 min (Figure 2C) and 36.2 min (Figure 2D) respectively. Tricine-PAGE showed the correlation between the purified fractions and their apparent molecular weight. Fractions c and d yielded the lowest bands between the molecular marker bands of 10 kDa and 15 kDa, where the band produced by fraction c resolved slightly above the band displayed by fraction d. Fraction f showed a strong 214 nm signal at 36.2 min in RP-HPLC analysis, however it was not possible to detect this fraction through Tricine-PAGE stained either with silver nitrate or colloidal Coomassie.

2.5. Cell Proliferation Inhibition by SSE and HPLC-Purified Fractions

As described in the Materials and Methods section, in order to estimate proliferation of HDFa, CaCo2 and MCF7 cells in the presence of SSE and HPLC fractions at 2 µg/mL, 4 µg/mL, 8 µg/mL, 16 µg/mL, 32 µg/mL, 64 µg/mL and 128 µg/mL, a colorimetric method based on bioreduction of tetrazolium into formazan by cells was selected. Results in Figure 3 are presented as a viability percentage calculated in relation to untreated cells representing 100% viability.

Interestingly, and contrary to what we were expecting, a continuous dose-response relationship was not observed in any of the cell lines tested with both the SSE and the most abundant HPLC fraction (fraction c, Figure 2B). Cells treated with SSE showed a discontinuous trend (Figure 3A). HDFa cells cultured in the presence of SSE showed its highest viability of 86.12% ± 4.30 at 2 µg/mL,

at 4 μg/mL cell viability decreased to its lowest value of 63.87% ± 5.71, then increased to 81.07% ± 6.36 at 8 μg/mL, dropped to 69.55% ± 2.35 at 16 μg/mL, increased at 32 μg/mL to 74.86% ± 3.94, decreased to 72.97% ± 4.58 at 64 μg/mL and continue decreasing to 68.82% ± 3.84 at 128 μg/mL.

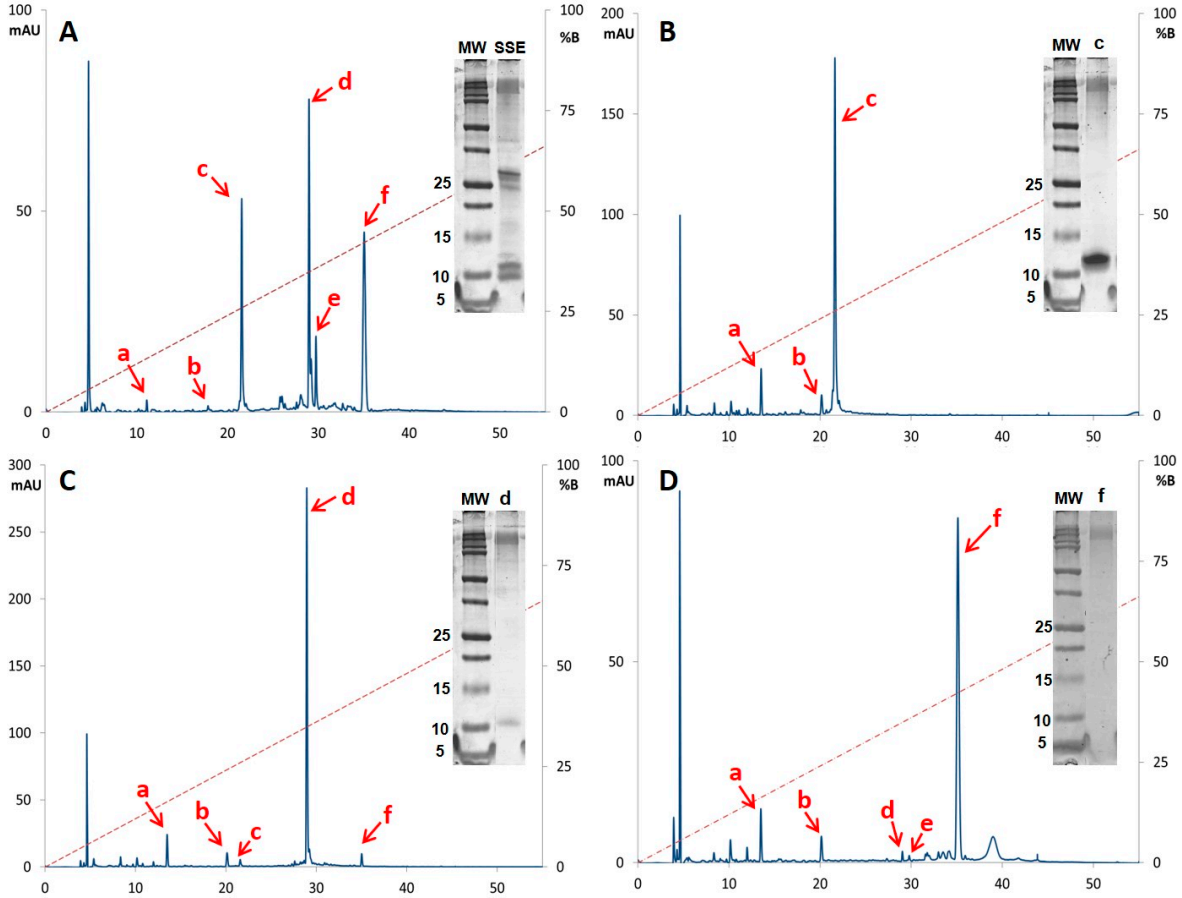

Figure 2. Analytical reverse-phase chromatograms and Tricine sodium dodecyl sulfate (SDS)-PAGE of the more abundant fractions recovered after SSE semi-preparative reversed-phase high-performance liquid chromatography (RP-HPLC) fractionation. (**A**) SSE with recovered fractions indicated by letters a, b, c, d, e and f. (**B**) Fraction c had a retention time of 22.3 min and an apparent molecular weight around 12 kDa. (**C**) Fraction d showed correlation with the 214 nm signal at 30.2 min and an apparent molecular weight around 11 kDa. (**D**) Fraction f showed 214 nm signal at 36.2 min, however it was not possible to correlate this fraction with any Tricine-PAGE band. Red dotted line represents the mobile phase composition for elution in relation to solvent B. M_W: Molecular Weight marker; mAU: milli-Absorbance Units.

Caco-2 cells treated with SSE at 2 μg/mL presented a viability of 87.45% ± 5.69 that increased to 105.25% ± 0.78 at 4 μg/mL, then decreased to 91.16% ± 6.95 at 8 μg/mL, increased to 99.61% ± 2.55 at 16 μg/mL, decreased to 90.36% ± 2.99 at 32 μg/mL, continued decreasing to 86.64% ± 5.17 at 64 μg/mL, and reached its lowest viability of 79.49% ± 1.73 at 128 μg/mL

The SSE effect on MCF7 cells was very similar to the response caused by HPLC fraction c also on MCF7 cells. At 2 μg/mL of SSE, MCF7 cell viability was 96.11% ± 3.36, at 4 μg/mL a 9.84% ± 5.55 surpass on the viability compared to untreated cells was observed, cell viability at 8 μg/mL decreased to 99.5% ± 6.06 and continued decreasing up to 80.80% ± 2.16 at 128 μg/mL.

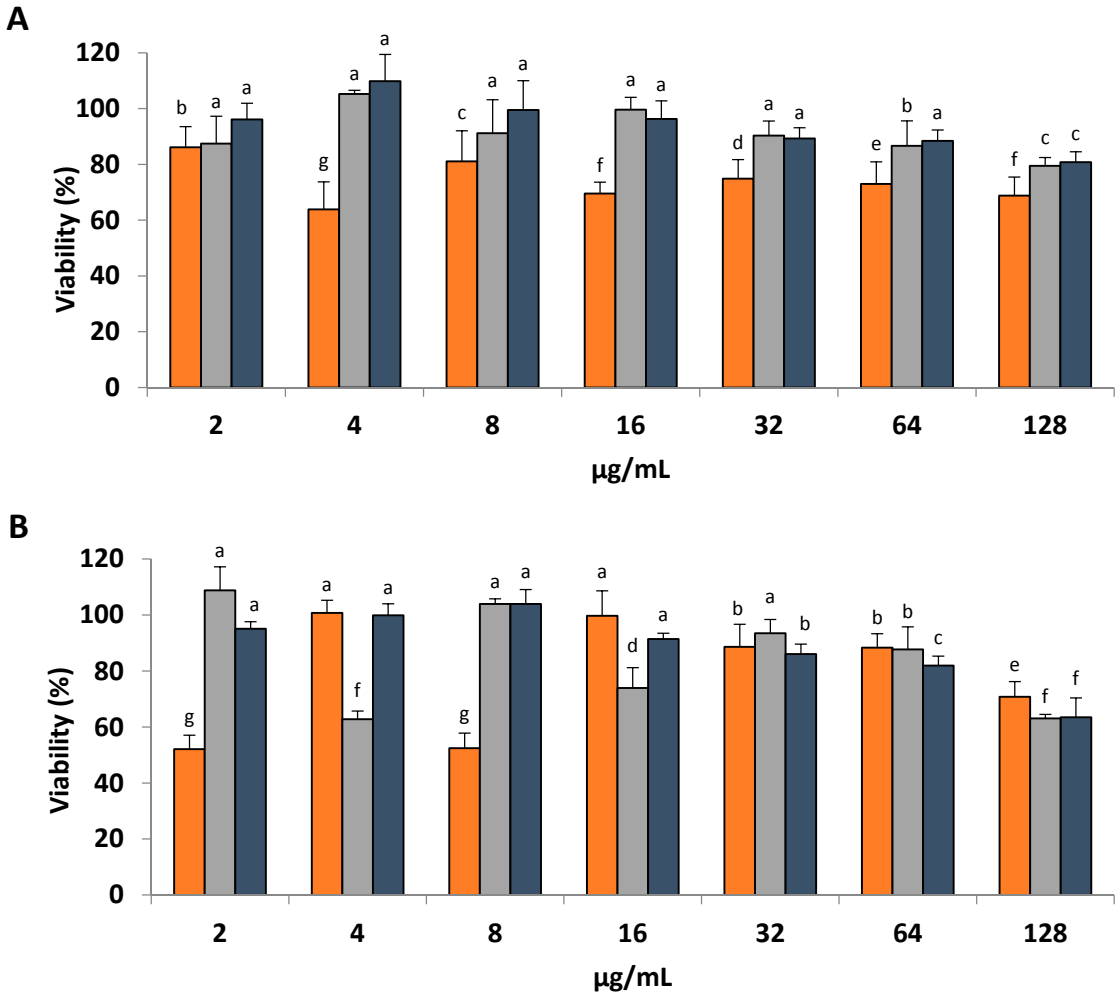

Figure 3. Cell proliferation assay. Viability of (■) HDFa, (■) CaCo-2 and (■) MCF7 cells cultured with different concentrations of (**A**) SSE and (**B**) HPLC Fraction c is presented as a percentage of the formazan signal recorded at 490 nm compared to untreated cells. According to the Tukey's test performed, significantly different means are identified with different significance letters.

HDFa cells treated with fraction c (Figure 3B) at 2 µg/mL and 8 µg/mL showed a significant reduction in viability, 52.1% ± 2.86 and 52.46% ± 3.08 respectively, while the viability of HDFa cells treated with 4 µg/mL of fraction c was almost the same as the viability of untreated cells. A continuous decline in HDFa cells viability was observed as fraction c concentration increased from 16 µg/mL to 128 µg/mL.

CaCo2 cells treated with 2 µg/mL of fraction c outperformed the viability of untreated cells by 8.8% ± 4.86, for 4 µg/mL viability dropped to 63.87% ± 5.71, at 8 µg/mL increased to 103.96% ± 1.05, dropped at 16 µg/mL to 73.95% ± 4.17, increased at 32 µg/mL to 93.47% ± 2.84, decreased to 87.72% ± 4.65 at 64 µg/mL and finally reached its lower viability of 63.09% ± 0.83 at 128 µg/mL.

A less discontinuous trend was observed for MCF7 cells treated with fraction c, although cells viability at 2 µg/mL was 95.09% ± 1.44, increased to 99.88% ± 2.39 at 4 µg/mL continued increasing to 103.96% ± 2.97 at 8 µg/mL, a tendency shift took place at 16 µg/mL with 91.46% ± 1.16 MCF7 cells viability and continued decreasing until 63.5% ± 2.16 at 128 µg/mL of fraction c.

2.6. Structural Characterization of Bioactive Fraction

Following the methodology described to elucidate the primary structure of the bioactive proteins in the SSE of *D. arenicolor*, several uncharacterized sequences were predicted using PEAKS

software-assisted de novo sequencing combined with the use of a tailored database containing all anuran mRNA and Protein entries available in NCBI. From the de novo sequencing analysis of fraction c, tryptic-digested peptide sequence SSFTYYYYDK (Figure 4) was predicted with high average local confidence (ALC) (>95%). A similarity sequence analysis using BLASTp showed 80% identity with a protein named anntoxin, first described in the skin secretions of *Hyla annectans* [19] and later on *Hyla simplex* [20]. Other peptides with lower ALC and matching different regions of the anntoxins accounting for 79.31% of the full sequences were also predicted since the anntoxin region Y^{36}RGXGGNGNRFK^{47} was not proposed by the de novo algorithm.

It was not possible to obtain any peptide with a high ALC from fractions d and f through the de novo sequencing strategy due to the reduced genomic and transcriptomic information available on anurans. Based on the predicted peptides, it is possible that fraction d is a protein which primary structure has none or low homology with any other anuran protein or peptide previously described. Meanwhile, due to its absorption at 214 nm, it is likely that fraction f is a peptide or even a protein, however this only would be confirmed through evidence at mRNA level.

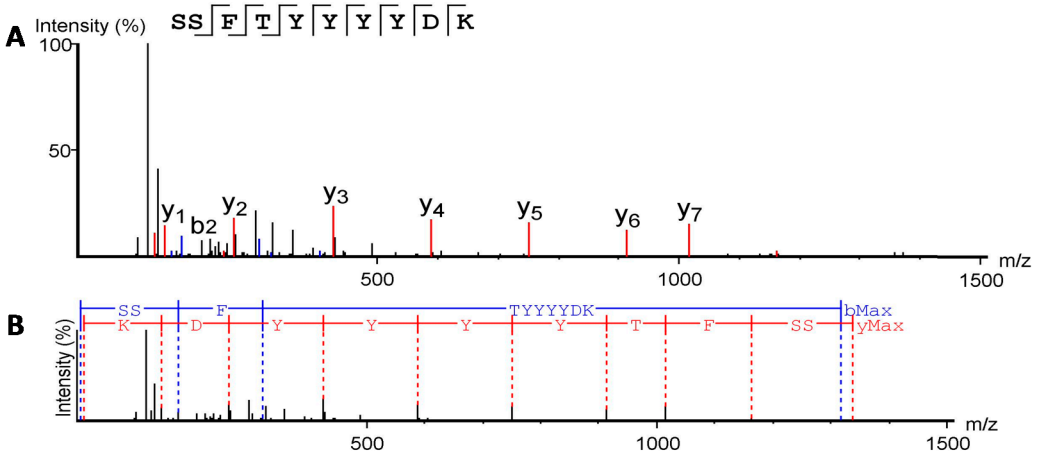

C

#	b	b-H2O	b-NH3	b (2+)	Seq	y	y-H2O	y-NH3	y (2+)	#
1	88.04	70.03	71.01	44.52	S					10
2	175.07	157.06	158.04	88.04	S	1249.54	1231.53	1232.51	625.27	9
3	322.14	304.13	305.11	161.57	F	1162.50	1144.50	1145.48	581.75	8
4	423.19	405.18	406.16	212.09	T	1015.45	997.43	998.41	508.22	7
5	586.25	568.24	569.22	293.63	Y	914.40	896.38	897.37	457.70	6
6	749.31	731.30	732.29	375.16	Y	751.33	733.32	734.30	376.16	5
7	912.38	894.37	895.35	456.69	Y	588.27	570.26	571.24	294.63	4
8	1075.44	1057.43	1058.41	538.22	Y	425.20	407.19	408.18	213.10	3
9	1190.47	1172.46	1173.44	595.73	D	262.14	244.13	245.11	131.57	2
10					K	147.08	129.10	130.09	74.06	1

Figure 4. De novo sequence prediction of the most abundant trypsin-digested peptide from fraction c. (**A**) Annotated spectrum of peptide SSFTYYYDK showing identified b (blue signal) and y (red signal) ions. (**B**) Alignment of the spectrum with the fragment ions generated from the peptide, bMax: is the most intense peak in the spectrum corresponding to b ions series (blue uppercase letter and lines); yMax: is the most intense peak in the spectrum corresponding to y ions series (red uppercase letter and lines). (**C**) Predicted b and y ions match table with the calculated mass of possible fragment ions; spectrum matching b ions are highlighted in blue and spectrum matching y ions are highlighted in red, #: identifies the order of the ions identified in the spectrum according to each ion series.

2.7. Identified Protein cDNA Synthesis

From the de novo sequencing of the most abundant trypsin-digested peptide from fraction c, SSFTYYYYDK, further BLASTp and partial homology correlation with the anntoxins from *H. annectans* and *H. simplex*, a degenerated 5′ primer, denominated RAnx1, was designed based on the amino acid

sequence KTSVVFL from the signal peptide sequence of the previously characterized anntoxins. 3′ rapid amplification of cDNA ends (RACE) PCR reactions that employed the universal primer mix (UPM) as 3′ primer and degenerated RAnx1 as 5′ primer yielded a 378 bp product. BLASTn of this PCR product showed overall nucleotide sequence similarity of 87% between *H. annectans*' anntoxin and the cDNA amplified with RAnx1 and UPM primers from the mRNA recovered from the skin secretions of *D. arenicolor*. The 378 bp PCR product encompasses signal peptide, mature peptide and poly A signal (Figure 5). Signal peptide was predicted just before the residue Ala^{22} using the SignalP 4.1 server and its nucleotide sequence showed 95% similarity with the signal peptide sequence of *H. annectans*' anntoxin. Meanwhile, the 58 amino acids mature protein encoded by the PCR product showed a 93% identity with the anntoxin from *H. annectans* and 82% with the anntoxin S1 from *H. simplex.* Following amino acids were unique in the protein from the skin secretions of *D. arenicolor* when aligned with *H. annectans* and *H. simplex* anntoxins: Glu^{6} Ser^{16} Tyr^{20} and Lys^{28}. Mature protein encoded by the cDNA generated from the skin secretions of *D. arenicolor* has been named by our research group as Arenin. The complete cDNA sequence was deposited in GenBank under the accession number MH898942.

Further BLASTp revealed that, as the anntoxins from *H. annectans* and *H. simplex*, arenin could have a Kunitz/Bovine pancreatic trypsin inhibitor (BPTI) domain, usually indicative of serine protease inhibitory activity. A possible trypsin interaction site *ku* [21] was also identified, comprising the residues $Lys^{13}Gly^{14}Ser^{15}Ser^{16}Ser^{17}Thr^{19}$.

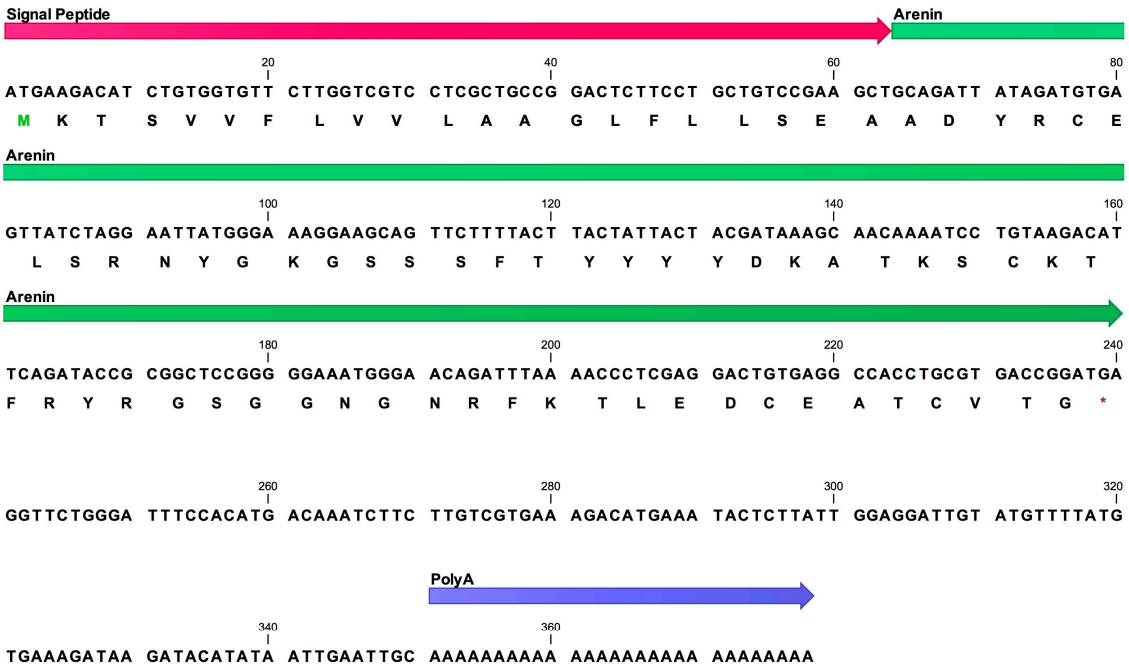

Figure 5. Full cDNA sequence of encoded arenin from *D. arenicolor* skin secretions. (■) Codified and translated signal peptide, (■) nucleotide and amino acid sequences of the mature polypeptide arenin, (■) Poly A signal. Green residue indicates translation initiation codon. Red asterisks indicates translation stop codon.

2.8. Structural Modeling of Arenin

The 3D model of arenin (Figure 6) generated based on the solution structure of anntoxin from *H. annectans* suggests that arenin keeps a very similar structure with anntoxin maintaining the two disulfide bonds Cys^{5}-Cys^{55} and Cys^{30}-Cys^{51} due to the proximity between the sulfhydryl groups of each pair of cysteines, 2 alpha-helix motifs Tyr^{3} to Glu^{6} and Leu^{48} to Cys^{55} and a twisted 2-stranded antiparallel beta sheets Phe^{18} to Asp^{24} and Ser^{29} to Tyr^{35}. In the ribbons model (Figure 6A,B),

the possible trypsin interaction site *ku* [21], $Lys^{13}Gly^{14}Ser^{15}Ser^{16}Ser^{17}Thr^{19}$, can be recognized as an outer loop in purple.

Polarity prediction model (Figure 6C,D) and amino acid composition of arenin suggests it has few hydrophobic zones, implying a proclivity to solubilize in aqueous solutions. This is in accordance with the RP-HPLC solvent composition of 26.87% ± 0.06 acetonitrile (ACN) that prompted the elution of arenin.

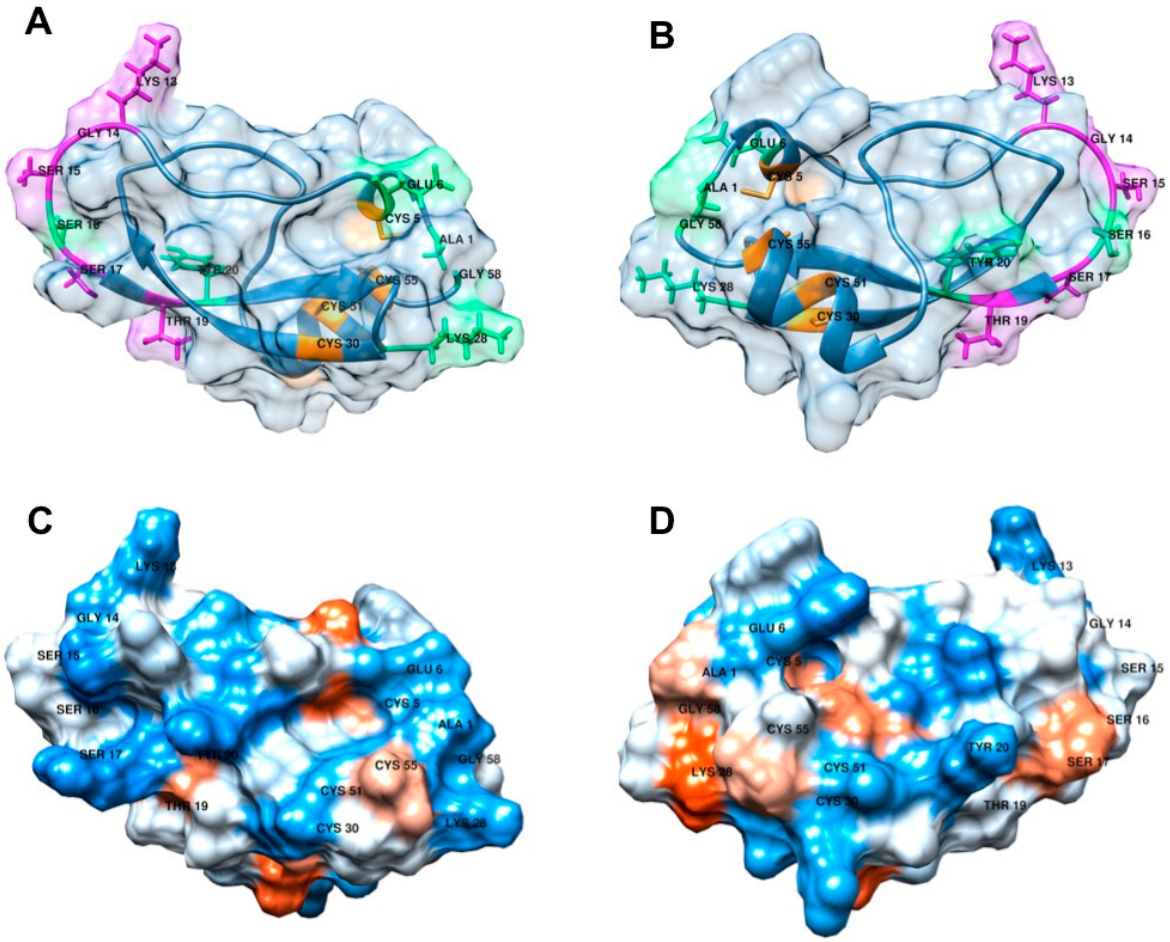

Figure 6. 3D model of arenin from *D. arenicolor* skin secretions. (**A**) Front and (**B**) back ribbon model of arenin, Unique amino acids Glu^6 Ser^{16} Tyr^{20} and Lys^{28} are highlighted in green, amino acids $Lys^{13}Gly^{14}Ser^{15}Ser^{16}Ser^{17}Thr^{19}$ possibly constitutes the trypsin interaction site *ku* and are highlighted in purple, amino acids Cys^5-Cys^{55} and Cys^{30}-Cys^{51} involved in the formation of disulfide bonds are highlighted in orange. (**C**) Front and (**D**) back polarity model prediction of arenin, blue zones represent polar residues, red zones non-polar residues and white zones neutral residues.

3. Discussion

Skin anti-predator defense systems of many anurans are enriched with various types of compounds including biogenic amines, bufogenines, bufotoxins, alkaloids, peptides and proteins. Biologically active peptides of 12 to 48 amino acids have been the most studied molecules in amphibian skin secretions with over 2000 peptides classified in more than 100 families including i.e., myotropical peptides, opioid peptides, angiotensins, neuropeptides, antioxidant peptides, wound-healing peptides, antimicrobial peptides, immunomodulatory peptides, insulin-release peptide, and other peptides [8]. However, there are many reports of anurans lacking peptides in their skin secretions [11] such as the Tomato Frog *Dyscophus guineti* (Microhylidae) [22] or *Pipa carvalhoi* [10] that displayed a Kunitz-like protease inhibitor polypeptide and kynurenic acid, respectively, as major constitutive components

in each species skin secretions. In the Hylidae family, at least 30 species have been suggested to lack host-defense peptides [23]. Although most amphibian skin secretions analysed through RP-HPLC display a complex profile with various peaks and similar intensities, *D. arenicolor's* SSE reverse-phase chromatogram (Figure 2A) show few peaks with similar intensities contrasting with the number of spots with relatively similar intensity in 2D-PAGE (Figure 1). Even though the resolution difference between 2D-PAGE and RP-HPLC profiles and the amount of sample analysed by each method was largely different (150 µg of SSE for Tricine-2D-PAGE and 20 µg of SSE for analytical RP-HPLC), skin secretions from other amphibians have also been reported to present RP-HPLC profiles of reduced complexity, such as the case with *Pipa carvalhoi* [10] and *Rana tigerina* [24].

Based on our findings, skin secretions of *D. arenicolor* are highly rich in proteins with an apparent molecular weight between 20 and 37 kDa (Figure 1). However, *D. arenicolor* skin secretions do not contain any of the typical defensive 12 to 48 amino acid-long peptides described in other members of the Hylidae family. At the same time, one of the major components in the skin secretion of *D. arenicolor* is a 58 amino acid polypeptide that shares homology with anntoxin, a Kunitz-like protease inhibitor and neurotoxin first described in the skin secretions of *H. annectans*. This polypeptide that was fractionated from the SSE of *D. arenicolor* through RP-HPLC (fraction c), further resolved through Tricine-PAGE (Figure 2B), in-gel digested and analysed through mass spectrometry, showed an experimental mass between 10 and 15 kDa every time it was analysed through Tricine-PAGE. Regarding fractions d and f, even though both fractions appear as abundant as fraction c in the RP-HPLC chromatogram (Figure 2A), when total soluble protein from d and f fractions were quantified, yields were very low in contrast with fraction c. Thus, sample quantity limited the design of activity assay for both fractions. Also, when analyzed through Tricine-PAGE, fraction d showed a faint band meanwhile fraction f did not show any band at all, making difficult the in-gel digestion for MS analysis. Fraction d analysis through MS and the de novo sequencing algorithm yielded some candidate peptides with ALC > 80% that did not match with any other protein or peptide in the databases used. Although it was not possible to identify fractions d and f proteins, it is of our interest to fully characterize both fractions in future research.

Protease inhibitors (PIs) and proteases are ubiquitous molecules in nature involved in a plethora of fundamental functions. In amphibian skin secretions, PIs are known to play a key role on inhibiting the catalytic activity of proteolytic enzymes in charge of the processing of defense peptide precursors [25]. However, in amphibians lacking defensive peptides, these molecules could play a key role in immunity as a protection against extrinsic proteases produced by invading microorganisms [3]. Generally, proteases are classified based on the catalytic amino acid within their active site (aspartic acid, threonine, cysteine, serine protease) or according to the cofactor essential for catalytic activity (metalloproteases). Similarly, protein-based PIs are commonly classified based on three defined structural motifs: Kunitz, Kazal and Bowman-Birk [26]. In amphibians, Kunitz-like PIs have been found in the skin secretions of various toads, ranid and hylid frogs, Kazal inhibitors in phyllomedusinae frogs and Bowman-Birk inhibitors in ranid frogs [25]. According to the 3D model predicted for arenin (Figure 6), its structure resembles a typical Kunitz-type fold constituted by a twisted antiparallel β-sheets hairpin (residues Phe^{18}-Tyr^{35}) an α-helix (Leu^{48}-Cys^{55}), and a short 3_{10} helix (residues Tyr^{3}-Glu^{6}) in the N terminus [25]. Amphibian Kunitz-like PIs differ from typical Kunitz PIs in the number of disulfide bonds, since the former contains 2 disulfide bonds (Cys^{5}-Cys^{55} and Cys^{30}-Cys^{51} in arenin), meanwhile typical Kunitz PIs are characterized by the presence of 3 disulfide bonds [8,25].

However, even though they share 93% sequence homology, comparing the 3D model of arenin with the nuclear magnetic resonance (NMR) crystallography of anntoxin from *H. annectans*, differences in the amino acid sequence could impact arenin's structure and, therefore, its activity. Substitution of anntoxin Gln^{7} by Glu^{6} in arenin may stabilize the short 3_{10} helix hosting the Cys^{5} residue that makes a disulfide bond with Cys^{55}, this shift may provide more stability between the 3_{10} helix and the α-helix. In anntoxin, Gly^{17} is localized in the most exposed area of the reactive loop that constitutes the trypsin interaction site (*ku* domain). In arenin, Gly^{17} is substituted by Ser^{16} that may reduce the

flexibility of the loop, this may decrease the selectivity of the protease inhibition activity, and at the same time, as Ser could accept or donate protons, its specific activity could be enhanced. At first glance, Asn^{21} substitution by Tyr^{20} in arenin may have little impact in overall protein stability-activity since both amino acids are polar, however the size and proximity of tyrosine's aromatic ring to the functional groups of Phe^{18}, Tyr^{35}, Arg^{44} and Lys^{46}, may reduce the flexibility of the reactive loop by stabilizing the twisted antiparallel β-sheets hairpin by hydrogen bonds with these 4 residues. Ser^{29} substitution by Lys^{28} may decrease protein solubility in water, since the hydroxyl group in Ser is more soluble in water than the amine in Lys.

Interestingly in PAGE (Figure 2A) analysis of the skin secretions of *D. arenicolor* and fraction c (Figure 2B), bands corresponding to arenin showed an apparent molecular weight between 10 and 15 kDa. Nonetheless, after in silico translation of its full cDNA, calculated molecular weight of the mature polypeptide based on its amino acid sequence resulted in 6578 Da. The difference between the calculated and the observed molecular weight could be explained through the formation of a homodimer between two arenin molecules, since the role of the Kunitz type domain in the formation of homodimers has been suggested previously [27]. An alternative hypothesis may be that this molecular weight shift is due to the presence of post-translational modifications such as glycosylation, methionine oxidation, tyrosine-sulfation, and/or carboxyterminal amidation. Even though these features may be found in Kunitz-like proteins from plants [28], these post-translational modifications have not been associated to amphibian Kunitz-like polypeptides. However, these features have been found in peptides and proteins from the skin secretions of other frogs [29], raising the possibility that arenin may contain them. Therefore, it is possible that arenin could be glycosylated such as the foetal human brain amyloid protein precursor that contains a Kunitz domain that has been described to present *N*- and *O*-glycosylations [30]. Yet, these hypotheses should be confirm through structural analysis of the purified protein.

At the beginning of our research we were interested in the antimicrobial potential of skin secretions of *D. arenicolor* based on ethnopharmacology studies pointing out its use in MTM activities for treatment of skin infections [16,17]. To explore this suggested antimicrobial property, *E. coli*, *S. mutans* and *S. aureus* cultures were subjected to microdilution assays to test its susceptibility against HPLC fractions and SSE at 5, 10 and 50 μg/mL. Although there is a small antimicrobial effect produced by the HPLC fractions or SSE over *E. coli*, *S. mutans* or *S. aureus*, it is not a significant response that could suggest that the main purpose of the skin secretions of *D. arenicolor* is protection against microorganisms. Moreover, the lack of classical antimicrobial peptides aids the notion that due to selective pressure, this species has developed skin secretions focused primarily, but not exclusively, on defense against non-microbial threats. This hypothesis could be supported by the demonstration of the lethal toxicity induced through the administration of high concentrations (0.05 to 3 mg/kg body weight) of anntoxin, that shares 93% homology with arenin, to potential predators such as insects, snakes, birds and mice [19]. Also, reduced or none antimicrobial activity has been observed in other Kunitz-like proteins [25].

Aside from their anti-protease activity, PIs have been associated with other underlying properties such as contribution in the termination of inflammatory processes through modulation of cytokine expression, signal transduction and tissue remodeling [26], playing a key role in the etiology and treatment of human pathologies such as cancer, inflammation and hemorrhage [25]. As a consequence of these bioactivities, PIs have been suggested as useful tools to study pathological processes along with the design of highly-specific drugs [31]. Amphibian Kunitz-like PIs have exhibited inhibition of tetrodotoxin-sensitive (TTX-S) voltage-gated sodium channel (VGSC) suggesting its application as analgesics when delivered at low concentrations [32]. While screening the effect of the skin secretions of *D. arenicolor* and arenin (fraction c) in normal human fibroblasts, colon cancer and breast cancer cells (Figure 3), a variable dose-response relationship was observed in the 3 cell lines. At low concentration of SSE and arenin (2, 4, 8 and 16 μg/mL), it is difficult to establish a trend in CaCo2 and HDFa cells; on the other hand, MCF7 cells maintain a less variable trend that is clearer with arenin alone,

suggesting a role impacting cell proliferation. Based on the switches in cell proliferation caused by arenin from 2 μg/mL to 4 μg/mL and then at 8 μg/mL in HDFa and CaCo2 cells, an opposed discrete dose-dependent effect could be distinguished between these cell lines where fibroblasts viability its near to half its maximum value at the same arenin concentration (2 μg/mL) at which colon cancer cells exceeds the viability displayed by the non-treated cells. This effect is inverted at 4 μg/mL of arenin where fibroblast cells shows a viability almost the same as the non-treated cells and colon cancer cells are at its lowest viability. Once again, inversion of this effect is observed at 8 μg/mL and 16 μg/mL of arenin. At higher concentrations of arenin (32, 64 and 128 μg/mL) viability inversion is still noticeable but less drastic. This effect is not produced by SSE, since the viability of HDFa cells was lower than CaCo2 and MCF7 cells in all the concentrations tested, suggesting that skin secretions from *D. arenicolor* are more toxic to normal cells than to adenocarcinoma cells at the concentrations assessed. Overall, the response observed by the increasing concentrations of arenin and SSE on HDFa, CaCo2 and MCF7 cells could be described as an effect with high variability at low doses that is gradually stabilized into a viability reduction trend at increasing concentrations.

Hormesis is a dose-response phenomenon characterized by low-dose stimulation and high-dose inhibition, independent of biological model and endpoint, as well as chemical class and physical agent [33]. The hormetic dose-response has been shown to describe the fundamental features of several dozen receptor systems, thus affecting a vast array of biological endpoints [34], aiding the suggestion that hormetic dose-responses may represent the first comprehensive quantitative estimation of biological plasticity [35]. Some examples of systems displaying an hormetic dose-response behavior include the work presented by Bogen and collaborators [36] where human keratinocytes (HEK001) cells exposed to low-doses of arsenite (As^{III}) displayed variable viability responses across the low-range of concentrations of As^{III} tested (0.25, 0.50, 1, 2, 3, 4 μM). Also, a number of cell lines displaying an hormetic dose-response when treated with a wide range of agents including antineoplastic drugs, nonneoplastic drugs, endogenous agonists and phytocompounds have been thoroughly described [37]. A molecular tactic proposed to explain hormetic dose-response relationships involves the presence of two receptors subtypes, one with high affinity and the other with low affinity for the agonist but with notably more capacity. Such an arrangement typically may lead to a biphasic dose-response, with the high-affinity receptor activated at low concentrations and the lower affinity/high-capacity receptor becoming dominant at higher concentrations [37]. Thus, it is proposed that the behavior observed in the viability of HDFa, CaCo-2 and MCF7 cells cultured in the presence of increasing concentrations of arenin and SSE displays an hormetic-like multiphasic dose-response relationship that may be regulated by more than two receptor subtypes.

Protease activated receptors (PARs) originally discovered in platelets, endothelial cells and fibroblasts, are seven-transmembrane-spanning receptors coupled to G proteins. PAR activation through protease hydrolyzation at a specific cleavage site in the extracellular N terminus of the receptor exposes a new N-terminal domain, which binds and activates the receptor initiating intracellular signals involved in responses such as platelet activation, vascular functions, inflammation, angiogenesis, neurodegeneration, proliferation, cell migration and even nociception [38,39]. Thrombin, trypsin, and human mast-cell tryptase have been found to activate the 4 PARs cloned thus far (PAR-1, PAR-2, PAR-3 and PAR-4) [40]. In theory, arenin could act as PARs antagonist through the inhibition of the proteases involved in PARs activation. This could explain the response observed at high concentration of arenin and SSE, but not the discrete effect at low concentration. It is possible that arenin could interact directly or indirectly with other cell membrane receptors additionally to PAR in a multi-targeted fashion dependent of arenin concentration according to the hormetic model hypothesis. Transcriptomic, proteomic and metabolomic analysis at different concentrations of arenin could shed light on the mechanism underlying the variable response noticed in our study.

4. Materials and Methods

4.1. Collection and Identification of D. arenicolor

Adult *D. arenicolor* of both sexes (n = 13, weight range 4–7 g) were collected from rocks near water bodies at Reserva de la Biosfera de Sierra Gorda, under SEMARNAT permission (SGPA/DGVS/06751/15). All specimens were kept in groups of 4 individuals in a 60 cm × 30 cm × 50 cm fish tank with soil, rocks and water, temperature in each terrarium was maintained between 20 °C to 25 °C with a heat mat, photoperiod was set to 12 h light and vitamin-supplemented live crickets were fed ad libidum. Species identification was determined through PCR amplification, sequencing and BLAST of mitochondrial DNA regions previously reported as useful markers for differential identification of *D. arenicolor* species [41]. Total genomic DNA was extracted from freeze-dried skin using the NucleoSpin® Tissue kit (Machinery-Nagel, Düren, Germany). PCR was performed with ExTaq DNA Polymerase (TaKaRa Bio Inc., Kusatsu, Shiga, Japan), primers MVZ-59^{F} (5′-ATAGCACTGAAAAYGCTDAGATG-3′) and tRNAVal^{R} (5′-GGTGTAAGCGARAGCTTTKGTTAAG-3′) [42], using the following thermocycler protocol: initial denaturation of 3 min at 95 °C; 30 cycles comprised by denaturation for 10 s at 98 °C, annealing for 30 s at 53 °C, extension for 70 s at 72 °C; and a final extension for 5 min at 72 °C. Products were visualized with a 0.7% gel, purified using a Wizard SV Gel and PCR Clean-up System (Promega Corporation, Madison, WI, USA), cloned into a pGEM-T vector system (Promega Corporation, Madison, WI, USA) and sequenced at Instituto de Biotecnología de la UNAM (Cuernavaca, Mexico). All sequences obtained were subjected to online BLAST searches against Gen-Bank for identification and to check for possible contamination.

4.2. Recovery of Skin Secretions Extract

To promote release of skin secretions, frogs were stimulated by injecting 40 nmol/grams body weight norepinephrine bitartrate salt (Sigma-Aldrich, St. Louis, MO, USA) dissolved in sterile 200 µL water at two sites into dorsal lymph sacs. Skin secretions were collected by placing the stimulated frog in a covered glass beaker with 40 mL of collection buffer, 25 mM NaCl and 25 mM ammonium acetate, pH 7.0, [43,44] for 15 min. After removing the frog, collected skin secretions were acidified with hydrochloric acid (1% v/v) and centrifuged 30 min at 5000× g. Supernatants were immediately desalted and concentrated using Sep-Pak C-18 cartridges (Waters Associates, Milford, MA, USA) as previously described [18]. Concentrated and desalted protein solution was named the skin secretions extract (SSE). Protein concentration was determined using Microplate BCA^{TM} Protein Assay Kit (Thermo Scientific, Rockford, IL, USA). After norepinephrine stimulation and recovery of SSE, none of the frogs tested showed any distress related to this process. This protocol was reviewed and approved by the Institutional Committee for the Use and Care of Lab Animals of Tecnologico de Monterrey (Comité Institucional para el Cuidado y Uso de Animales de Laboratorio (CICUAL) del Tecnologico de Monterrey) under the protocol number 2015-007 (8 May 2015).

4.3. SSE Characterization by Reverse-Phase HPLC and 2D-PAGE

RP-HPLC profile of SSE was assessed to determine sample complexity by injecting 20 µg of skin secretions into a XBridge Peptide BEH C-18 column (4.6 mM inner diameter (i.d.) × 250 mM, 5 µm) connected to an Agilent 1200 HPLC-UV System (Agilent, Santa Clara, CA, USA). Elution was conducted at 0.75 mL/min employing solutions A (water: Trifluoroacetic acid (TFA) 99.9:0.1 v/v) and B (ACN:water:TFA 70.0:29.9:0.1, $v/v/v$) using a linear gradient from 0% to 100% solution B over 85 min. Absorbance was monitored at 214 nm and 280 nm. Absorbance spectra (190 nm to 600 nm) of most abundant peaks were analyzed as a preliminary identification step.

To evaluate the protein composition of the skin secretions, 150 µg of SSE were loaded into a 7 cm immobilized pH gradient (IPG) strip (3-10L). Isoelectric focusing (IEF) was carried out on an Ettan IPGphorTM 3 (GE Healthcare, Uppsala, Sweden). After completion of the IEF, reduction and alkylation steps as per manufacturer instructions, IPG strips were placed on home casted 10%

SDS/Tricine-PAGE [45]. Second dimension electrophoresis was performed in a mini-PROTEAN Tetra Cell (Bio-Rad, Hercules, CA, USA). Gels were stained overnight with GelCode™ Blue Stain Reagent (Thermo Scientific, Rockford, IL, USA). Gels were rinsed with water several times over 6 h to remove background before being scanned in a GE Image Scanner III (GE Healthcare Bio-Sciences AB, Uppsala, Sweden)

4.4. Protein Isolation for Activity Evaluation

For activity screening assays to identify bioactive fractions, SEE were separated into a Zorbax SB-C18 (Agilent, Santa Clara, CA, USA) semi-preparative column (9.4 mM i.d. × 250 mM, 5 µm) connected to an Agilent 1100 HPLC-UV system (Agilent, Santa Clara, CA, USA) equipped with a fraction collector. The mobile phase system was the same as described for SSE characterization by RP-HPLC. Fractionation was performed using the following method: a linear gradient from 10% to 25% of solution B from 0 to 5 min at a flow rate of 1.5 mL/min, linear gradient to 30% of solvent B from 5 to 10 min at a flow rate of 1.5 mL/min, linear gradient to 50% of solvent B from 10 to 25 min at a flow rate of 2.5 mL/min, and a linear gradient to 100% of solvent B from 25 to 30 min at a flow rate of 3 mL/min. Total method time was 35 min. Fractions with same retention time were pooled and evaporated in a GeneVac EZ-2 series (Genevac Ltd., Ipswich, UK); protein quantification was performed as describe in the Recovery of Skin Secretions Extract section. Purity of fractions collected was assessed using HPLC and 10% SDS/Tricine-PAGE.

4.5. Cell Proliferation Inhibition by SSE and HPLC-Purified Fractions

To evaluate the potential effect on the inhibition of cell proliferation, SSE and HPLC-purified fractions were tested at different concentrations (2 µg/mL, 4 µg/mL, 8 µg/mL, 16 µg/mL, 32 µg/mL, 64 µg/mL and 128 µg/mL) by triplicate in two independent experiments in normal human dermal fibroblasts (HDFa, ATCC® PCS-201-012), human epithelial cells from colorectal adenocarcinoma (CaCo2, ATCC® HTB-37) and human epithelial cells from breast adenocarcinoma (MCF7, ATCC® HTM-22). Cells were cultured in Dulbecco's modified Eagle medium (DMEM) containing 5% fetal calf serum in flat-bottomed 96-well microtiter trays at 5×10^4 cells per well at 37 °C in a humidified incubator with 5% CO_2. After 24 h incubation, culture media was removed and fresh media containing SSE or HPLC-purified fractions was added to each well and incubated for 48 h at 37 °C in a humidified incubator with 5% CO_2. To estimate proliferation of viable cells, 20 µL of phenazine methosulfate 3-(4,5-dimethyl thiazole-2-yl)-2,5-diphenyl tetrazolium bromide mix-based (MTS) CellTiter 96® AQueous One Solution Cell Proliferation Assay (Promega Corporation, Madison, WI, USA) were added to each well and after 45 min incubation at 37 °C, absorbance at 490 nm was recorded using a 96-well plate reader. Percentage of viable treated cells was calculated in relation to untreated controls (viability percentage = treated cells Optical Density/untreated cells Optical Density × 100%) [46].

4.6. Statistical Analysis

Results are expressed as the mean ± standard error (SE). Statistical analysis was carried out with the statistical software JMP version 14.1.0 (SAS, Cary, NC, USA). One way-analysis of variance (ANOVA) was used to analyze the variation between groups. Tukey's test was used to identify significantly different means. Results were considered significant if $p \leq 0.05$. Significantly different means are identified with different significance letters.

4.7. Structural Characterization of Bioactive Protein

4.7.1. In Gel Digestion of Bioactive Proteins

Isolated fractions were solubilized in sodium dodecyl sulfate (SDS) and resolved in a 12% Tricine-SDS-PAGE. Gel was stained with Colloidal Coomassie Blue and protein bands were cut and destained in 50% ACN containing 25 mM ammonium bicarbonate (ABB).

In gel digestion of proteins was performed as previously described [47], with minor modifications. Briefly, gel bands were cut in 1-mm^2 cubes and proteins were reduced in 10 mM dithiothreitol in 25 mM ABB at 60 °C for 1 h. Proteins were subsequently alkylated with 55 mM iodoacetamide in 25 mM ABB at room temperature for 45 min protected from the light. Gel cubes were then dehydrated with ACN in two washes of 1 min/each and dried during 5 min in the speedvac. Tryptic digestion of proteins was performed at 37 °C overnight by the addition of 10 ng/µL of sequencing grade trypsin prepared in 25 mM ABB. Tryptic digested peptides were extracted from the gel cubes twice with 50% ACN, 5% acetic acid during 15 min with vigorous vortexing. Subsequently, two rounds of extraction were performed with 50% ACN, 5% formic acid (FA) for 15 min/each. The obtained supernatants were combined and dried in the speedvac. Dried peptides were resuspended in 3% ACN, 0.1% FA for their subsequent analysis by liquid chromatography mass spectrometry.

4.7.2. Liquid Chromatography Mass Spectrometry (LC-MS) Analysis of Bioactive Proteins

Primary structure of the bioactive proteins was characterized by MS as previously described [48,49] with minor modifications. Analysis of peptides was performed using a QExactive mass spectrometers coupled with a Dionex UltiMate 3000 UHPLC system from Thermo Fisher Scientific Inc. (Bremen, Germany). Peptide separation was performed using a reverse-phase EASY-Spray LC column (75 µm ID × 15 cm, 3 µm particle size, Thermo Scientific Inc., Bremen, Germany) maintained at 35 °C and working at 300 nL/min. Eluents A (0.1% FA) and B (90% ACN, 0.1% FA) were used to establish the following 60-min gradient: 7–18% B for 30 min, 18–32% B for 15 min, 32–50% B for 4 min, 50–90% B for 1 min, 90–5% B for 0.1 min, 5% B for 7.9 min, 5–7% B for 2 min. Spray was generated using a Thermo Scientific EASY-Spray source (Bremen, Germany) at 1.75 kV. QExactive mass spectrometer was set to positive mode for data acquisition with Xcalibur 3.0.63 software (Thermo Fisher Scientific Inc., Bremen, Germany) software alternating between full Fourier transform-mass spectrometry (FT-MS) (350−1600 m/z, resolution 75,000, with 1 µscan per spectrum) and FT-MS/MS (resolution 35000, with 1 µscan per spectrum). Fragmentation of the 10 most intense precursors with charge > +2 and isolated within a 2 Da window was performed using a normalized collision energy of 28%. A threshold of 500 counts was enabled. For full FT-MS and FT-MS/MS automatic gain control was set to 3×10^6 and 2×10^5, respectively.

4.7.3. Bioinformatics and Data Analysis

The raw MS/MS data were processed using PEAKS software version 7.5 (Bioinformatics Solutions, Waterloo, ON, Canada) for the de novo sequencing of peptides [50]. In parallel data were searched using PEAKS software against a tailored database containing all anuran mRNA (648,884) and protein (425,093) entries available in the National Center for Biotechnology Information (NCBI, https://www.ncbi.nlm.nih.gov/). For the de novo sequencing of peptides, local confidence was considered as the confidence (%) that a particular amino acid was present in the de novo peptide at a particular position. The sum of the total confidence scores (0 to 1) from each amino acid in the peptide sequence divided by the number of amino acids is presented to be ALC used to assess the accuracy of the interpretation. The database search was performed as previously described [51], allowing a precursor ion tolerance of 10 ppm, a fragment tolerance of 0.05 Da MS/MS and a false discovery rate of 1% at peptide level. Carbamidomethylation at Cys residues was set as a fixed modification.

4.8. Identified Protein cDNA Synthesis

To identify the DNA sequence codifying for the protein analyzed by MS, cDNA synthesis was performed using mRNA isolated from skin secretions as template for retro-transcription. After neuroendocrine stimulation, skin secretions were recovered by directly rubbing the stimulated skin with a sterile tip and immediately transferred into a sterile polypropylene tube containing 1 mL of lysis/binding buffer provided by the Dynabeads® mRNA purification kit (Ambion, Carlsbad, CA, USA). Polyadenylated mRNA was isolated as per manufacturer's instructions.

First strand cDNA synthesis was carried out using the 3′RACE CDS Primer A from SMARTer RACE 5′/3′ kit (Clontech, Mountain View, CA, USA) and the Improm-II Reverse Transcriptase (Promega Corporation, Madison, WI, USA). 3′-RACE PCR was performed using a universal primer mix (UPM), supplied with the SMARTer RACE 5′/3′ kit, a degenerated sense primer (RAnx1: 5′-GAARACWTCTGTKGTKTTYYTGG-3′) and high fidelity polymerase TaKaRa Ex Taq (Clontech, Mountain View, CA, USA) with the following program: initial denaturation step: 60 s at 94 °C; 35 cycles: denaturation 30 s at 94 °C, primer annealing for 30 s at 56 °C, extension for 180 s at 72 °C. The resulting PCR fragments (378 bp) were purified with a Wizard SV Gel and PCR Clean-Up System (Promega Corporation, Madison, WI, USA), cloned using a pGEM-T vector system (Promega Corporation, Madison, WI, USA) and sequenced at Instituto de Biotecnología de la UNAM (Cuernavaca, Mexico). All sequences obtained were subjected to online BLAST (Available online: https://blast.ncbi.nlm.nih.gov/Blast.cgi) searches against GenBank for identification and to check for possible contamination. cDNA was confirmed by in silico translation of sequenced PCR products and further alignment against digested peptides with highest ALC. Signal peptide of the sequenced cDNA was predicted in the SignalP 4.1 server (Available online: http://www.cbs.dtu.dk/services/SignalP/) [52].

4.9. Structural Modeling of Arenin

After confirmation of the correlation between the cDNA generated with the mRNA recovered from the skin secretions of *D. arenicolor* and the MS analysis performed to fraction's c protein, a 3D model of the in silico translated protein was generated using the SWISS MODEL server (Available online: https://swissmodel.expasy.org/) [53,54]. Protein model generated was downloaded and modified with the molecular visualization software UCSF Chimera (RBVI, San Francisco, CA, USA) [55]. A structural comparison between the identified *D. arenicolor*'s skin secreted protein and anntoxin, the protein used as a template for modeling (PDB: 2kcr) [19], was performed in order to detect conformational differences.

5. Conclusions

The current work demonstrates the lack of classical defensive peptides in the skin secretions of *D. arenicolor*. At the same time, we present the full cDNA of the third gene-encoded anntoxin-like protein from amphibian skin secretions, arenin. Based on the cell proliferation assay and the homology between arenin and the Kunitz-type protease inhibitor anntoxin, arenin is proposed to induce a hormetic-like dose-dependent behavior in the proliferation of normal and cancerous cells, partially through the protection of PARs. Nonetheless, further research focused on transcriptomics, metabolomics and proteomics changes is needed in order to confirm this hypothesis and to identify other receptors and routes involved in order to elucidate the mechanism of action behind the dose-response relationship observed in HDFa, CaCo2 and MCF7 cells cultured with low concentrations of arenin.

Author Contributions: Conceptualization, J.H.-P. and J.B.; Methodology, J.H.-P.; formal analysis, J.H.-P., A.S., S.K.S. and J.B.; investigation, J.H.-P. and A.S.; resources, A.S., S.K.S., P.L.C., J.S. and J.B.; data curation, J.H.-P.; writing—original draft preparation, J.H.-P. and J.B.; writing—review and editing, A.S., S.K.S., P.L.C. and J.S.; visualization, J.H.-P.; supervision, P.L.C., J.S. and J.B.; project administration, J.B.; funding acquisition, P.L.C., J.S. and J.B.

Acknowledgments: Authors acknowledge the Ph.D. scholarship No. 391089 from the Consejo Nacional de Ciencia y Tecnología (CONACyT) to support Jesus Hernandez-Perez, and the financial support from Tecnológico de Monterrey (Bioengineering, Biosystems and Synthetic Biology Research Group). We also thank Marilena Antunes-Ricardo, Javier Villela-Castrejón and Alejandro Robles for technical advice with cell viability assays.

Conflicts of Interest: The authors declare no conflicts of interest.

Abbreviations

ABB	Ammonium bicarbonate
ACN	Acetonitrile
ALC	Average local confidence
BPTI	Bovine pancreatic trypsin inhibitor
FA	Formic Acid
FT-MS	Fourier transform-mass spectrometry
IEF	Isoelectric focusing
IPG	Immobilized pH gradient
MS	Mass spectrometry
MTM	Mexican Traditional Medicine
MTS	Phenazine methosulfate 3-(4,5-dimethyl thiazole-2-yl)-2,5-diphenyl tetrazolium bromide mix-based
PAR	Protease activated receptor
PIs	Protease inhibitors
SDS	Sodium dodecyl sulfate
SSE	Skin secretions extract
TEAB	Triethylammonium bicarbonate
TFA	Trifluoroacetic acid
TTX-S	Tetrodotoxin-sensitive
VGSC	Voltage-gated sodium channel

References

1. Calderon, L.; Stabeli, R. *Changing Diversity in Changing Environment*; Grillo, O., Ed.; InTech: Rijeka, Croatia, 2011; ISBN 978-953-307-796-3.
2. Xi, X.; Li, B.; Chen, T.; Kwok, H. A Review on Bradykinin-Related Peptides Isolated from Amphibian Skin Secretion. *Toxins (Basel)* **2015**, *7*, 951–970. [CrossRef] [PubMed]
3. Song, G.; Zhou, M.; Chen, W.; Chen, T.; Walker, B.; Shaw, C. HV-BBI-A novel amphibian skin Bowman-Birk-like trypsin inhibitor. *Biochem. Biophys. Res. Commun.* **2008**, *372*, 191–196. [CrossRef] [PubMed]
4. Bai, B.; Zhang, Y.; Wang, H.; Zhou, M.; Yu, Y.; Ding, S.; Chen, T.; Wang, L.; Shaw, C. Parallel peptidome and transcriptome analyses of amphibian skin secretions using archived frozen acid-solvated samples. *Mol. Biotechnol.* **2013**, *54*, 187–197. [CrossRef] [PubMed]
5. Thompson, A.H.; Bjourson, A.J.; Orr, D.F.; Shaw, C.; McClean, S. Amphibian skin secretomics: Application of parallel quadrupole time-of-flight mass spectrometry and peptide precursor cDNA cloning to rapidly characterize the skin secretory peptidome of Phyllomedusa hypochondrialis azurea: Discovery of a novel peptide fa. *J. Proteome Res.* **2007**, *6*, 3604–3613. [CrossRef] [PubMed]
6. De Sousa, L.Q.; Machado, K.D.; Oliveira, S.F.; Araújo, L.D.; Monção-Filho, E.D.; Melo-Cavalcante, A.A.; Vieira-Júnior, G.M.; Ferreira, P.M. Bufadienolides from amphibians: A promising source of anticancer prototypes for radical innovation, apoptosis triggering and Na+/K+-ATPase inhibition. *Toxicon* **2017**, *127*, 63–76. [CrossRef] [PubMed]
7. Rollins-Smith, L.A.; Reinert, L.K.; O'Leary, C.J.; Houston, L.E.; Woodhams, D.C. Antimicrobial Peptide defenses in amphibian skin. *Integr. Comp. Biol.* **2005**, *45*, 137–142. [CrossRef] [PubMed]
8. Xu, X.; Lai, R. The Chemistry and Biological Activities of Peptides from Amphibian Skin Secretions. *Chem. Rev.* **2015**, *115*, 1760–1846. [CrossRef] [PubMed]
9. König, E.; Wesse, C.; Murphy, A.C.; Zhou, M.; Wang, L.; Chen, T.; Shaw, C.; Bininda-Emonds, O.R.P. Molecular cloning of the trypsin inhibitor from the skin secretion of the Madagascan Tomato Frog, Dyscophus guineti (Microhylidae), and insights into its potential defensive role. *Org. Divers. Evol.* **2013**, *13*, 453–461. [CrossRef]

10. Mariano, D.O.C.; Yamaguchi, L.F.; Jared, C.; Antoniazzi, M.M.; Sciani, J.M.; Kato, M.J.; Pimenta, D.C. Pipa carvalhoi skin secretion profiling: Absence of peptides and identification of kynurenic acid as the major constitutive component. *Comp. Biochem. Physiol. C Toxicol. Pharmacol.* **2014**, *167C*, 1–6. [CrossRef] [PubMed]
11. König, E.; Bininda-Emonds, O.R.P.; Shaw, C. The diversity and evolution of anuran skin peptides. *Peptides* **2015**, *63*, 96–117. [CrossRef] [PubMed]
12. Nguyen, L.T.; Haney, E.F.; Vogel, H.J. The expanding scope of antimicrobial peptide structures and their modes of action. *Trends Biotechnol.* **2011**, *29*, 464–472. [CrossRef] [PubMed]
13. Faivovich, J.; Haddad, C.F.B.; Garcia, P.C.A.; Frost, D.R.; Campbell, J.A.; Wheeler, W.C. Systematic Review of the Frog Family Hylidae, With Special Reference To Hylinae: Phylogenetic Analysis and Taxonomic Revision. *Bull. Am. Mus. Nat. Hist.* **2005**, *294*, 1. [CrossRef]
14. Conlon, J.M.; Kolodziejek, J.; Nowotny, N. Antimicrobial peptides from the skins of North American frogs. *Biochim. Biophys. Acta Biomembr.* **2009**, *1788*, 1556–1563. [CrossRef] [PubMed]
15. Duellman, W.E.; Marion, A.B.; Hedges, S.B. *Phylogenetics, Classification, and Biogeography of the Treefrogs (Amphibia: Anura: Arboranae)*; Magnolia Press: Auckland, New Zealand, 2016; Volume 4104.
16. Alonso-Castro, A.J. Use of medicinal fauna in Mexican traditional medicine. *J. Ethnopharmacol.* **2014**, *152*, 53–70. [CrossRef] [PubMed]
17. Alonso-Castro, A.J.; Carranza-Álvarez, C.; Maldonado-Miranda, J.J.; Del Rosario Jacobo-Salcedo, M.; Quezada-Rivera, D.A.; Lorenzo-Márquez, H.; Figueroa-Zúñiga, L.A.; Fernández-Galicia, C.; Ríos-Reyes, N.A.; de León-Rubio, M.Á.; et al. Zootherapeutic practices in Aquismón, San Luis Potosí, México. *J. Ethnopharmacol.* **2011**, *138*, 233–237. [CrossRef] [PubMed]
18. Conlon, J.M. Purification of naturally occurring peptides by reversed-phase HPLC. *Nat. Protoc.* **2007**, *2*, 191–197. [CrossRef] [PubMed]
19. You, D.; Hong, J.; Rong, M.; Yu, H.; Liang, S.; Ma, Y.; Yang, H.; Wu, J.; Lin, D.; Lai, R. The first gene-encoded amphibian neurotoxin. *J. Biol. Chem.* **2009**, *284*, 22079–22086. [CrossRef] [PubMed]
20. Wu, J.; Liu, H.; Yang, H.; Yu, H.; You, D.; Ma, Y.; Ye, H.; Lai, R. Proteomic analysis of skin defensive factors of tree frog Hyla simplex. *J. Proteome Res.* **2011**, *10*, 4230–4240. [CrossRef] [PubMed]
21. Otlewski, J.; Jelen, F.; Zakrzewska, M.; Oleksy, A. The many faces of protease-protein inhibitor interaction. *EMBO J.* **2005**, *24*, 1303–1310. [CrossRef] [PubMed]
22. Conlon, J.M.; Kim, J.B. A protease inhibitor of the Kunitz family from skin secretions of the tornato frog, Dyscophus guineti (Microhylidae). *Biochem. Biophys. Res. Commun.* **2000**, *279*, 961–964. [CrossRef] [PubMed]
23. Erspamer, V.; Erspamer, G.F.; Cei, J.M. Active peptides in the skins of two hundred and thirty American amphibian species. *Comp. Biochem. Physiol. C* **1986**, *85*, 125–137. [CrossRef]
24. Sai, K.P.; Jagannadham, M.V.; Vairamani, M.; Raju, N.P.; Devi, A.S.; Nagaraj, R.; Sitaram, N. Tigerinins: Novel antimicrobial peptides from the Indian frog Rana tigerina. *J. Biol. Chem.* **2001**, *276*, 2701–2707. [CrossRef] [PubMed]
25. Chen, X.; Wang, H.; Shen, Y.; Wang, L.; Zhou, M.; Chen, T.; Shaw, C. Kunitzins: Prototypes of a new class of protease inhibitor from the skin secretions of European and Asian frogs. *Biochem. Biophys. Res. Commun.* **2016**, *477*, 302–309. [CrossRef] [PubMed]
26. Shigetomi, H.; Onogi, A.; Kajiwara, H.; Yoshida, S.; Furukawa, N.; Haruta, S.; Tanase, Y.; Kanayama, S.; Noguchi, T.; Yamada, Y.; et al. Anti-inflammatory actions of serine protease inhibitors containing the Kunitz domain. *Inflamm. Res.* **2010**, *59*, 679–687. [CrossRef] [PubMed]
27. Ben Khalifa, N.; Tyteca, D.; Courtoy, P.J.; Renauld, J.C.; Constantinescu, S.N.; Octave, J.N.; Kienlen-Campard, P. Contribution of Kunitz protease inhibitor and transmembrane domains to amyloid precursor protein homodimerization. *Neurodegener. Dis.* **2012**, *10*, 92–95. [CrossRef] [PubMed]
28. Rustgi, S.; Boex-Fontvieille, E.; Reinbothe, C.; von Wettstein, D.; Reinbothe, S. The complex world of plant protease inhibitors: Insights into a Kunitz-type cysteine protease inhibitor of Arabidopsis thaliana. *Commun. Integr. Biol.* **2018**, *11*, e1368599. [CrossRef] [PubMed]
29. Pinkse, M.; Evaristo, G.; Pieterse, M.; Yu, Y.; Verhaert, P. MS approaches to select peptides with post-translational modifications from amphibian defense secretions prior to full sequence elucidation. *EuPA Open Proteomics* **2014**, *5*, 32–40. [CrossRef]
30. Godfroid, E.; Octave, J.N. Glycosylation of the amyloid peptide precursor containing the Kunitz protease inhibitor domain improves the inhibition of trypsin. *Biochem. Biophys. Res. Commun.* **1990**, *171*, 1015–1021. [CrossRef]

31. Christeller, J.T. Evolutionary mechanisms acting on proteinase inhibitor variability. *FEBS J.* **2005**, *272*, 5710–5722. [CrossRef] [PubMed]
32. Wei, L.; Dong, L.; Zhao, T.; You, D.; Liu, R.; Liu, H.; Yang, H.; Lai, R. Analgesic and anti-inflammatory effects of the amphibian neurotoxin, anntoxin. *Biochimie* **2011**, *93*, 995–1000. [CrossRef] [PubMed]
33. Calabrese, E. Hormesis and Pharmacology. *Pharmacology* **2009**, 75–102. [CrossRef]
34. Cornelius, C.; Graziano, A.; Perrotta, R.; Di Paola, R.; Cuzzocrea, S.; Calabrese, E.J.; Calabrese, V. Cellular Stress Response, Hormesis, and Vitagens in Aging and Longevity: Role of mitochondrial "Chi". *Inflamm. Adv. Age Nutr.* **2014**, 309–321. [CrossRef]
35. Calabrese, E.J.; Mattson, M.P. Hormesis provides a generalized quantitative estimate of biological plasticity. *J. Cell Commun. Signal.* **2011**, *5*, 25–38. [CrossRef] [PubMed]
36. Bogen, K.T.; Arnold, L.L.; Chowdhury, A.; Pennington, K.L.; Cohen, S.M. Low-dose dose-response for reduced cell viability after exposure of human keratinocyte (HEK001) cells to arsenite. *Toxicol. Rep.* **2017**, *4*, 32–38. [CrossRef] [PubMed]
37. Calabrese, E.J. Cancer biology and hormesis: Human tumor cell lines commonly display hormetic (biphasic) dose responses. *Crit. Rev. Toxicol.* **2005**, *35*, 463–582. [CrossRef] [PubMed]
38. Vergnolle, N.; Ferazzini, M.; D'Andrea, M.R.; Buddenkotte, J.; Steinhoff, M. Proteinase-activated receptors: Novel signals for peripheral nerves. *Trends Neurosci.* **2003**, *26*, 496–500. [CrossRef]
39. Day, J.R.S.; Landis, R.C.; Taylor, K.M. Aprotinin and the protease-activated receptor 1 thrombin receptor: Antithrombosis, inflammation, and stroke reduction. In *Seminars in Cardiothoracic and Vascular Anesthesia*; SAGE: Thousand Oaks, CA, USA, 2006; Volume 10, pp. 132–142.
40. Rezaie, A. Protease-activated receptor signalling by coagulation proteases in endothelial cells. *Thromb. Haemost.* **2014**, *112*, 876–882. [CrossRef] [PubMed]
41. Klymus, K.E.; Carl Gerhardt, H. AFLP markers resolve intra-specific relationships and infer genetic structure among lineages of the canyon treefrog, Hyla arenicolor. *Mol. Phylogenet. Evol.* **2012**, *65*, 654–667. [CrossRef] [PubMed]
42. Goebel, A.M.; Donnelly, J.M.; Atz, M.E. PCR primers and amplification methods for 12S ribosomal DNA, the control region, cytochrome oxidase I, and cytochrome b in bufonids and other frogs, and an overview of PCR primers which have amplified DNA in amphibians successfully. *Mol. Phylogenet. Evol.* **1999**, *11*, 163–199. [CrossRef] [PubMed]
43. Conlon, J.M.; Leprince, J. Identification and Analysis of Bioactive Peptides in Amphibian Skin Secretions. In *Peptidomics, Methods in Molecular Biology*; Humana Press: New York, NY, USA, 2010; Volume 615, pp. 145–157.
44. Gammill, W.M.; Scott Fites, J.; Rollins-Smith, L.A. Norepinephrine depletion of antimicrobial peptides from the skin glands of Xenopus laevis. *Dev. Comp. Immunol.* **2012**, *37*, 19–27. [CrossRef] [PubMed]
45. Schägger, H. Tricine–SDS-PAGE. *Nat. Protoc.* **2006**, *1*, 16–22. [CrossRef] [PubMed]
46. Groot, H.; Muñoz-Camargo, C.; Moscoso, J.; Riveros, G.; Salazar, V.; Kaston Florez, F.; Mitrani, E. Skin micro-organs from several frog species secrete a repertoire of powerful antimicrobials in culture. *J. Antibiot. (Tokyo)* **2012**, *65*, 461–467. [CrossRef] [PubMed]
47. Gallart-Palau, X.; Serra, A.; Lee, B.S.T.; Guo, X.; Sze, S.K. Brain ureido degenerative protein modifications are associated with neuroinflammation and proteinopathy in Alzheimer's disease with cerebrovascular disease. *J. Neuroinflamm.* **2017**, *14*, 1–12. [CrossRef] [PubMed]
48. Serra, A.; Hemu, X.; Nguyen, G.K.T.; Nguyen, N.T.K.; Sze, S.K.; Tam, J.P. A high-throughput peptidomic strategy to decipher the molecular diversity of cyclic cysteine-rich peptides. *Sci. Rep.* **2016**, *6*, 23005. [CrossRef] [PubMed]
49. Serra, A.; Zhu, H.; Gallart-Palau, X.; Park, J.E.; Ho, H.H.; Tam, J.P.; Sze, S.K. Plasma proteome coverage is increased by unique peptide recovery from sodium deoxycholate precipitate. *Anal. Bioanal. Chem.* **2016**, *408*, 1963–1973. [CrossRef] [PubMed]
50. Ma, B.; Zhang, K.; Hendrie, C.; Liang, C.; Li, M.; Doherty-Kirby, A.; Lajoie, G. PEAKS: Powerful software for peptide de novo sequencing by tandem mass spectrometry. *Rapid Commun. Mass Spectrom.* **2003**, *17*, 2337–2342. [CrossRef] [PubMed]
51. Serra, A.; Gallart-Palau, X.; Park, J.E.; Lim, G.G.Y.; Lim, K.L.; Ho, H.H.; Tam, J.P.; Sze, S.K. Vascular Bed Molecular Profiling by Differential Systemic Decellularization In Vivo. *Arterioscler. Thromb. Vasc. Biol.* **2018**, *38*, 2396–2409. [CrossRef] [PubMed]

52. Nielsen, H. Predicting Secretory Proteins with SignalP. In *Methods in Molecular Biology*; Kihara, D., Ed.; Springer: New York, NY, USA, 2017; Volume 1611, pp. 59–73, ISBN 978-1-4939-7013-1.
53. Bertoni, M.; Kiefer, F.; Biasini, M.; Bordoli, L.; Schwede, T. Modeling protein quaternary structure of homo- and hetero-oligomers beyond binary interactions by homology. *Sci. Rep.* **2017**, *7*, 1–15. [CrossRef] [PubMed]
54. Waterhouse, A.; Bertoni, M.; Bienert, S.; Studer, G.; Tauriello, G.; Gumienny, R.; Heer, F.T.; De Beer, T.A.P.; Rempfer, C.; Bordoli, L.; et al. SWISS-MODEL: Homology modelling of protein structures and complexes. *Nucleic Acids Res.* **2018**, *46*, W296–W303. [CrossRef] [PubMed]
55. Pettersen, E.F.; Goddard, T.D.; Huang, C.C.; Couch, G.S.; Greenblatt, D.M.; Meng, E.C.; Ferrin, T.E. UCSF Chimera—A visualization system for exploratory research and analysis. *J. Comput. Chem.* **2004**, *25*, 1605–1612. [CrossRef] [PubMed]

Vitae

Jesús Hernández Pérez was born on Tuesday 10th January of 1989 at 1:00 pm in Puebla, Puebla, México. He is the only son of María de Lourdes Pérez Ramírez and Manuel Hernández Herrera. Jesus attended preschool, elementary school, middle school and high school at Colegio Benavente in Puebla, Puebla.

At the age of 18 he moved to Monterrey to pursue a bachelor's degree in Biotechnology Engineering at Tecnológico de Monterrey. In 2010 he joined Dr. Cardineau's lab where he learned molecular biology and tissue culture techniques. In 2011 he participated in the iGEM competition along with 9 teammates with a project demonstrating the surface display of active enzymes in *Escherichia coli*'s membrane. In December 2012 he graduated from Biotechnology Engineering with a specialization in bioprocesses and in January 2013 he joined Dr. Cardineau's lab as full-time researcher where he worked in the recombinant expression of proteins in tobacco cells.

In August 2014 he joined the PhD in Biotechnology program at Tecnológico de Monterrey under Dr.Jorge Benavides and Dr. Guy Cardineau supervision. From January 2018 to July 2018 he did a research stay at the NTU Food Technology Centre of the Nanyang Technological University in Singapore under Prof. Patricia Conway and Prof. Jørgen Schlundt supervision.

His Ph.D. project was conceived as a means of fulfilling two of his interests; to develop skills in analytical techniques and to introduce him in the research of nature derived compounds through the isolation and identification of bioactive molecules from the skin secretions of an amphibian previously described on Mexican Traditional Medicine practices. His interests remain to study natural compounds to elucidate its role in nature and propose therapeutic applications as part of a drug discovery platform.

This document was typed in using Microsoft Word by Jesús Hernández-Pérez